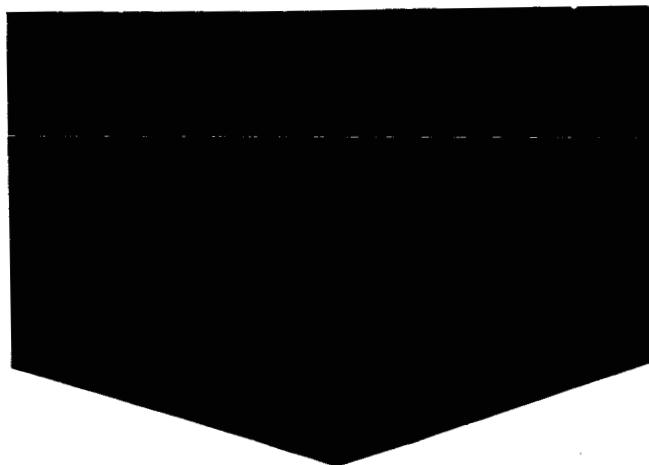


Nas 5 1081



N65-34974

FACILITY FORM 502

(ACCESSION NUMBER)	(THRU)
57	1
(PAGES)	(CODE)
1267267	C7
(NASA CR OR TNX OR AD NUMBER)	(CATEGORY)

GPO PRICE \$ _____

CFSTI PRICE(S) \$ _____

Hard copy (HC) _____

Microfiche (MF) _____

ff 653 July 65

BALL BROTHERS

RESEARCH CORPORATION

LABORATORIES IN BOULDER, COLORADO AND MUNCIE, INDIANA





BALL BROTHERS RESEARCH CORPORATION

BOULDER, COLORADO

FINAL REPORT
DESIGN, FABRICATION, TEST, AND
FLIGHT OF BBRC TYPE SPC 300
SOLAR POINTING CONTROLS
AND
BBRC TYPE TEL 200
TELEMETRY SYSTEMS

F65-2

March 10, 1965

Contract NAS5-1081

Prepared for
National Aeronautics and Space Administration
Goddard Space Flight Center

PREPARED

R. L. Campbell
Electronics Engineer

APPROVED

R. A. Hamel
Project Engineer

R. E. Hathaway
Program Manager



ABSTRACT

This report summarizes a four-year contract with its modifications to design, fabricate, test, and provide launch services for three BBRC type SPC 300 solar pointing controls and three BBRC type TEL 200 telemetry systems suitable for use with specific scientific research instruments.

The BBRC type SPC 300 solar pointing control provides orientation of scientific instrumentation toward the center of the solar disc during the upper atmospheric portion of an Aerobee sounding rocket flight. The BBRC type SPC 300B also provides instrument restraint and shielding during re-entry into the earth's atmosphere to enhance the possibility of successful parachute recovery.

The BBRC type TEL 200 telemetry system provides FM-FM radio transmission of instrument electronic data outputs, vehicle performance monitor outputs, and solar pointing control performance data outputs during the flight.



FOREWORD

This document is the final report required by NASA-GSFC Contract NAS5-1081. The contract and contract modification commitments as well as the results of these commitments are documented and summarized. Recommendations and conclusions are based upon included flight report excerpts. The purpose of the hardware fabricated under this contract is discussed to provide a thorough understanding of the contract objectives.



SUMMARY

Three BBRC type SPC 300 solar pointing controls (SPC 308, SPC 309, and SPC 310) were fabricated under this contract. Two of these were subsequently modified to become type SPC 300B solar pointing controls.

Three BBRC type TEL 200 telemetry systems were fabricated under this contract. Serial numbers TEL 206, TEL 207, and TEL 208 were assigned to these units.

SPC 308B and TEL 206 were expended in the launch of NASA Flight No. 4.21US on November 27, 1962. Excerpts from the BBRC flight report of NASA Flight No. 4.21US are contained in Section 2.

SPC 309B and TEL 208 were launched on NASA Flight No. 4.33GS on October 15, 1963, and successfully recovered. Excerpts from the BBRC flight report of NASA Flight No. 4.33GS are contained in Section 3.

SPC 310 and TEL 207 were expended in the launch of NASA Flight No. 4.22US on September 6, 1963. Excerpts from the BBRC flight report of NASA Flight No. 4.22US are contained in Section 4.

SPC 309B and TEL 311 (transferred to this contract from NAS5-3462) were expended in the launch of NASA Flight No. 4.116GS on October 30, 1964. Excerpts from the BBRC flight report of NASA Flight No. 4.116GS are contained in Section 5.



CONTENTS

Section		Page
	ABSTRACT	ii
	FOREWORD	iii
	SUMMARY	iv
	ILLUSTRATIONS	vi
1	CONTRACT HISTORY	1-1
	1.1 Contract Objectives	1-1
	1.2 Contract Modifications	1-3
	1.3 Conclusions	1-17
2	FLIGHT OF SPC 308B AND TEL 206	2-1
	2.1 General	2-1
	2.2 Flight Data	2-1
	2.3 Conclusions	2-3
3	FLIGHT OF SPC 309B AND TEL 208	3-1
	3.1 General	3-1
	3.2 Flight Data	3-1
	3.3 Conclusions	3-4
4	FLIGHT OF SPC 310A AND TEL 207	4-1
	4.1 General	4-1
	4.2 Flight Data	4-1
	4.3 Conclusions	4-3
5	FLIGHT OF SPC 309B AND TEL 311	5-1
	5.1 General	5-1
	5.2 Reduced Flight Data	5-2
	5.3 Conclusions	5-6



ILLUSTRATIONS

Figure		Page
1-1	SPC 300 With Cylindrical Nose Cone	1-4
1-2	SPC 300B (Cylindrical Nose Cone With Restow)	1-5
1-3	TEL 200 Without In-Flight Calibrator	1-6
1-4	TEL 200 With In-Flight Calibrator	1-8
1-5	High-Vacuum Nose Cone Evacuation System	1-12
2-1	Instrument Elevation Angle versus Time	2-5
2-2	Temperature Probe Output versus Time	2-6
2-3	Chamber Pressure Voltage Output versus Time and Accelerometer Voltage Output versus Time	2-7
2-4	Elevation and Azimuth Error versus Time	2-8
2-5	Acquisition	2-9
2-6	Bias Voltage and A + Voltage versus Time	2-10
3-1	Instrument Elevation Angle versus Time	3-6
3-2	Azimuth and Elevation Pointing Errors versus Time	3-7
3-3	Rocket Spin Rate versus Time	3-8
3-4	Performance Data versus Time	3-9
3-5	SPC Bias Voltage versus Time	3-10
3-6	NASA Accelerometer Output versus Time	3-11
3-7	Biaxial Accelerometer Output versus Time	3-12
3-8	NASA Chamber Pressure Transducer Output versus Time	3-13
3-9	Temperature Probe Output versus Time	3-14
4-1	Rocket Spin Rate versus Time	4-4
4-2	Accelerometer and Chamber Pressure Transducer Voltages versus Time	4-5
4-3	Elevation and Azimuth Error versus Time	4-6



Figure		Page
4-4	Instrument Elevation Angle versus Time	4-12
4-5	Acquisition Functions versus Time	4-15
5-1	Instrument Elevation Angle versus Time	5-8
5-2	Azimuth and Elevation Pointing Errors versus Time	5-9
5-3	Rocket Spin Rate versus Time	5-10
5-4	SPC Performance Data versus Time	5-12
5-5	SPC Bias Voltage versus Time	5-14
5-6	Biaxial Accelerometer Output versus Time	5-15
5-7	NASA Chamber Pressure Transducer Output versus Time	5-21
5-8	Temperature on Inside of Casting at Station 87 versus Time	5-22



Section 1

CONTRACT HISTORY

1.1 CONTRACT OBJECTIVES

NASA Contract NAS5-1081 was formulated as a result of BBRC solicited proposal PROP 161, dated September 19, 1960, as amended through subsequent negotiations prior to the contract date. BBRC was directed by NASA to proceed on January 19, 1961, and advised that the contract would be received at a later date. This directive was followed with a letter contract. Definitive Contract NAS5-1081, dated April 12, 1962, was received by BBRC in May 1962.

Contract NAS5-1081 specified the following articles:

Article I

- Item 1 Design, fabricate, and test three (3) BBRC type SPC 300 solar pointing controls.
- Item 2 Design, fabricate, and test three (3) BBRC type TEL 200 telemetry systems.
- Item 3 Provide 9 man weeks of engineering services at BBRC for each SPC 300 and 3 man weeks of engineering services at BBRC for each TEL 200 for integration of scientific instrumentation.
- Item 4 Provide 8 man weeks of engineering field services at the rocket launch site for each SPC 300 and 4 man weeks of engineering field services at the rocket launch site for each TEL 200.



Item 5 Prepare an evaluation report of each SPC 300 after its flight.

Item 6 Submit monthly progress reports.

Item 7 Submit a final report at the conclusion of the contract.

Article II - Delivery schedule of all items called out in Article I.

Article III - All GFE to be utilized on NAS5-1081.

Article IV - Technical directions to be utilized on NAS5-1081.

Article V - Location of inspection and acceptance and the inspection authority.

Article VI - Terms of shipment.

Article VII - Date of incurrence of cost.

Article VIII - Payment of fixed fee.

Article IX - Submittal of invoices.

Article X - Method of preservation and packing.

Article XI - Method of negotiating overhead rates.

Article XII - Contract alterations.

Article XIII - Requirements of Director of Procurement and Supply approval.

Article XIV - Reference of this definitive contract to the letter contract of an earlier date.

NASA General Provisions Form 417, dated June 1961, and NASA Clause 50 were a contract attachment. NASA Clause 50 specified the contract data



requirements.

All contract items specified in NAS5-1081 have been completed. Serial numbers were assigned as follows:

SPC 300 Solar Pointing Controls

SPC 308B, SPC 309B, and
SPC 310

TEL 200 Telemetry Systems

TEL 206, TEL 207, and
TEL 208

Photographs of the SPC 300 and TEL 200 are shown in Figs. 1-1, 1-2, and 1-3.

SPC 308B and TEL 206 were launched on NASA Flight No. 4.21 on November 27, 1962, and were not recovered. SPC 310 and TEL 207 were launched on NASA Flight No. 4.22 on August 6, 1963, and were not recovered. SPC 309B and TEL 208 were launched on NASA Flight No. 4.33 on October 15, 1963, and were recovered virtually undamaged. SPC 309B and TEL 311 were launched on NASA Flight No. 4.116GS on October 30, 1964, and were not recovered.

1.2 CONTRACT MODIFICATIONS

Contract NAS5-1081 was modified by eight contract modifications prior to its completion, as outlined below.

Modification No. 1	Definitive contract, dated April 12, 1962. This modification contained all applicable deliverable item specifications, listed all GFE, and listed all applicable notes, articles,
--------------------	--

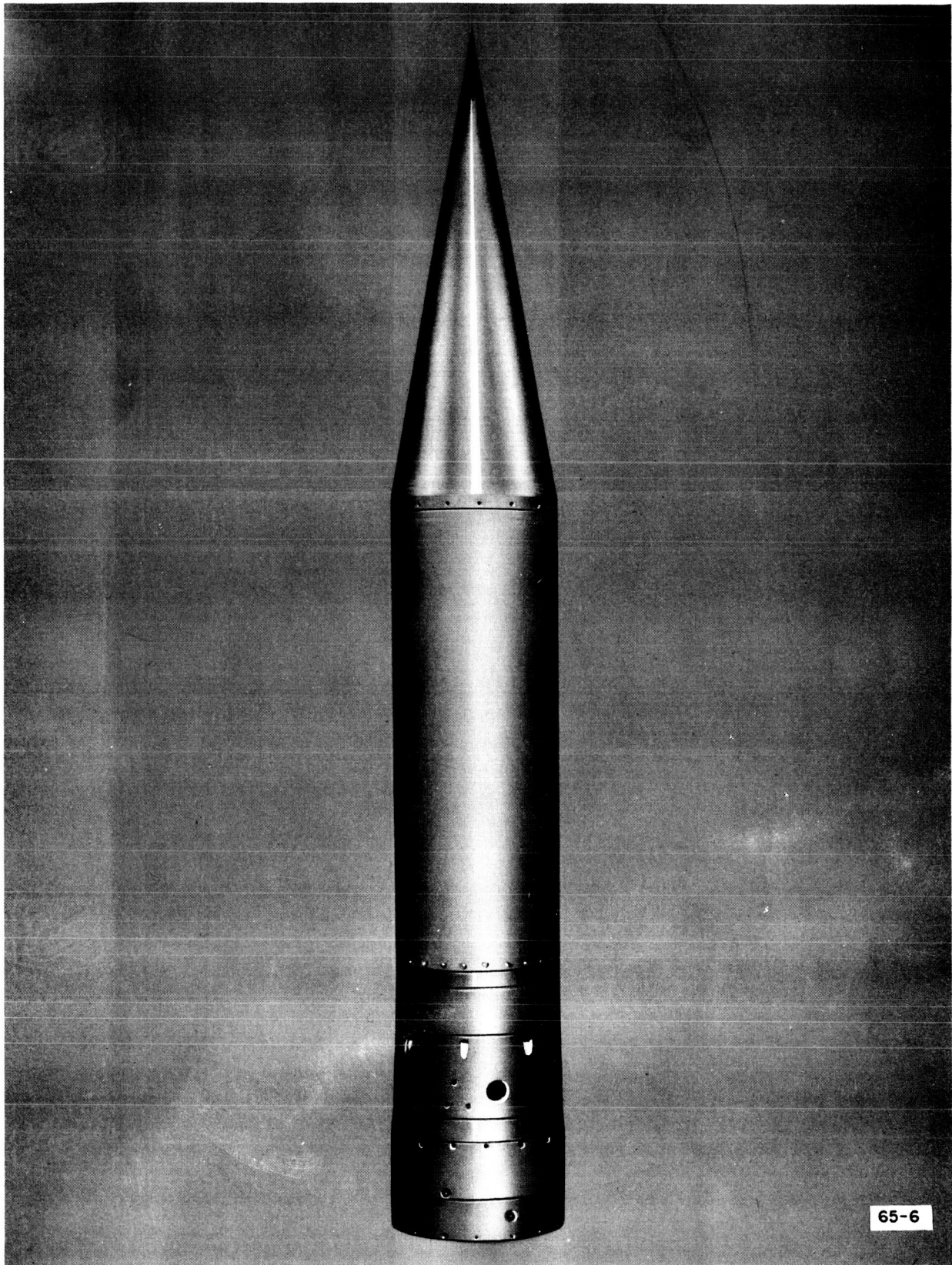


Fig. 1-1 SPC 300 With Cylindrical Nose Cone

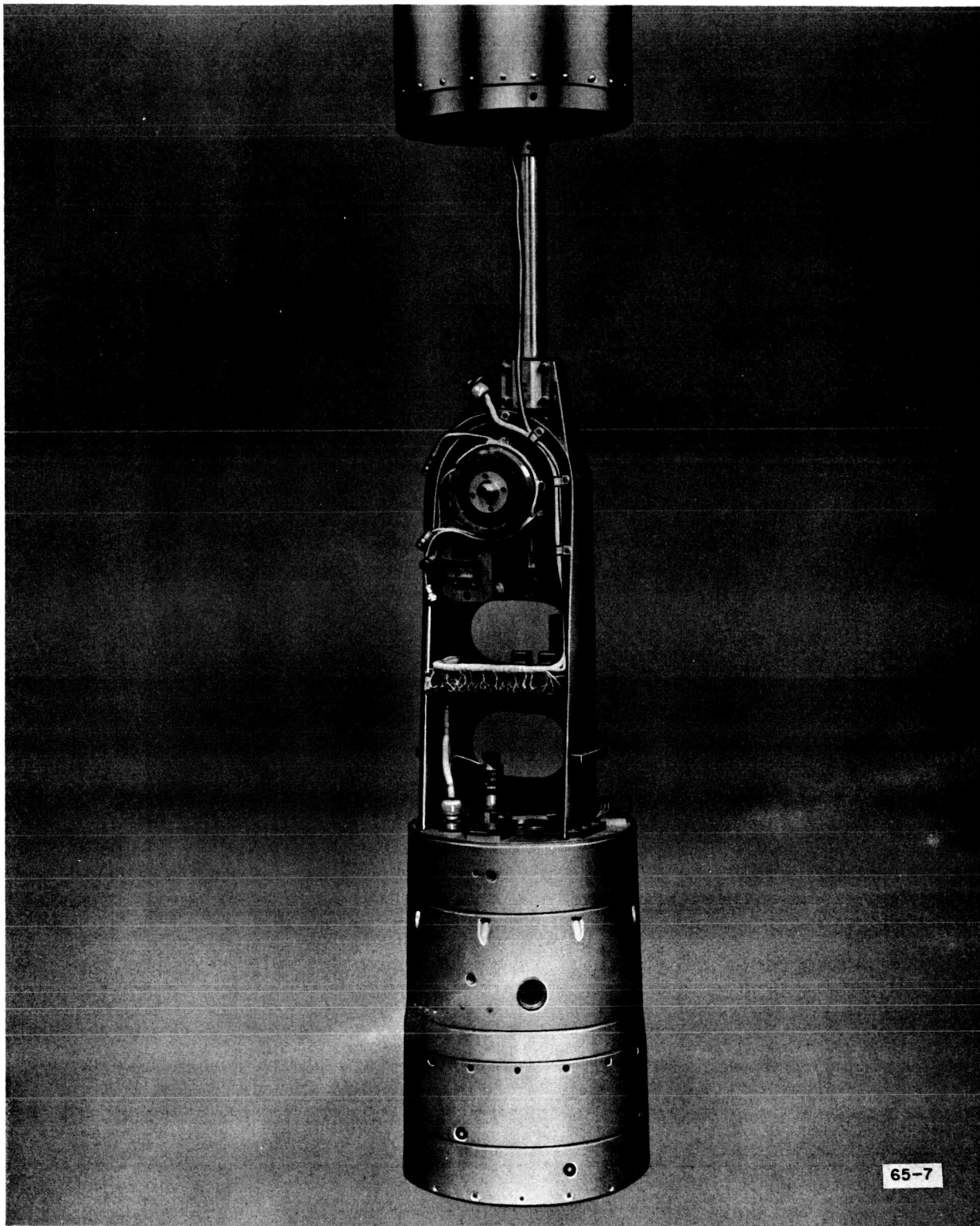
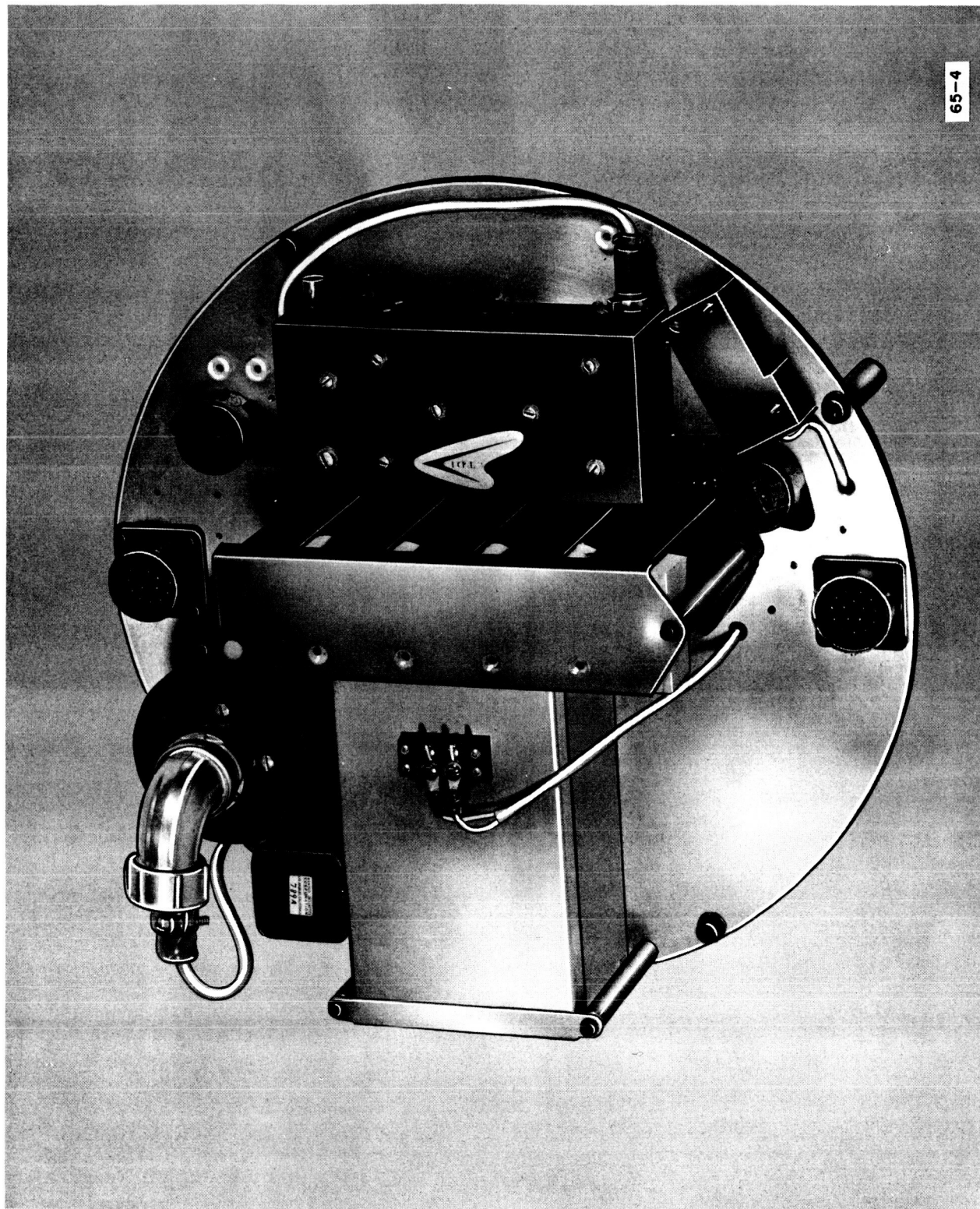


Fig. 1-2 SPC 300B (Cylindrical Nose Cone With Restow)



65-4

Fig. 1-3 TEL 200 Without In-Flight Calibrator



and general provisions as specified under the contract objective above.

- Modification No. 2 Increased the scope of work by requesting that three each TC100 telemetry calibrators be fabricated and one each be installed on each deliverable telemetry system. The telemetry system delivery dates were amended to provide sufficient time to incorporate the telemetry calibrators. Contract Article XIV was amended to include a statement that any costs or payments made under the letter contract will be considered to have been made under the definitive contract. Article XV, which defined the estimated cost and fixed fee, was added. The TC100 telemetry calibrators were fabricated, tested, and installed prior to the telemetry system deliveries. The TEL 200 with calibrator is shown in Fig. 1-4.
- Modification No. 3 Included in Modification No. 4.
- Modification No. 4 Increased the scope of work by specifying that two of the three SPC 300 solar pointing controls (SPC 308 and SPC 309) being fabricated be modified to include mechanisms and control circuits required to lock the experiment into the stow position and to retract and lock the skin assembly in the closed position at the termination of the pointing phase of the flight.



F65-2

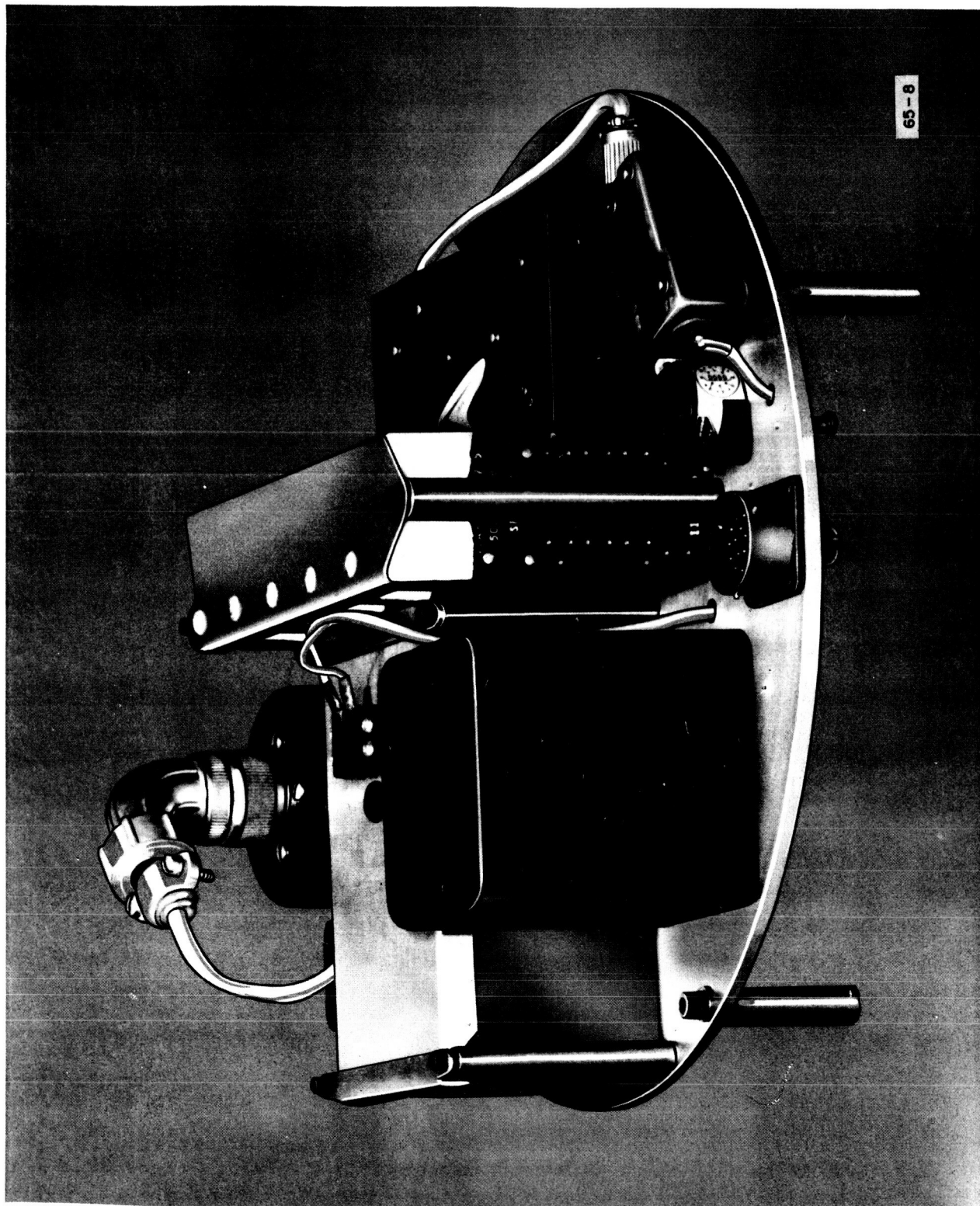


Fig. 1-4 TEL 200 With In-Flight Calibrator



This modification also requested that the telemetry transmitting frequency of two of the three TEL 200 systems (TEL 206 and TEL 207) being fabricated be changed from 235 mc to 234 mc. The delivery dates of the deliverable hardware items were modified suitably to allow sufficient time to incorporate the requested modifications.

Item 4 of Article I was modified to include White Sands Proving Ground, New Mexico, as a possible launch site. Article XV was modified to include the increase in estimated cost and fixed fee due to the increase in scope of work. Article XVI added 150 hours overtime authorization to be utilized in the period from September 20, 1962, through November 20, 1962. Article XVII, which referenced allowable costs of this modification to Clause No. 4 of the General Clauses, was added. The hardware modifications authorized by this modification were completed prior to delivery.



Modification No. 5 Requested that the scope of work be increased to include modifications to two of the SPC 300 solar pointing controls (SPC 308B and SPC 310).

These modifications incorporated a relay and associated wiring; incorporated an electrical circuit to override separation command during the powered phase of the flight; and replaced the existing stepping type commutator with an improved solid-state-type commutator. The above changes were to be completed prior to the scheduled launch date of November 27, 1962. All changes requested in Modification No. 5 were completed prior to launch date.

Modification No. 6 Increased the scope of work, due to additional requirements. Article I, Item 8, specified that one SPC 300 (SPC 310) delivered under this contract be modified to incorporate additional wiring and components as required for compatibility with the revised Harvard College Observatory instrument and to make minor revisions for electrical noise suppression. Item 8 also specified that the nose cone assembly be modified to facilitate evacuation prior to launch and that the nose cone lift mechanism be modified to eject the nose cone at operational altitude.



Article I, Item 9, specified the design, fabrication, and test of one high-vacuum evacuation system for use with the modified pointing control. The vacuum system is shown in Fig. 1-5.

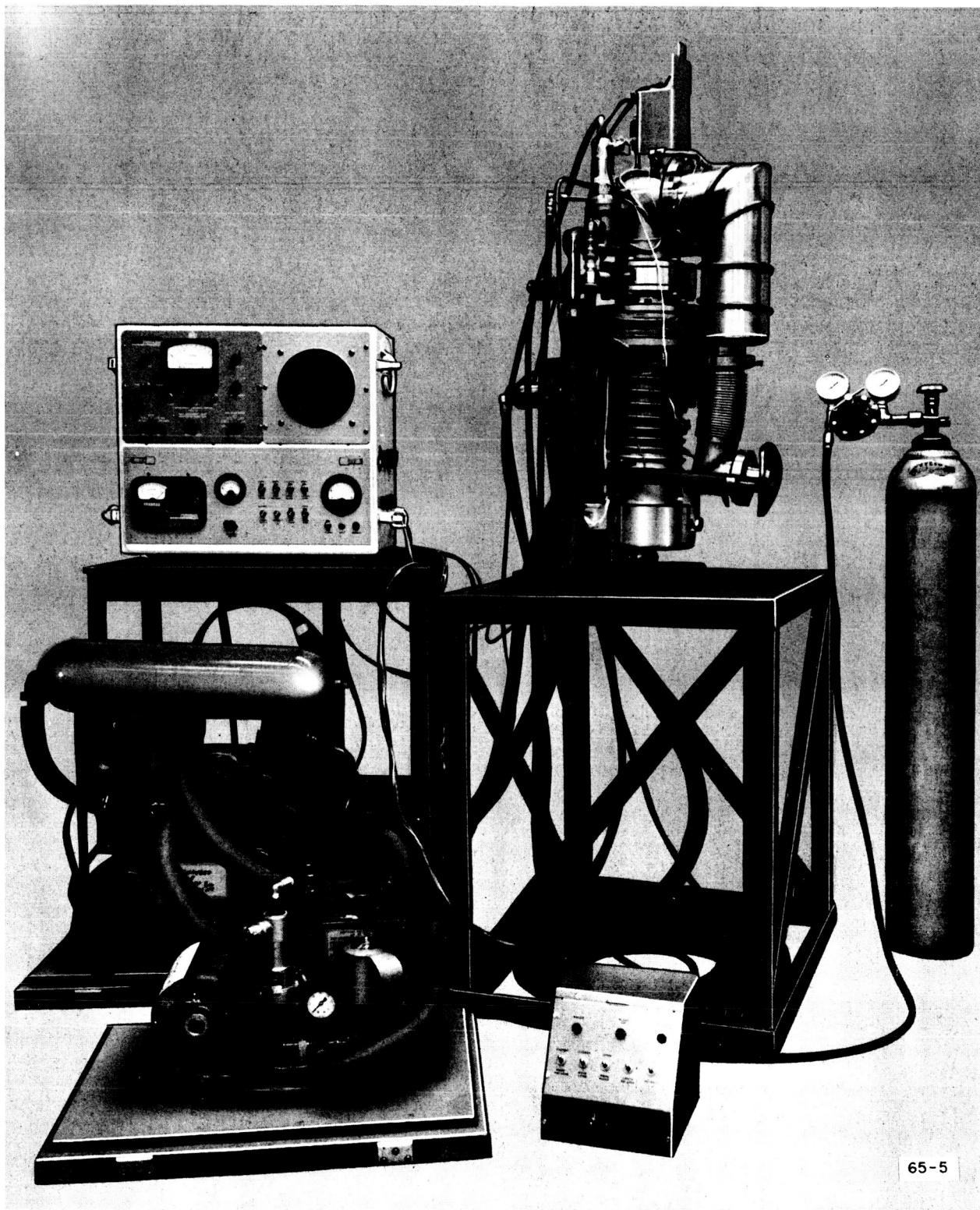
Article II was modified to include the delivery dates of Items 8 and 9.

Article III was modified to make available to the contractor on a rent-free, non-interference basis, all test equipment accountable under Contract NASw-113.

Article XV was revised to include the cost of the additional work in the estimated cost and fixed fee.

Article IV, as it was previously defined, referencing technical directions, was deleted in its entirety and a new Article IV referencing technical directions was added.

Modification No. 6 was completed prior to final acceptance of the solar pointing control modified under Modification No. 6.



65-5

Fig. 1-5 High-Vacuum Nose Cone Evacuation System



Modification No. 7 Provided for photographic documentary coverage of the integration of the Harvard College Observatory instrument with two solar pointing controls by increasing the scope of work.

Article I, Item 10, was added to the contract to provide this photographic coverage.

Article II, Item 10, was added to the contract to specify delivery of Article I, Item 10.

Article XV was revised to include the photographic coverage in the estimated cost and fixed fee portion of the contract. This photographic coverage was provided at BBRC during the integration checks of the Harvard College Observatory instrument with SPC 308B and SPC 310.

Modification No. 8 Specified that modifications be performed on SPC 308B by adding Article I, Item 11. Item 11 specified:

- (a) that the stepping type commutator be replaced with a solid-state type commutator and that the SPC 300 type elevation bridge be replaced with an SPC 400 type elevation bridge,



- (b) that the azimuth servo system be modified to increase pointing accuracy and that some additional switching circuits be provided;
- (c) that the transmitter frequency of TEL 208 be changed from 235 mc to 234 mc and that quadraloop antennas be mounted to the telemetry extension and wired;
- (d) that power and telemetry circuitry be provided for the vehicle accelerometer and chamber pressure transducers during the thrust portion of the flight;
- (e) that an accelerometer be mounted in the telemetry section and its associated wiring be installed; and
- (f) that a lockout circuit be added to prevent premature range safety stage separation.

Article III was modified to provide two quadraloop antennas as GSF to BBRC.

Article XV was revised to include the cost of Modification No. 8 in the estimated cost and fixed fee. The hardware modifications specified in Modification No. 8 were completed prior to the specified launch date.



- Modification No. 9 Revised Article XVI to increase the authorized overtime from 150 to 630 hours.
- Modification No. 10 TWX authorization to proceed with refurbishment of SPC 309B and was included in Modification No. 11.
- Modification No. 11 Provided for the modification and refurbishment of solar pointing control SPC 309B and the modification of TEL 311 to be compatible with SPC 309B and experimentation requirements. The following items were added to Article I:
- Item 12, modify and refurbish solar pointing control SPC 309B for reflight.
- Item 13, modify telemetry system TEL 311 per experiment requirements for operation with solar pointing control SPC 309B.
- Item 14, integration effort for reflight of SPC 309B and TEL 311.
- Item 15, engineering field services.
- Item 16, refurbish SPC 309B and TEL 311 for a second reflight.
- Item 17, integration effort for second reflight of SPC 309B and TEL 311.
- Item 18, engineering field services.



Item 19, flight performance evaluation report.

Item 20, submit monthly progress reports.

Item 21, submit final letter report.

Article II was modified to specify the delivery dates of all items added to Article I.

Article III was modified to include the following listed items as Government furnished property:

- (a) telemetry system TEL 311 accountable to Contract NAS5-3462
- (b) two each Aerobee cone-cylinder nose cones
- (c) one each Aerobee 10-inch fiberglass extension
- (d) furnish launch area facilities
- (e) furnish telemetry data records
- (f) furnish special test equipment on a noninterference basis.

A clause was added to Article V specifying that all reports be inspected and accepted at NASA.



Article VI concerning the terms of shipment was modified and Article IX, concerning invoices was modified.

Article XV estimated cost and fixed fee was increased to include this modification.

Article XVIII was added designating a new technology representative and patent representative.

Article XII concerning alterations was revised.

Modification No. 12 Corrected an error in Article XV of
Modification No. 11.

1.3 CONCLUSIONS

The three solar pointing controls (SPC 308B, SPC 309B, SPC 310) and the three telemetry systems (TEL 206, TEL 207, TEL 208) fabricated under this contract have all been flown, and in each case the pointing accuracy was well within the scientific instrumentation requirements. SPC 309B and TEL 208 were recovered virtually undamaged after the first flight. SPC 309B and TEL 311 were not recovered after the second flight of SPC 309B.

Based upon the flight results of SPC 310, it is recommended that the SPC 300 be modified to eject the nose cone if recovery is not required. Based upon the flight results of SPC 309B, it has been determined that some modifications to the azimuth system can improve azimuth accuracy; and that by replacing the SPC 300 elevation bridge with the new design SPC 400 bridge, the elevation accuracy can be improved. Based upon the results



of the flight of SPC 310 and the second flight of SPC 309B, it has been determined that the cylindrical nose cone can be evacuated by adding stiffening rings to the skin assembly and adding a vacuum valve to hold the vacuum during launch.

The new BBRC types SPC 400 and SPC 300D solar pointing controls provide higher accuracy than the SPC 300 and are recommended for use in the future.

It is recommended that the new BBRC type TEL 300 telemetry system be utilized in the future rather than the TEL 200. The TEL 300 telemetry system has the capabilities of more subcarrier oscillators thereby allowing the transmission of more in-flight data. The TEL 300 has the added advantage of being lighter, more stable, and having a lower battery power requirement for the same power output.



Section 2

FLIGHT OF SPC 308B AND TEL 206

2.1 GENERAL

SPC 308B and TEL 206 were launched on NASA Aerobee 4.21US at 11:00 a.m. MST, November 27, 1962.

The flight experiment consisted of spectral measurements of solar ultra-violet radiation in the 500 to 1,500 Angstroms region by means of a scanning spectrometer developed by the Harvard College Observatory. In addition to the primary function of data acquisition, this experiment provided flight test and calibration information required for a similar spectrometer scheduled for inclusion in the S-17 Orbiting Solar Observatory.

2.2 FLIGHT DATA

Investigation of the telemetry record indicated normal target acquisition by the pointing control. Evaluating the real-time telemetry record of the flight, we are able to report the following performance compared with predicted performance:

<u>Occurrence</u>	<u>Predicted</u>	<u>Actual</u>
Zenith altitude	124 miles	126 miles
Spin rate	1.8 rps	2.0 rps
SPC operation initiated	80.0 seconds	81.8 seconds
SPC nose cone unlock and lift	107.0 seconds	106.8 seconds
SPC pointing initiated	124.0 seconds	123.0 seconds



<u>Occurrence</u>	<u>Predicted</u>	<u>Actual</u>
Harvard high voltage ON	150.0 seconds	150.4 seconds
Harvard high voltage OFF	358.0 seconds	354.3 seconds
SPC restow initiated	360.0 seconds	357.0 seconds
Payload severance	399.0 seconds	407.0 seconds
Parachute deployment	540.0 seconds	None

According to verbal reports from WSMR, the parachute recovery package was severely damaged during the severance and/or parachute deployment phase of the flight, thus preventing a successful recovery. This parachute failure was not known immediately and BBRC personnel stayed at WSMR until November 30, to assist in recovery. The payload was recovered by the WSMR recovery crews on December 1, 1962, and returned to Ball Brothers for inspection on December 5, 1962.

Reference is made to the enclosed graphs for information as to servo performance and attitude of the rocket.

Figure 2-1 is a plot of elevation position pot information and represents the angle between the solar vector and the vehicle transverse axis. The vehicle precessional motion was approximately 20.5 degrees with a period of approximately 95 seconds.

Figure 2-2 is a plot of temperature inside the instrument versus time.

Figure 2-3 is a plot of NASA accelerometer and chamber pressure voltage outputs versus time.



Figure 2-4 is a plot of pointing errors versus time during the periods from 138 to 146 seconds, 200 to 208 seconds, and 276 to 284 seconds. These particular periods were displayed to show the pointing errors existing during different parts of the precessional motion. Pointing performance during the remainder of the oriented portion of the flight was essentially identical with no pointing errors greater than those indicated on the plot.

Figure 2-5 is a plot of various telemetry signals associated with target acquisition nose cone lift, instrument release, restow, etc.

Figure 2-6 is a plot of the pointing control solar sensor reference voltage and primary battery voltage.

2.3 CONCLUSIONS

The unexpectedly high azimuth error was found to be primarily due to three factors:

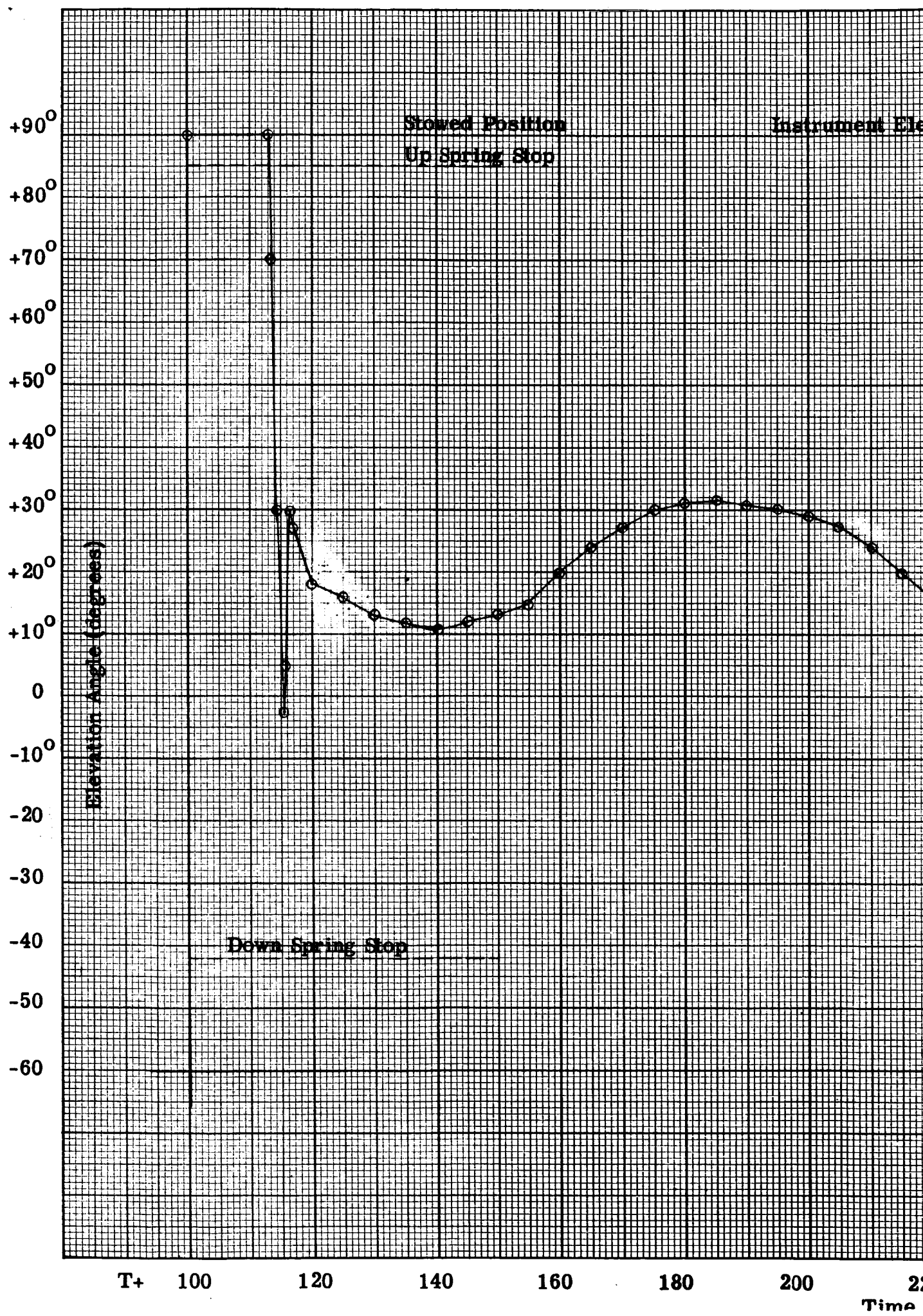
- a higher than anticipated spin rate,
- the effects of Aerobee mass unbalance about the spin axis, and
- the resultant effects of the vehicle unbalance on the increased mass of the modified nose cone.

On future flights, these effects can be significantly reduced by adopting the following corrective measures. If the modified nose cone configuration is to be utilized and recovery is not required, skin ejection is advised to eliminate the large, pendulous mass effect of the nose cone during the



pointing phase of the flight. Reduce the mass unbalance of the Aerobee, and utilize lower spin rates within the vehicle stability range.

In spite of the unexpected amplitude of azimuth errors, the pointing control performance was well within the requirements of the flight experiment, and all pointing control and telemetry system operations were performed successfully.



SPC-308

Elevation Angle vs. Time

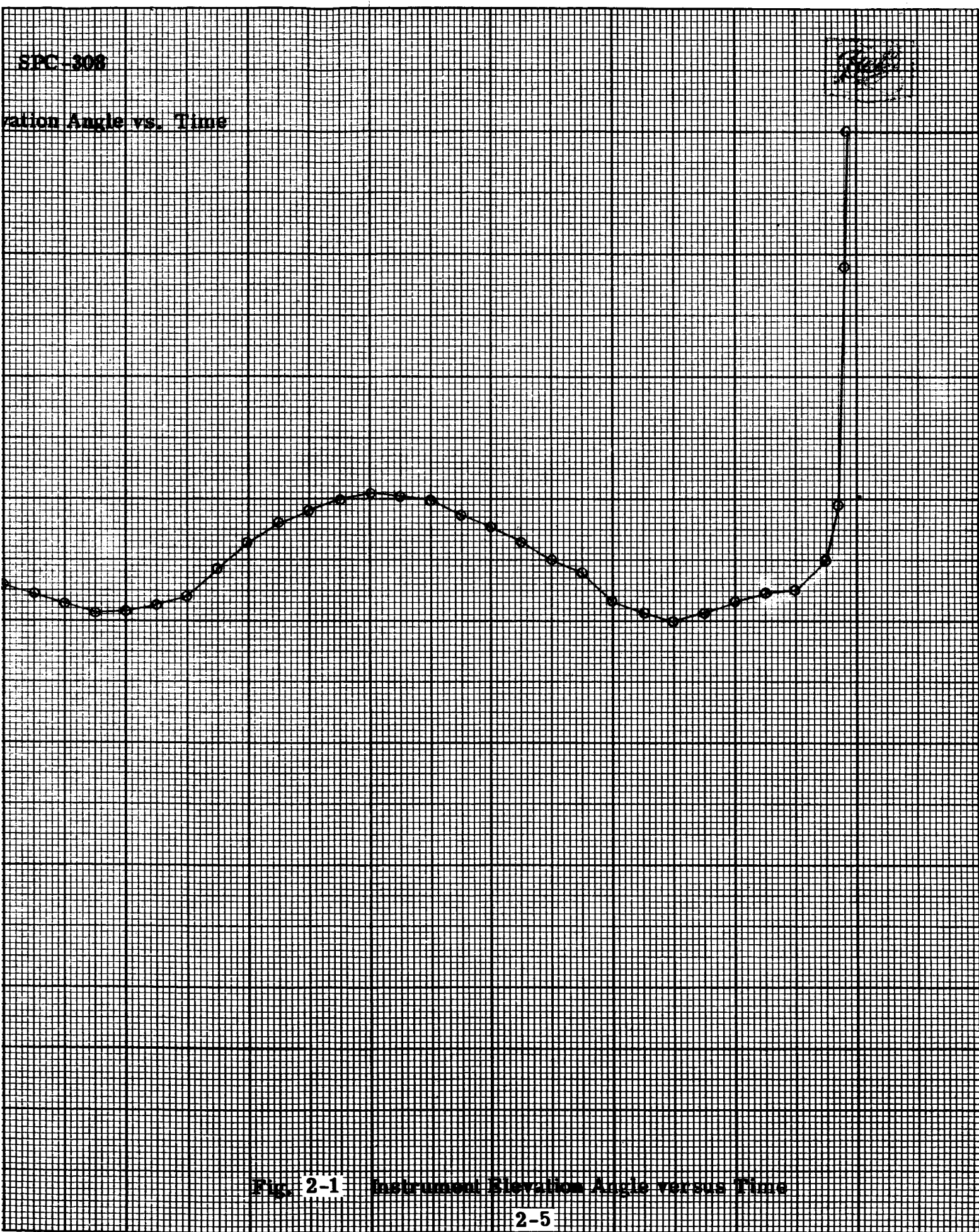


Fig. 2-1 Instrument Elevation Angle versus Time

SPC

Temperature Pro

Temperature in Degrees C.

 $+13^{\circ}$ $+5.2^{\circ}$ -22.5°

0

40

80

120

160

200

240

280

Time (Seconds from Launch)

e Output vs. Time



Fig. 2-2 Temperature Pulse Output Versus Time

2-6

320

360

400

Chamber Pressure Voltage Output

Accelerometer Voltage Output

4
3
2
1
0
-0.5 0 1 2 3 4 5 10 15 20 25

Chamber Pressure Volts
Accelerometer Volts

* See Text

* See Text

Time (Seconds)

4
3
2
1
0

0

ge Output vs. Time and
ge Output vs. Time

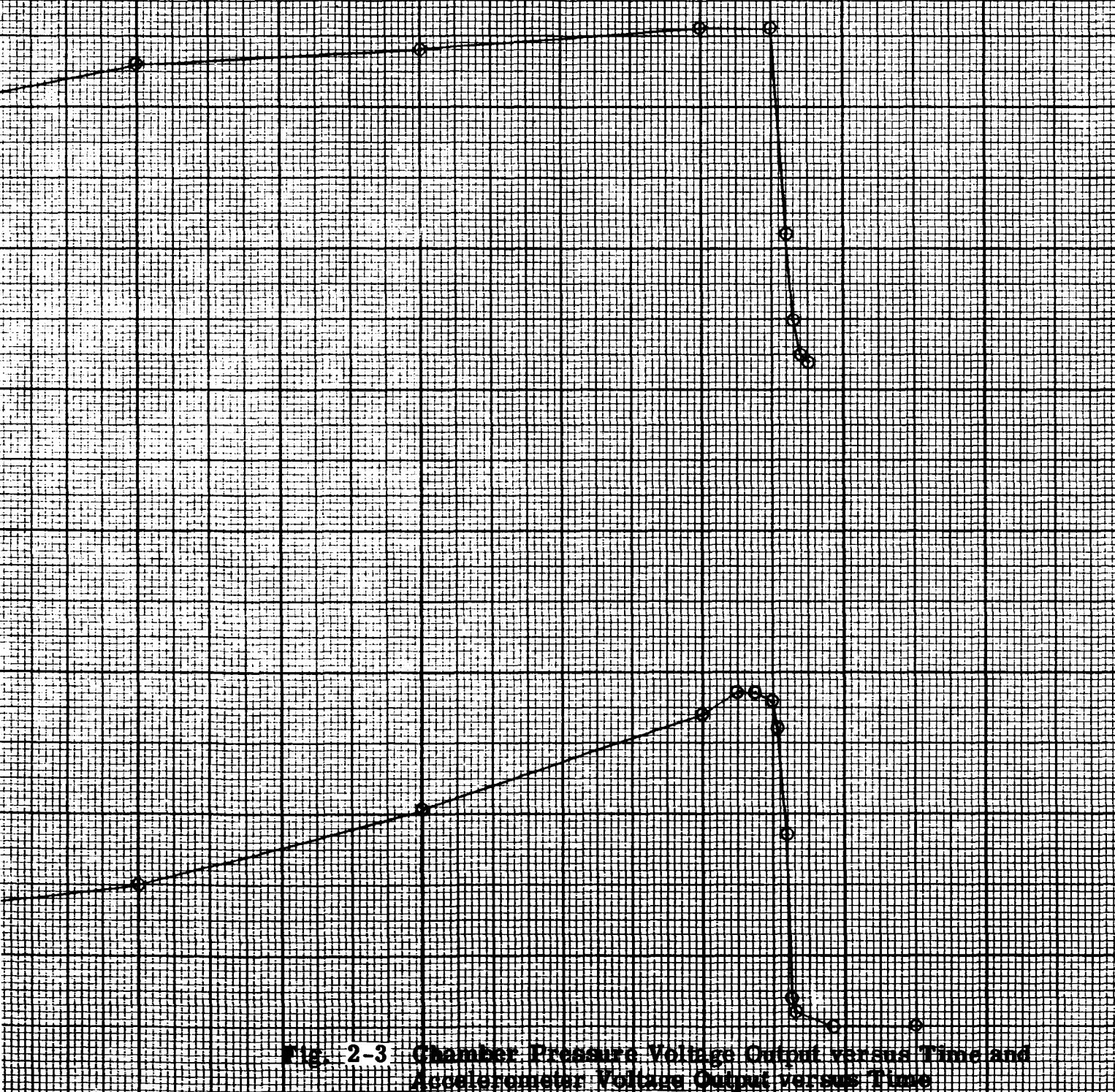
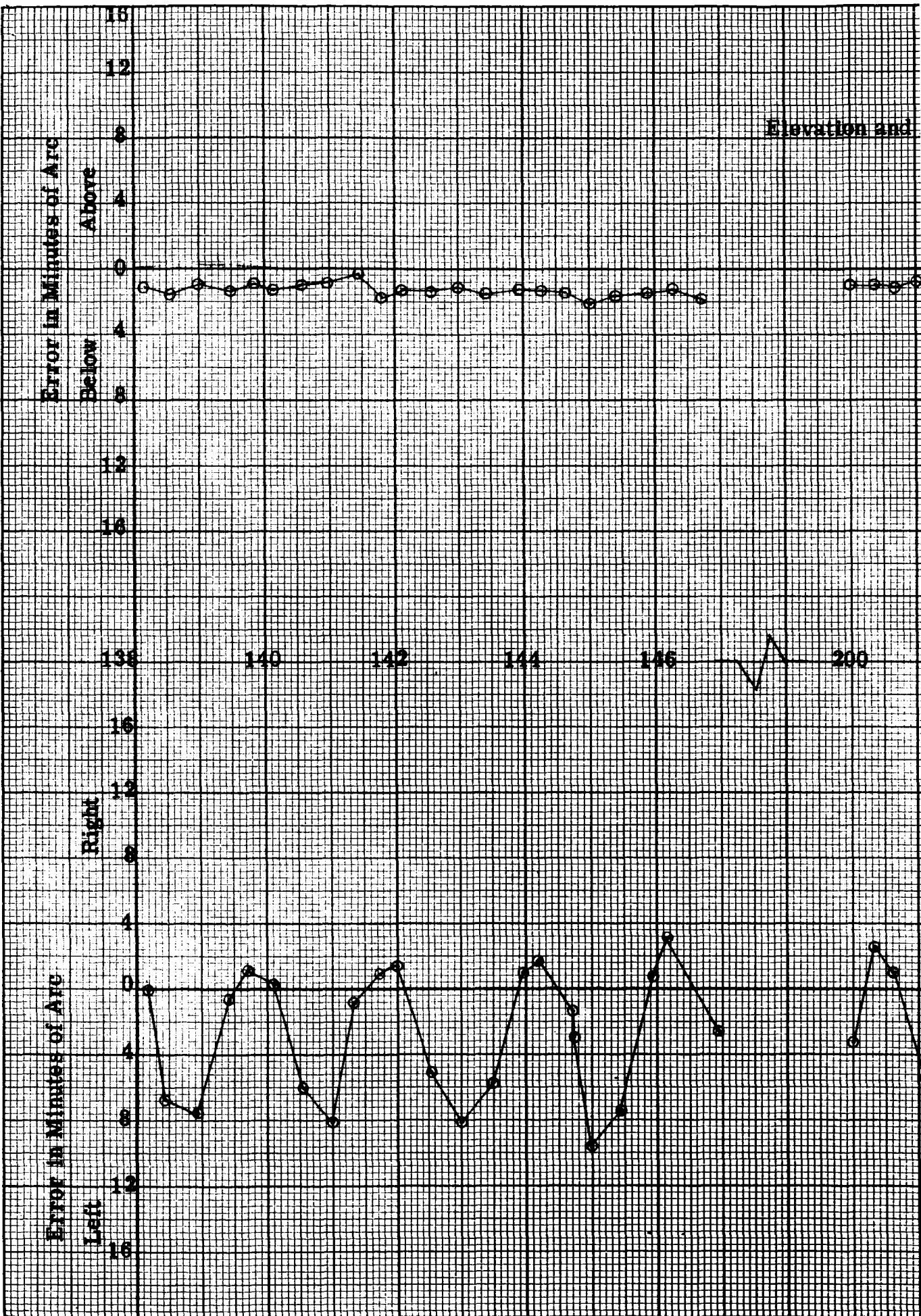


Fig. 2-3 Chamber Pressure Voltage Output versus Time and Accelerometer Voltage Output versus Time

30 35 40 45 50 55 60
2-7
s from Launch)



SPC-308

Azimuth Error vs. Time

Elevation System



202 204 206 276 278 280 282 284

Time (Seconds After Launch)

Azimuth System

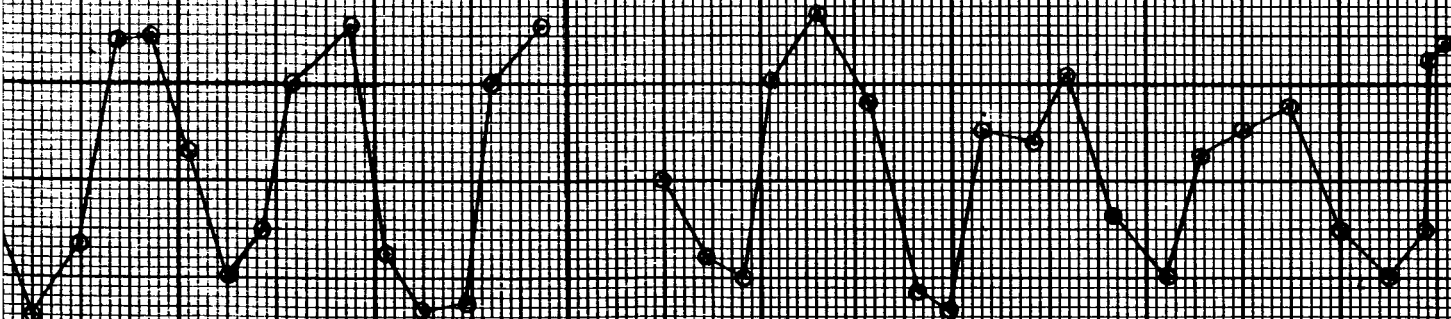
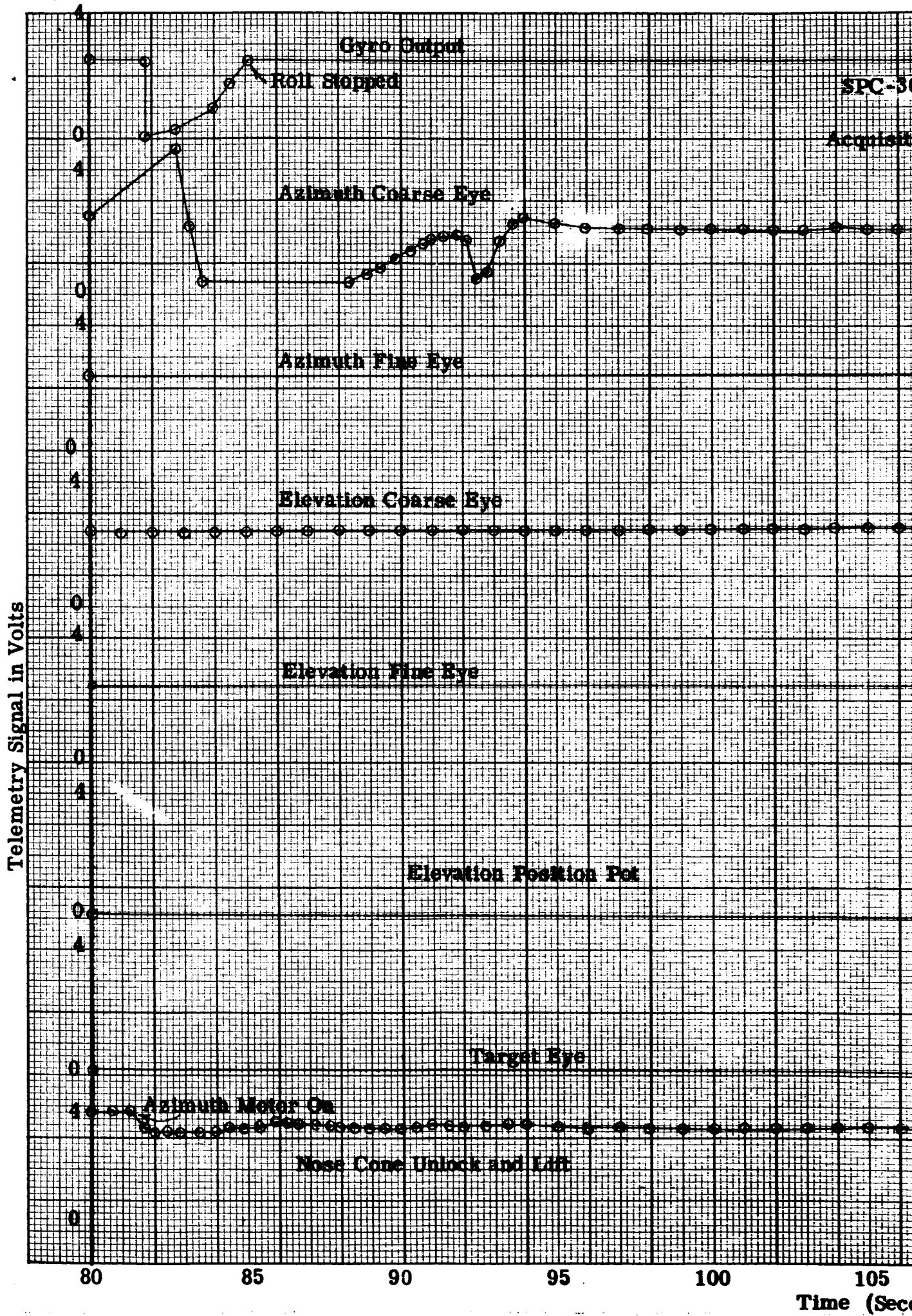
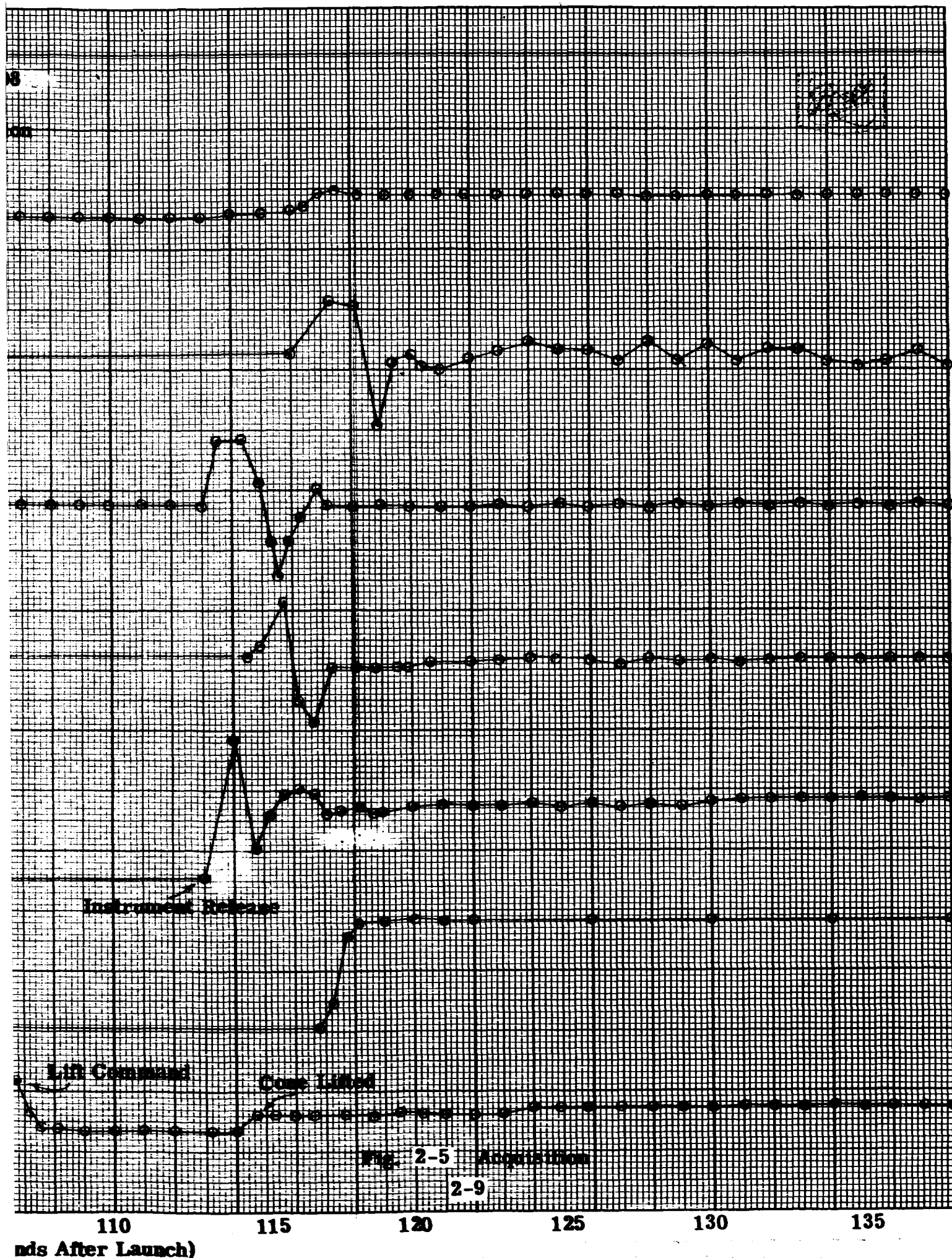
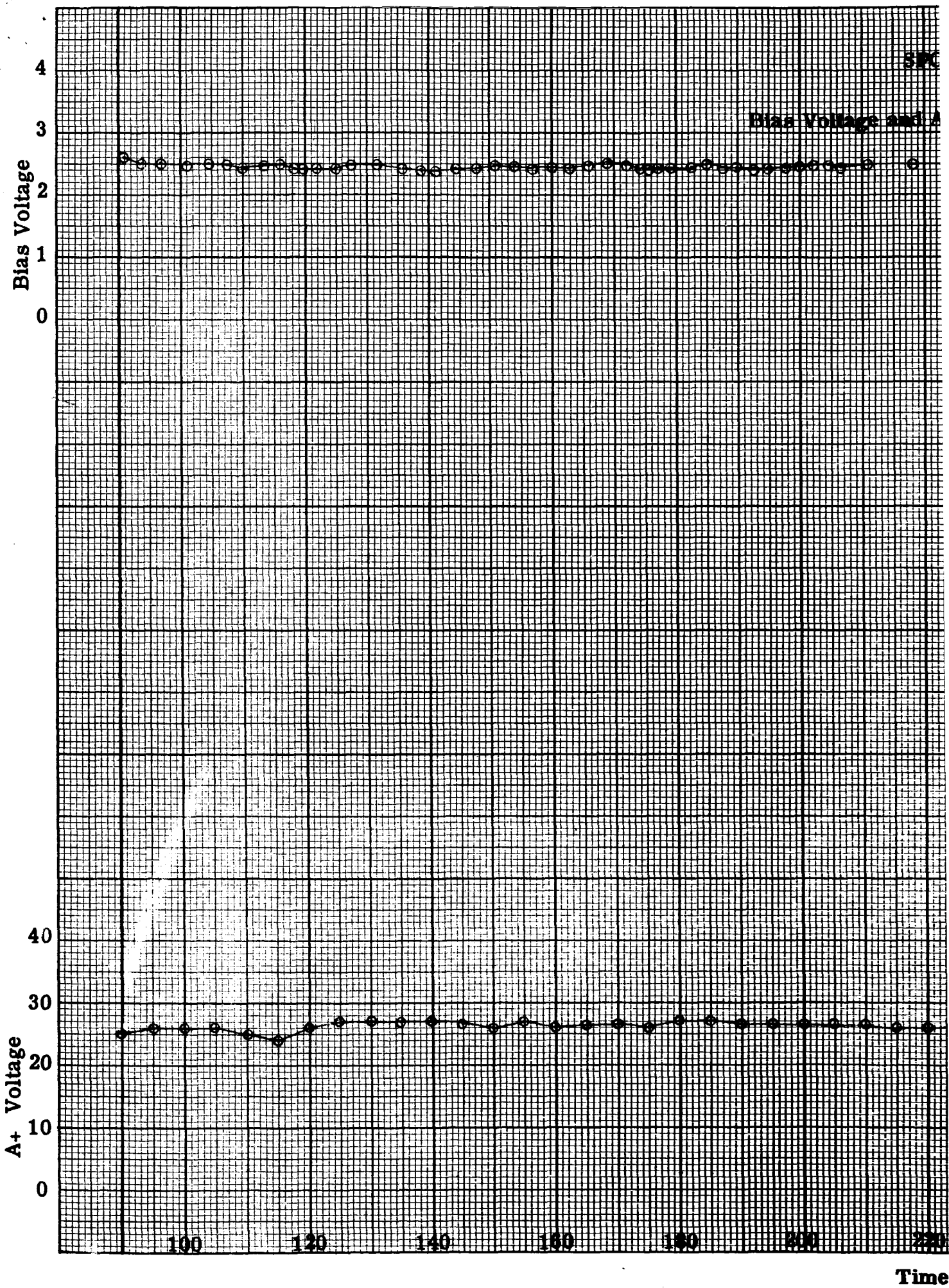


Fig. 2-4 Elevation and Azimuth Error versus Time







500

Voltage vs. Time

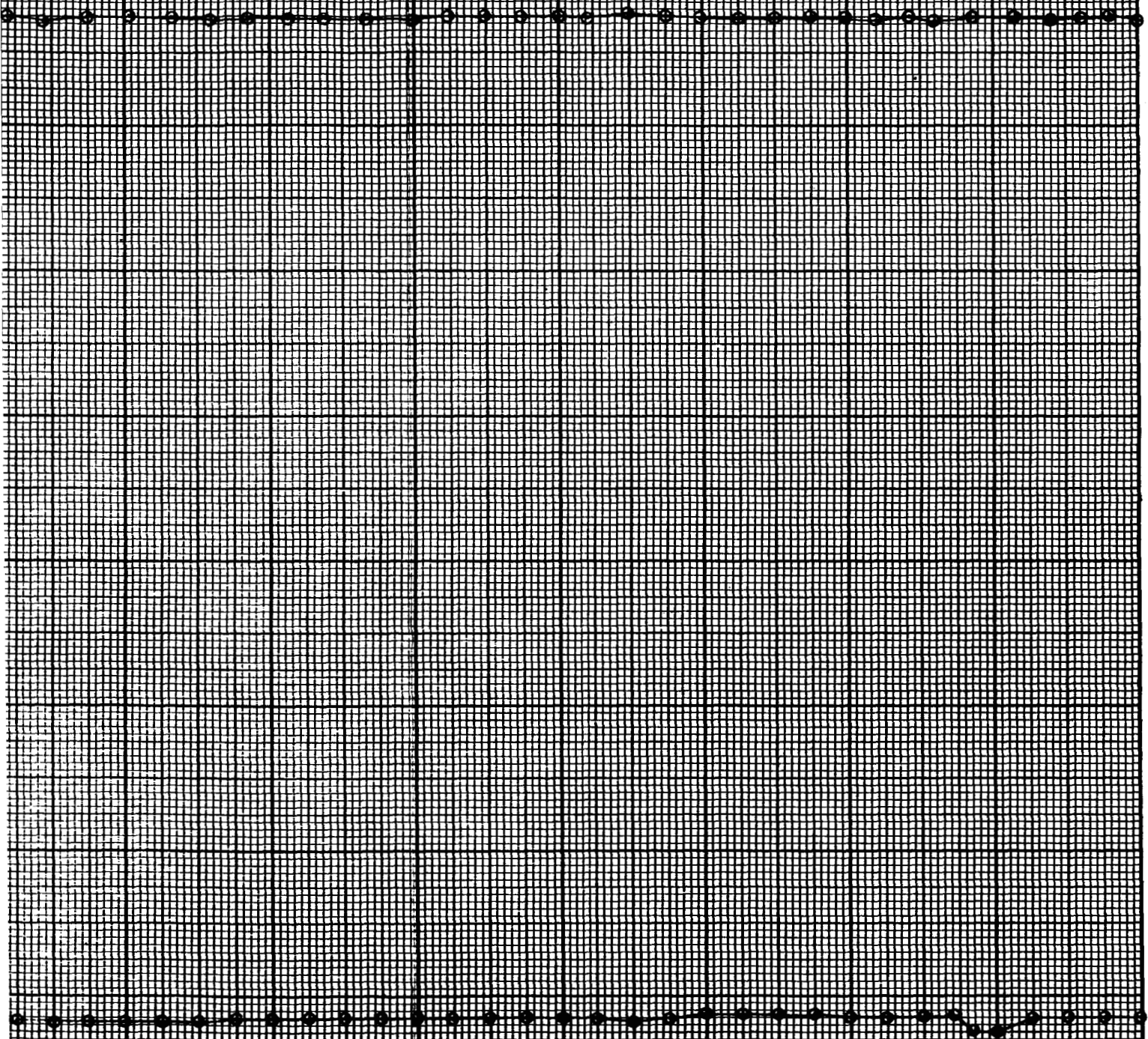


Fig. 2-6 B+ Voltage and A+ Voltage versus Time

2-10

140 160 180 200 220 240 260 280 300

(Seconds from Launch)



Section 3
FLIGHT OF SPC 309B AND TEL 208

3.1 GENERAL

SPC 309B and TEL 208 were launched on NASA Aerobee 4. 33GS at 9:05 a. m. MST, October 15, 1963.

Telemetry data monitored during the flight indicated both systems were functioning normally and evaluation of the flight telemetry record later confirmed this. The restow, payload severance, and parachute deployment systems operated normally and SPC 309B, TEL 208, and the NASA-GSFC instrument were recovered with no apparent damage to any of the systems.

3.2 FLIGHT DATA

The following tabulated data compares the predicted flight performance with the actual flight performance.

<u>Occurrence</u>	<u>Predicted</u>	<u>Actual</u>
Zenith altitude	123 miles	123.4 miles
Spin rate (before acquisition)	1.6 rps	1.1 rps
Spin rate (after acquisition)	1.8 rps	1.35 rps
SPC 309B servo operation initiated	T + 75 seconds	T + 72.5 seconds
SPC 309B nose cone lift	T + 97 seconds	T + 95 seconds
SPC 309B instrument restow	T + 369 seconds	T + 364.5 seconds
Payload severance	T + 391 seconds	T + 396.5 seconds



The performance data listed above and the information that follows was reduced from the telemetry records recorded at Ground Station Jig 44. The following graphs present information regarding pointing control and rocket performance.

Figure 3-1 is a plot of instrument elevation angle versus time. Ninety degrees corresponds to alignment of the instrument optical axis parallel to the vehicle longitudinal axis (stowed position), and zero degrees corresponds to alignment of the instrument optical axis along the vehicle transverse axis.

Figure 3-2 is a plot of the elevation and azimuth pointing errors and illustrates the commutated fine detector error signal outputs versus time. The output of the fine detectors is a direct function of their angular displacement from the solar center. Each fine detector error signal is sampled by the commutator 5.14 times per second with a sample bit duration of 6.65 milliseconds. The maximum plus and minus error during each second was plotted to generate the envelopes shown. Actual pointing error at any specified time therefore falls within the pointing envelope. Short-term errors were within ± 0.4 arc minutes in elevation and ± 1.5 arc minutes in azimuth. Long-term errors were within ± 1.0 arc minute in elevation and ± 2.2 arc minutes in azimuth. Long-term errors have a cyclic pattern corresponding to vehicle precessional rate and are the result of variations in reflected earthlight into the coarse detectors.

Figure 3-3 shows the variations in rocket spin rate in cycles per second versus time. The graph does not show the spin of the rocket during the thrust phase of the flight; however, it shows that after sustainer burnout, the spin rate is constant at 1.1 cps until the start of payload despin.



Figure 3-4 presents azimuth rate gyro, azimuth coarse detector, composite nose cone and instrument functions, elevation coarse detector, target detector, and battery voltage outputs as a function of time. These curves are all presented on the same sheet to illustrate the operational sequence when viewed simultaneously. There is a break in the graph from T+115 seconds to T+360 seconds since there were no changes in these functions during that period.

Figure 3-5 presents the changes in the pointing control bias voltage as a function of time. It is apparent that there were no significant changes in the bias voltage for the flight duration. This bias voltage is used by the pointing control as a reference and the slight changes in this voltage are taken into account when determining the pointing error curves.

Figure 3-6 presents the NASA accelerometer output voltage as a function of time. The NASA accelerometer was mounted in the rocket forward skirt section and its output voltage routed through the BBRC telemetry deck. Calibration for this accelerometer is not available at BBRC, therefore, the voltage output has not been converted to acceleration.

Figure 3-7 presents the biaxial accelerometer output in G's as a function of time. This accelerometer was mounted to the electronics base plate in the BBRC telemetry section and was added to provide data on re-entry and parachute shock forces. No re-entry acceleration information was acquired due to a change from the quadraloop antennas to the tail notch antenna shortly before the flight. Since the tail antenna is lost at payload severance, transmission of the re-entry data could not be accomplished.



Figure 3-8 presents the NASA chamber pressure transducer output voltage as a function of time. The chamber pressure transducer was mounted in the rocket tail section and its output routed through the BBRC telemetry section. Chamber pressure data was not plotted since the transducer calibration curves are not available at BBRC.

Figure 3-9 presents the eyeblock temperature in degrees Centigrade as a function of time. The temperature monitor was mounted on a thin metal plate on the eyeblock to reduce the time lag between the ambient and the monitor temperature.

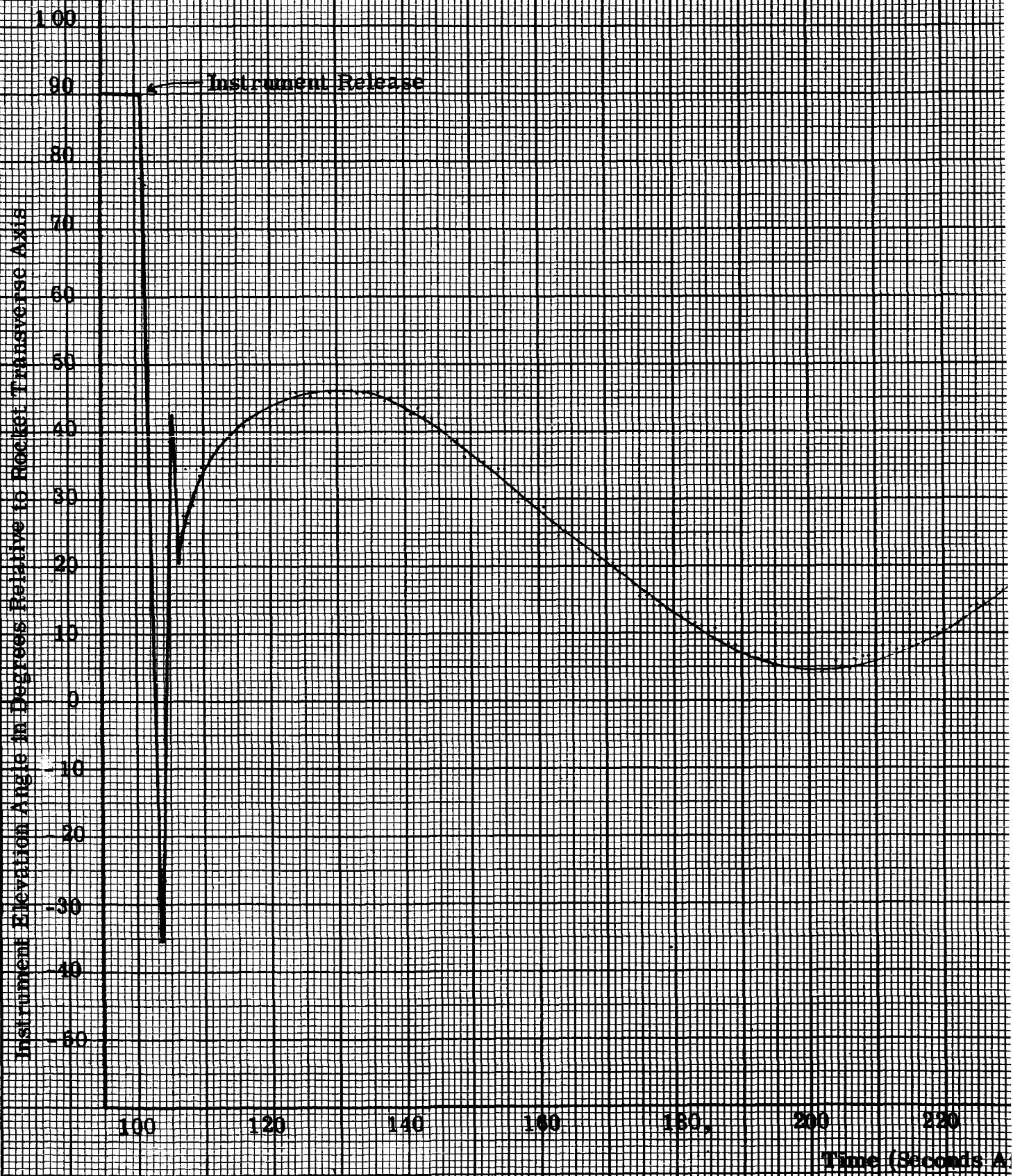
3.3 CONCLUSIONS

Flight performance of the solar pointing control and telemetry system was excellent. Pointing accuracy for a type SPC 300 was better than normal, reflecting the several revisions authorized by contract amendment No. 8 and the lower than normal vehicle spin rate.

The major forcing functions affecting pointing accuracy are introduced by mass unbalance of the rocket vehicle about its spin axis. Reduction of the spin rate reduces the amplitude of these forcing functions and correspondingly increases short-term pointing accuracy. Unfortunately, reduction of the spin rate also reduces vehicle stability as reflected by the 42.5-degree precessional cone, illustrated in Fig. 3-1 of this report. This precessional motion is corrected by the pointing control in two control axes. The third axis motion, however, introduces roll of the instrument about the solar vector and effectively reduces the resolution of the long exposure solar spectroheliograms. In addition, the excessive precessional motion

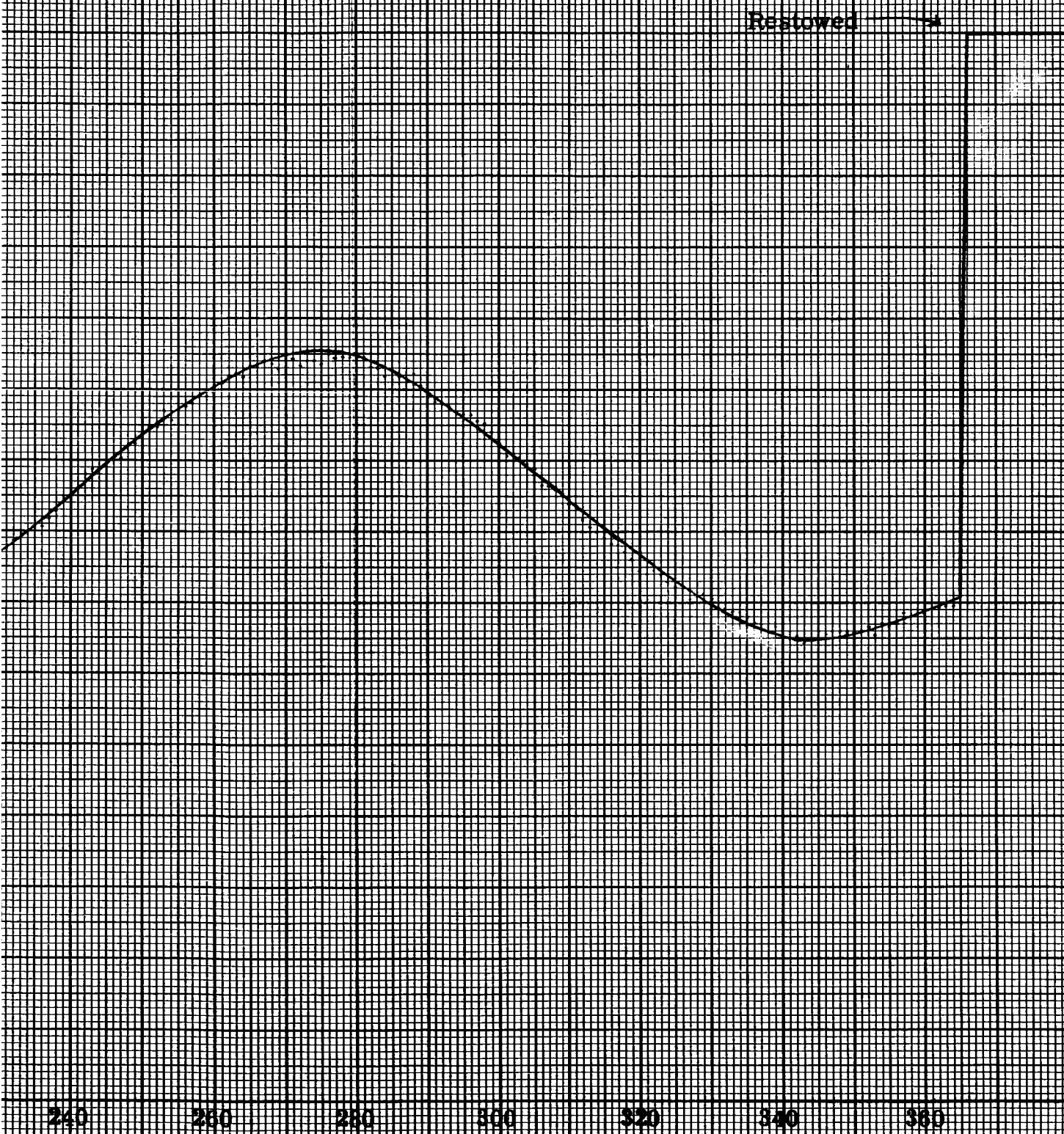


contributed to long-term pointing inaccuracies by increasing the effects of reflected earthlight on the coarse detectors. The effects of this reflected light are illustrated by Fig. 3-2.



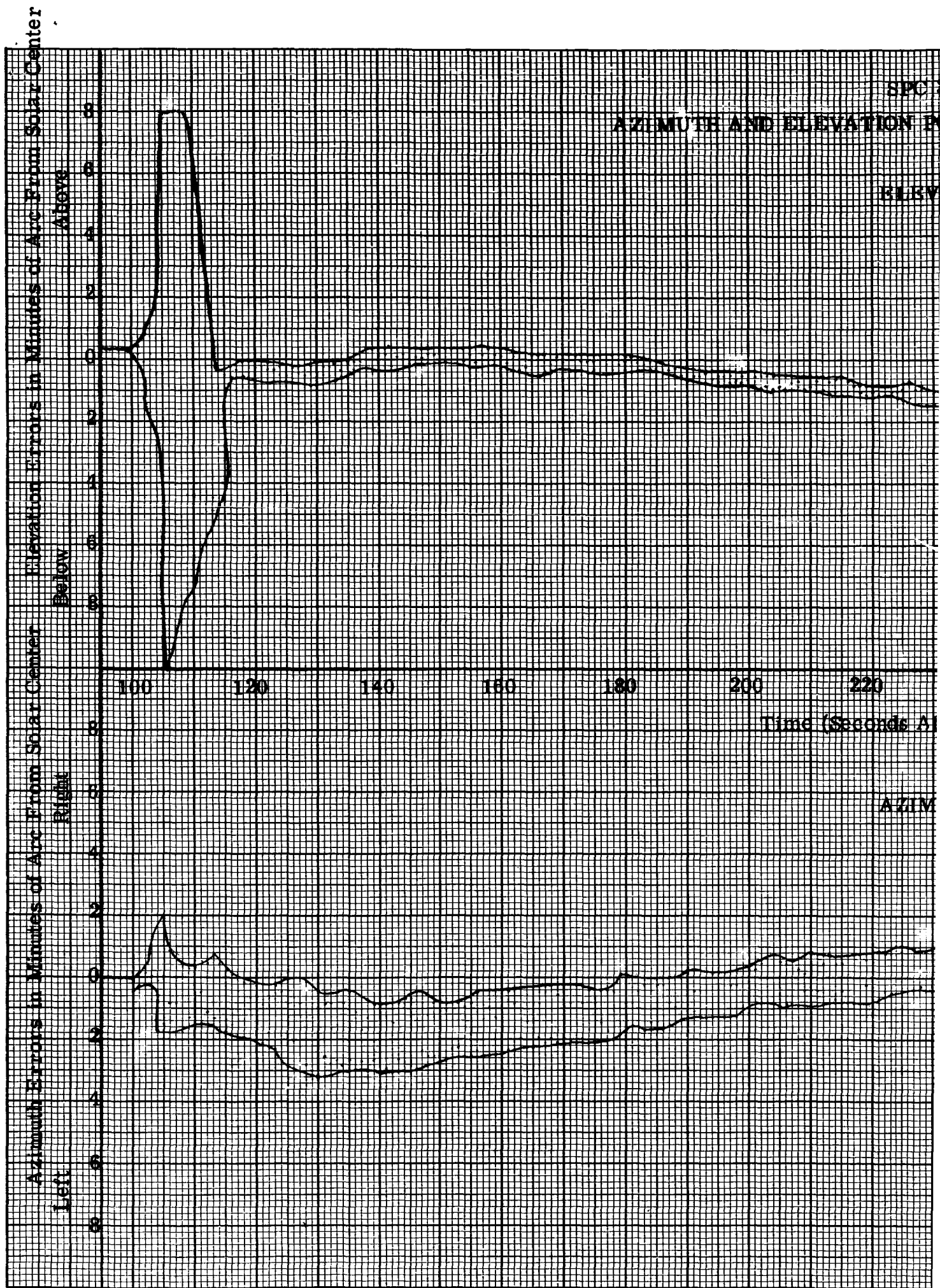
309B

N ANGLE VERSUS TIME



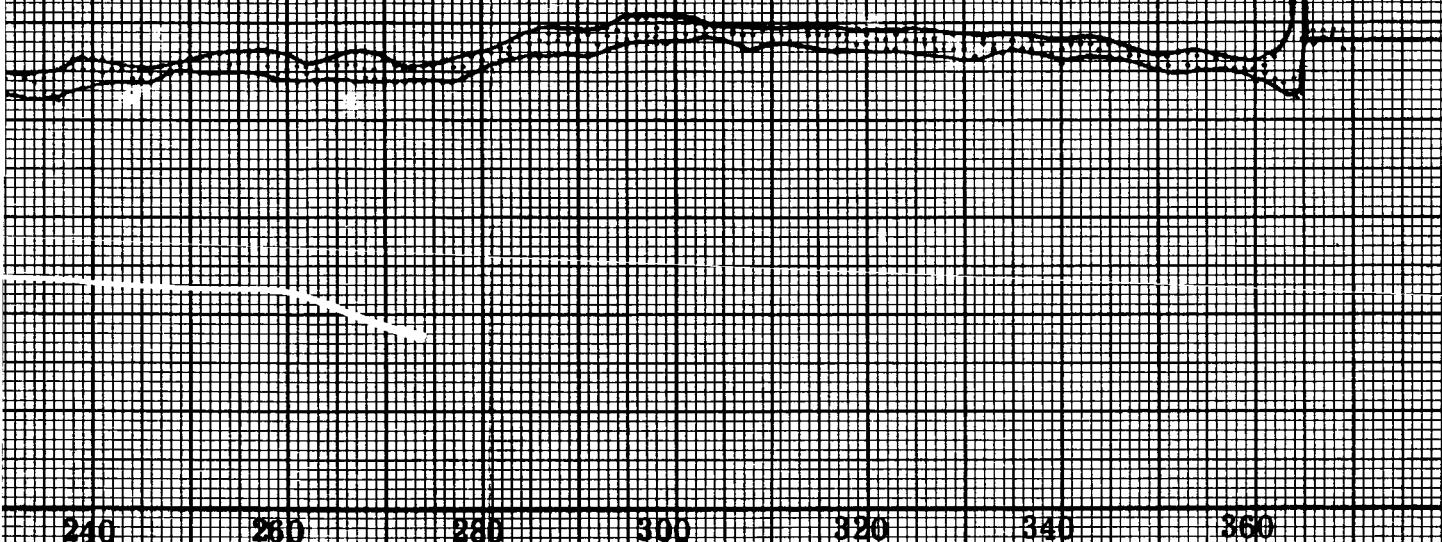
(er Launch)

Fig. 3-1 Instrument Elevation Angle versus Time



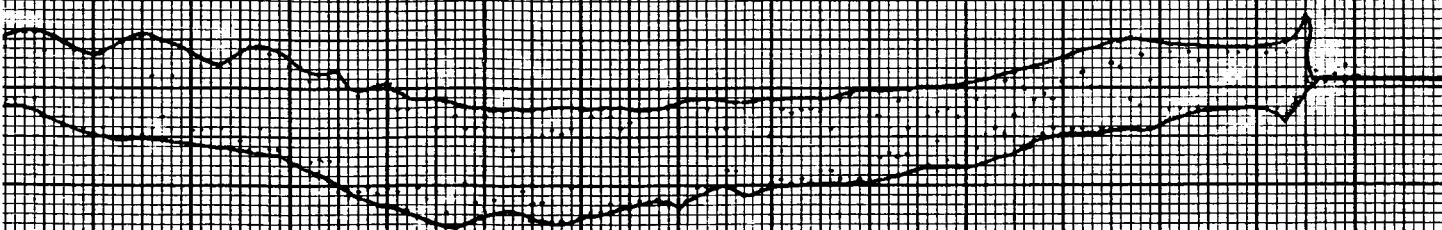
10013
POINTING ERRORS VERSUS TIME

ACTION



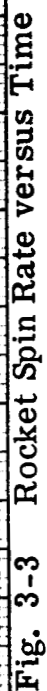
ter Launch)

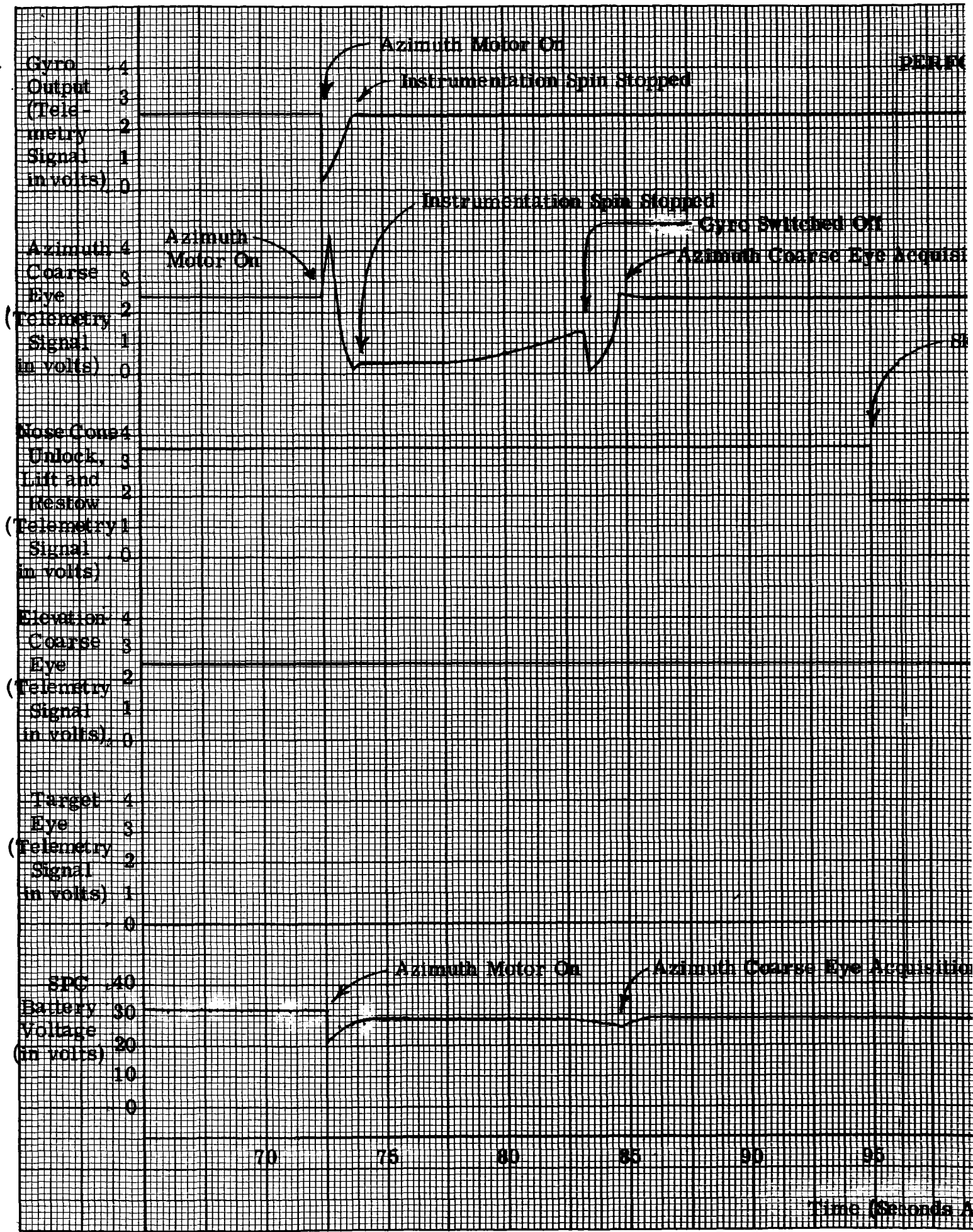
UTH



Note: These graphs show the maximum error points recorded each second.

Fig. 3-2 Azimuth and Elevation Pointing Errors versus Time





PERFORMANCE DATA VERSUS TIME

ion Complete

in Lift Command

Skin Lift Complete

Instrument Restow Command

Instrument Restowed

Skin Down

Skin Locked

Instrument Release

Elevation Fine Eye Acquisition

Start Instrument Restow

Instrument Restowed

Instrument On Target

Instrument Restowed

Start Elevation Coarse Eye Acquisition

Elevation Coarse Eye Acquisition Complete

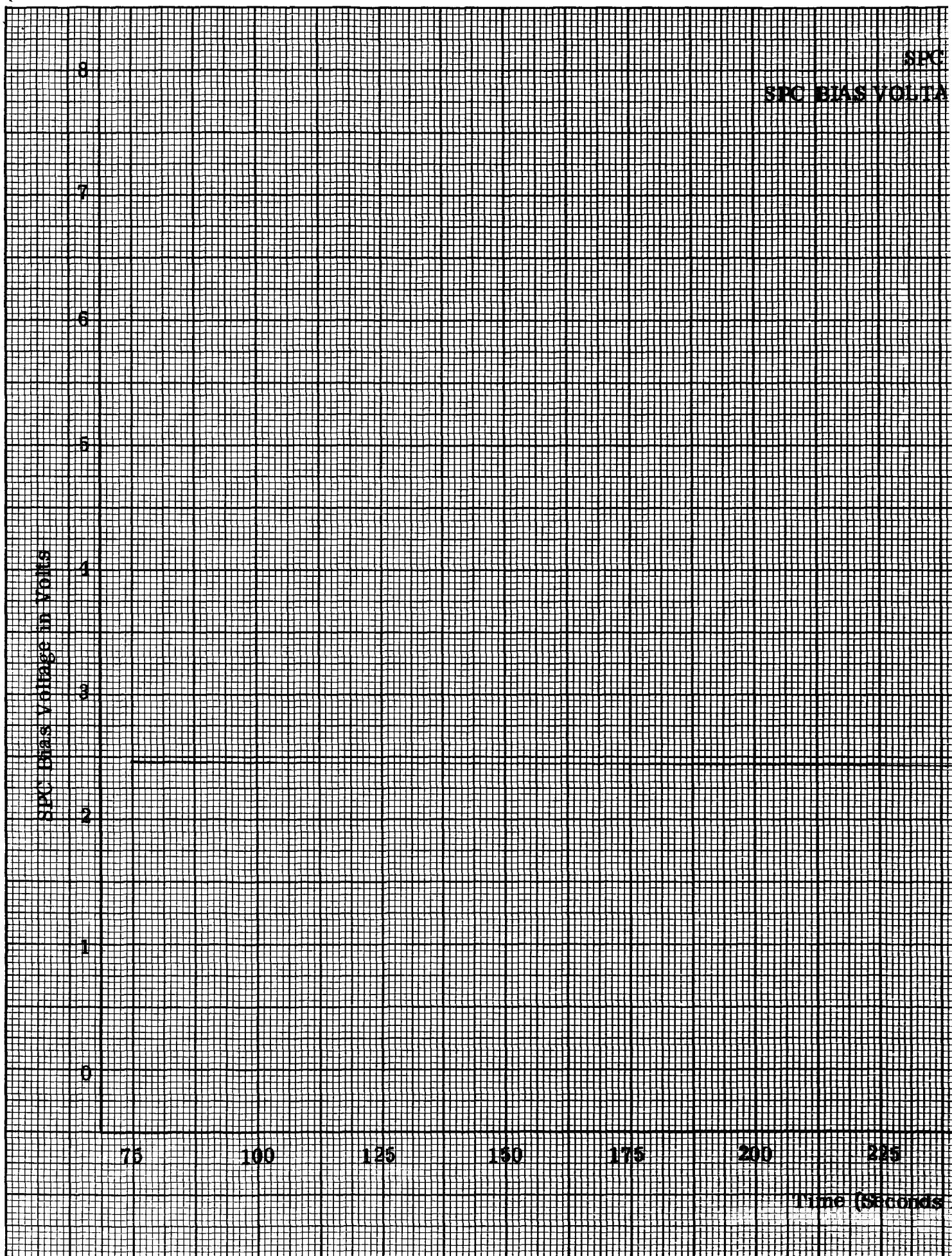
Start Restow Sequence

Skin Closure Complete

00 105 110 360 365 370 375

ter Launch)

Fig. 3-4 Performance Data versus Time



2000

Ball

VS VERSUS TIME

250

275

300

325

350

375

(After Launch)

Fig. 3-5 SPC Bias Voltage versus Time

3-10

NASA Accelerometer Output in Volts

8
7
6
5
4
3
2
1
0

Booster Burnout

4

8

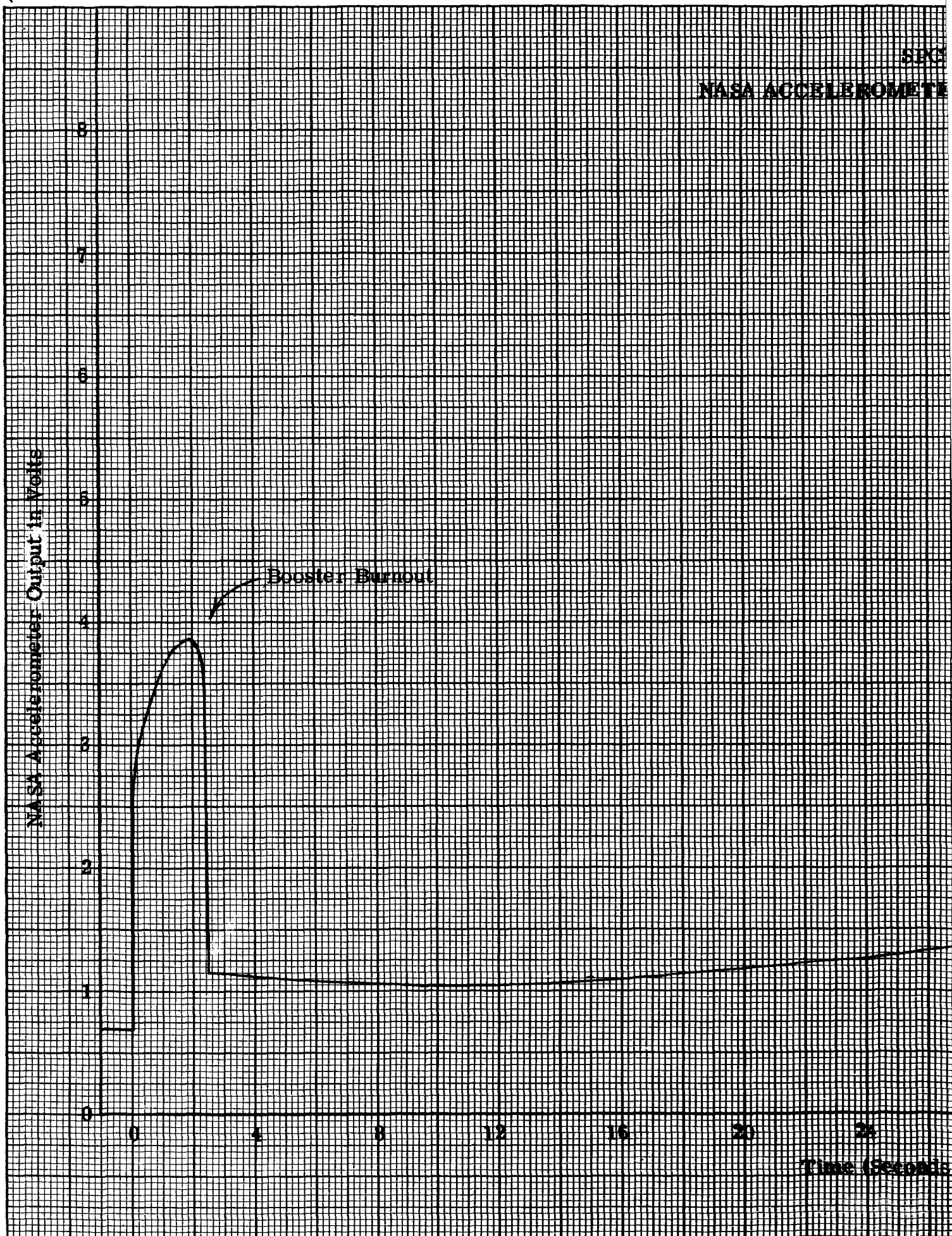
12

16

20

24

Time (Seconds)



309B

R OUTPUT VERSUS TIME

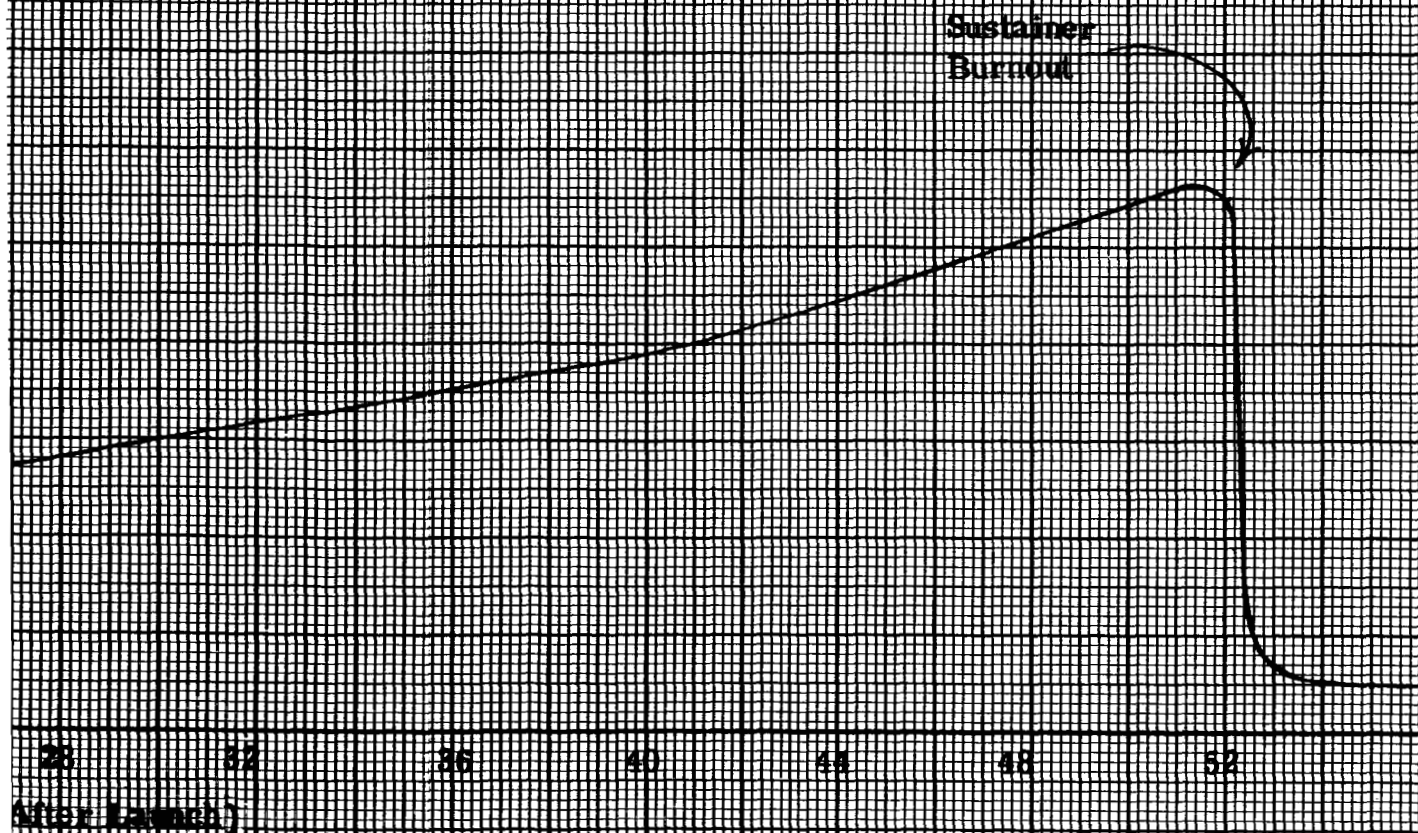
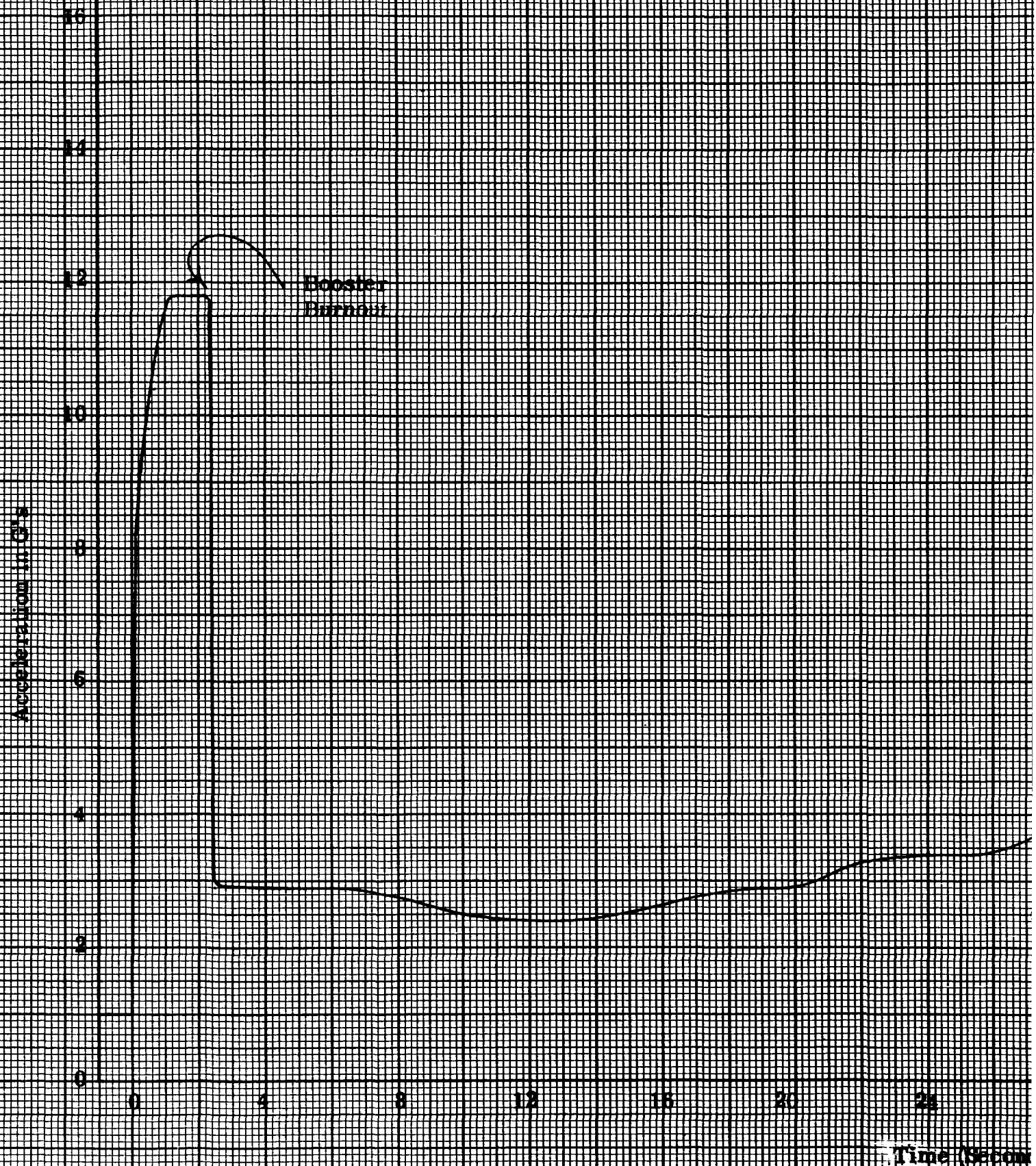
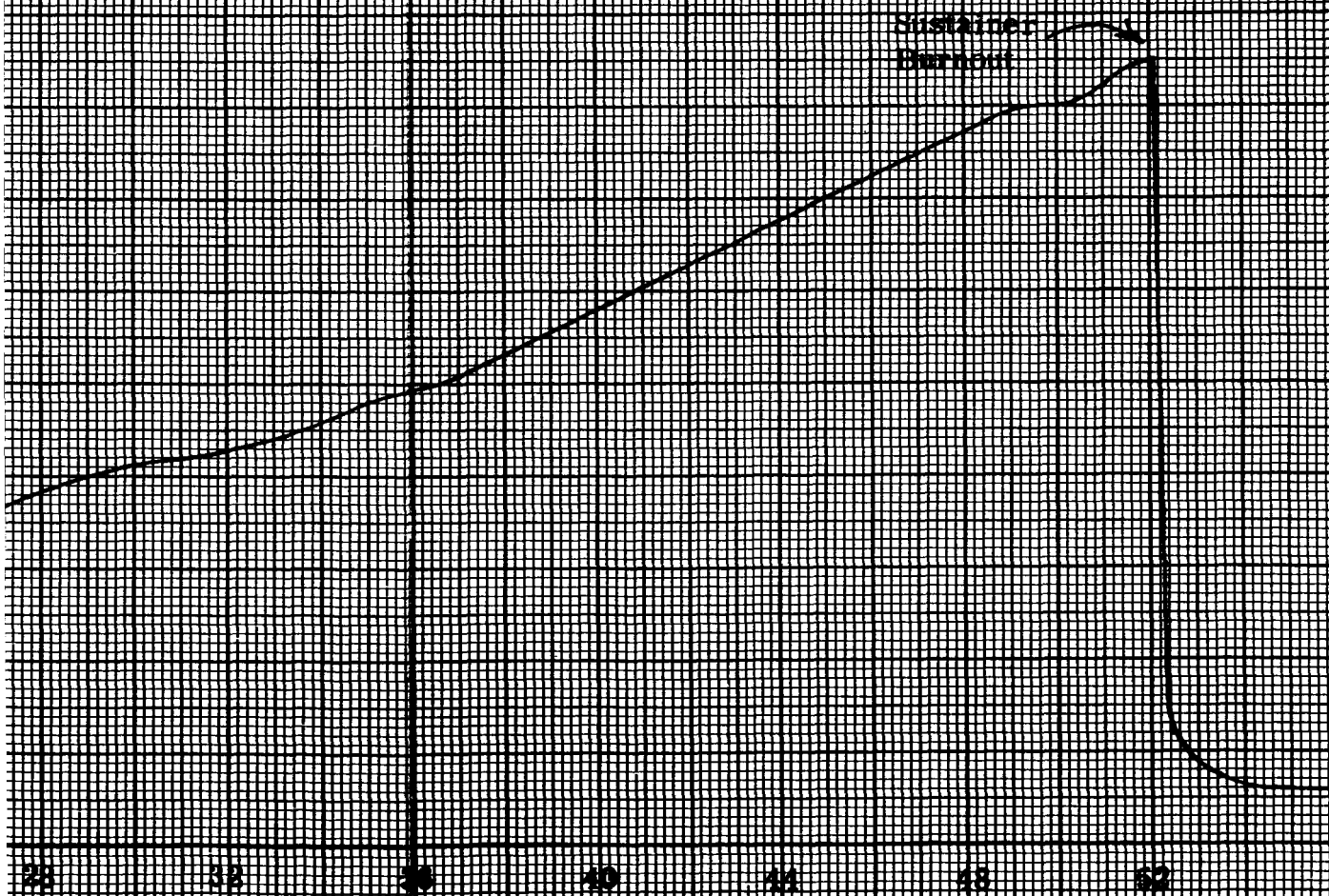


Fig. 3-6 NASA Accelerometer Output versus Time

BIAXIAL ACCELEROMETER



8
OUTPUT VERSUS TIME



(s After Launch)

Fig 3-7 Biasing Accelerometer Output versus Time

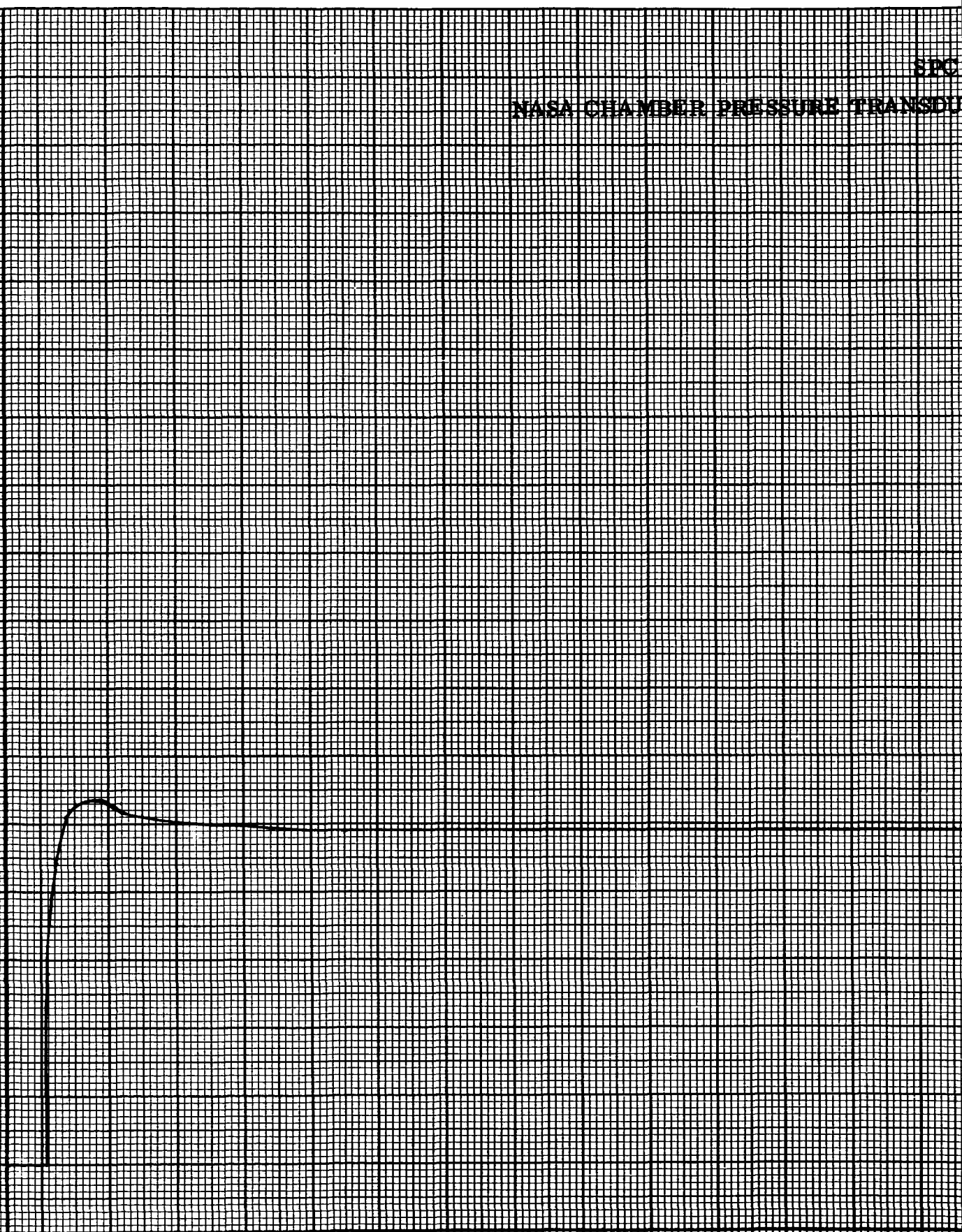
NASA CHAMBER PRESSURE TRANSDU

Chamber Pressure Transducer Output in Volts

8
7
6
5
4
3
2
1
0

0 4 8 12 16 20 24

Time (Seconds)



309B

CER OUTPUT VERSUS TIME

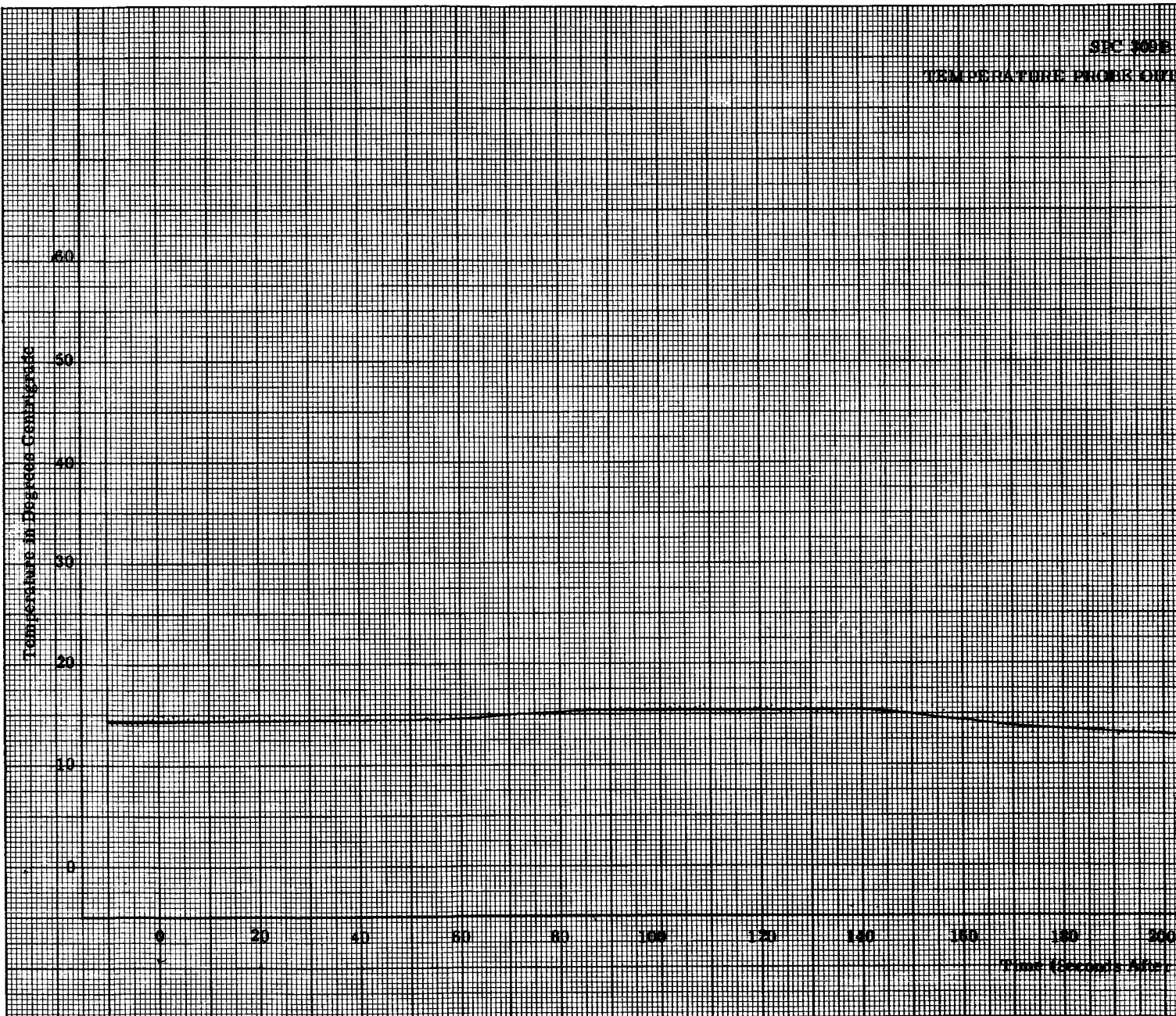


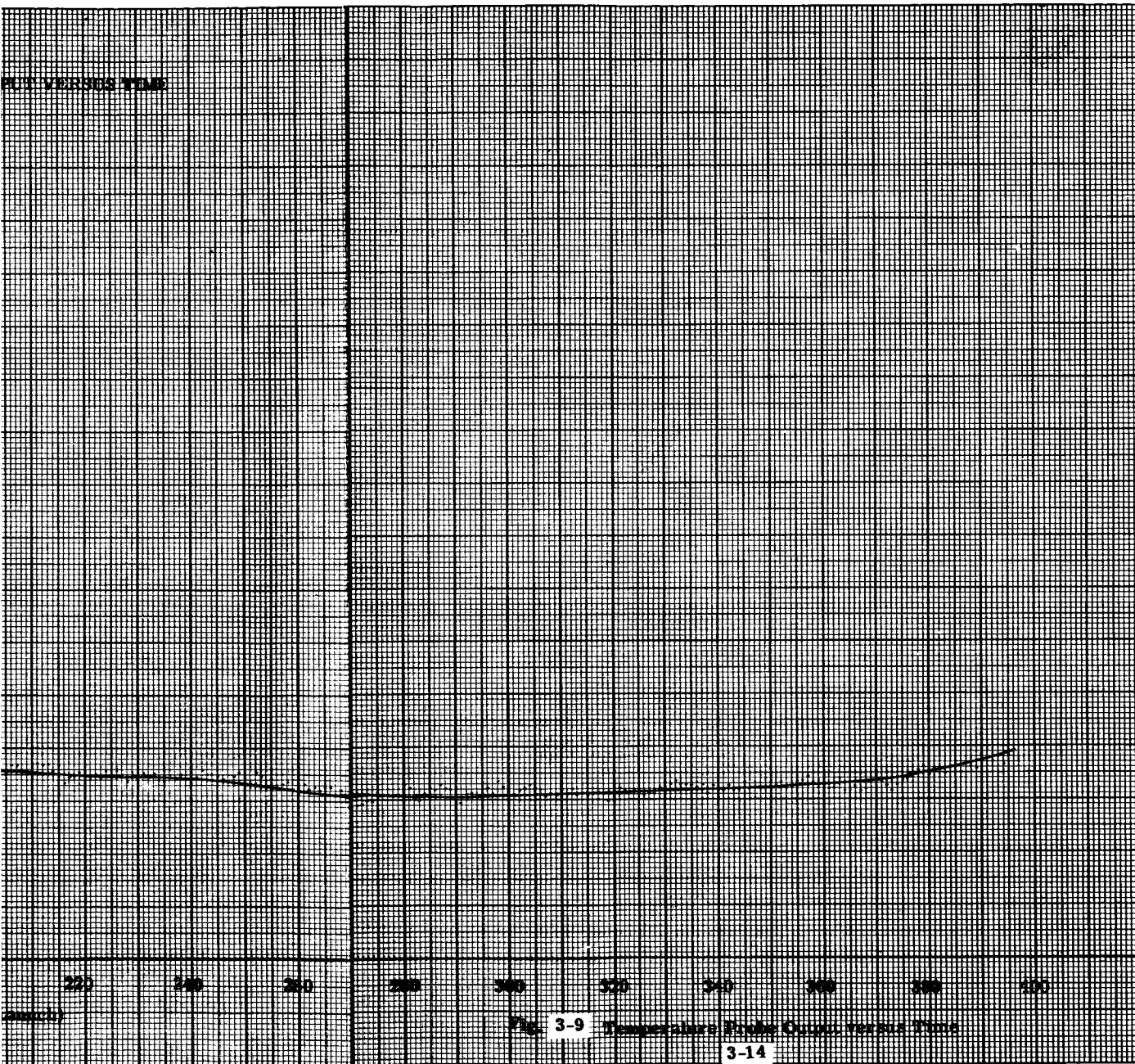
After Launch

Fig. 3-8 NASA Chamber Pressure Transducer Output versus Time

SIC 3033

TEMPERATURE PROCK OVI







Section 4

FLIGHT OF SPC 310A AND TEL 207

4.1 GENERAL

SPC 310A and TEL 207 were launched on NASA Aerobee 4.22US at 2:30 p. m. MST, on September 6, 1963.

Telemetry data monitored during the flight indicated both systems were functioning normally and evaluation of the flight telemetry record later confirmed this.

4.2 FLIGHT DATA

The following tabulated data compares the predicted flight performance with the actual flight performance.

<u>Occurrence</u>	<u>Predicted</u>	<u>Actual</u>
Zenith altitude	142 miles	135 miles
Spin rate before SPC acquisition	1.8 rps	1.8 rps
Spin rate after SPC acquisition	2.0 rps	2.0 rps
SPC servo operation initiated	T + 78 seconds	T + 80 seconds
SPC nose cone ejected	T + 111 seconds	T + 109 seconds
Instrument high voltage ON	T + 150 seconds	T + 150 seconds

The performance data listed above and the information that follows was reduced from the telemetry records recorded at ground stations Jig 44, Jig 36, and Jig 5. The following figures present information regarding pointing control and rocket performance.



Figure 4-1 is a plot of the vehicle spin rate versus time taken from Jig 36 and Jig 5 telemetry signal strength records. The spin rate was approximately 1.8 rps at burnout. The first functional operation of the SPC is to despin the payload. The transfer of energy from the payload to the vehicle during this operation increased the spin rate to approximately 2.2 rps.

Figure 4-2 is a plot of NASA accelerometer and chamber pressure telemetry voltage outputs versus time. BBRC was not furnished calibration data for these signals and no attempt was made to interpret the data.

Figure 4-3 is a plot of the SPC pointing errors versus time. The information is taken from commutated data and is presented as a point-to-point plot. During the period $T + 122$ seconds to $T + 427$ seconds, the maximum azimuth error was 4.4 arc minutes and the maximum elevation error was 1.0 arc minute. The average errors during this period were approximately 2 arc minutes in azimuth and 0.5 arc minutes in elevation.

Figure 4-4 is a plot of elevation position which represents the angle between the solar vector and the vehicle transverse axis. The vehicle precessional motion was approximately 18 degrees with a period of 69 seconds.

Figure 4-5 presents azimuth rate gyro, azimuth coarse detector, composite nose cone and instrument function, elevation coarse detector and elevation position as a function of time. These curves are all presented on the same sheet to illustrate the flight operational sequence. There is a break in the graph from $T + 136$ seconds to $T + 420$ seconds since there were no changes in these functions, except elevation position which is



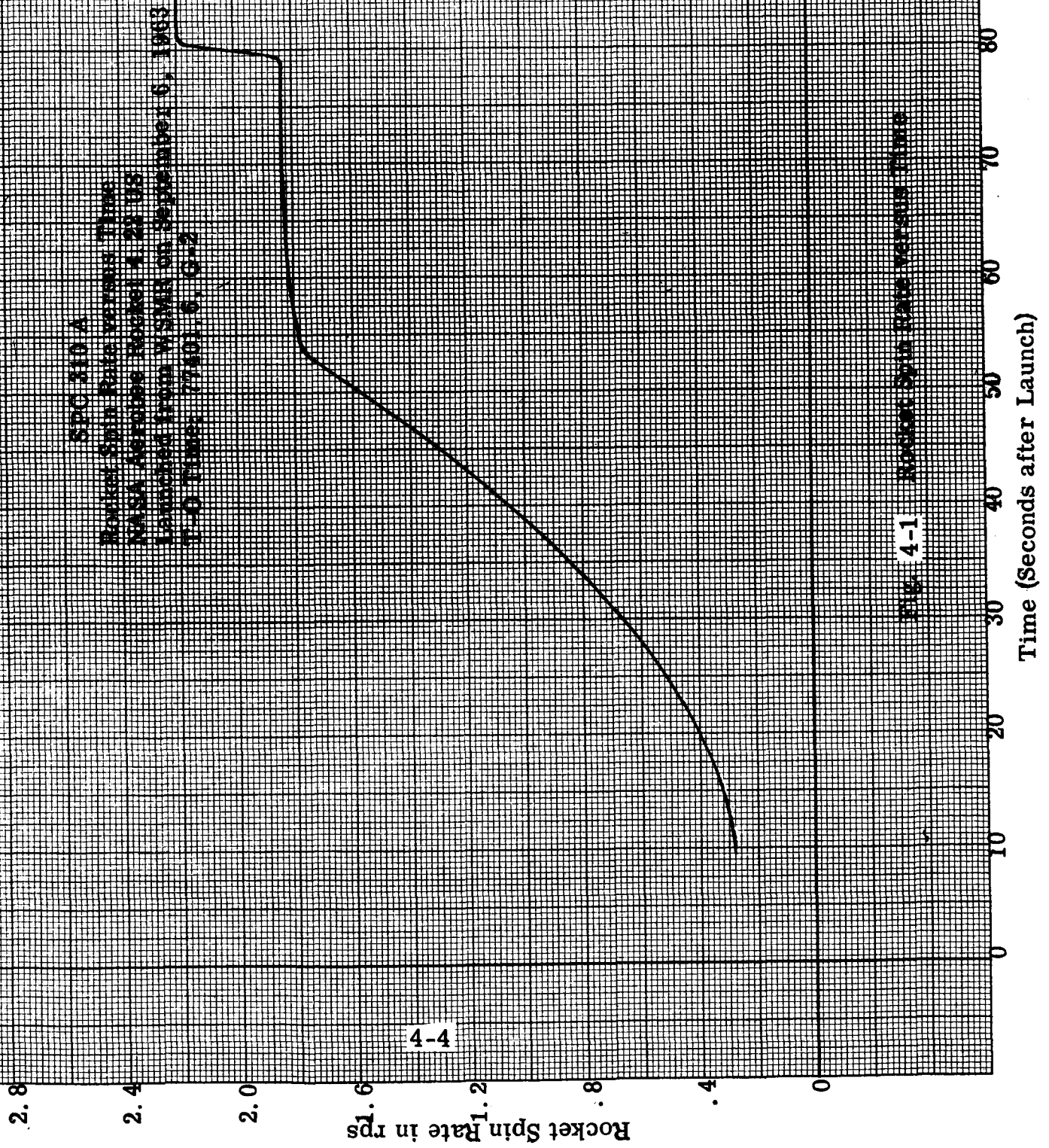
presented separately in Fig. 4-4, during that period. These curves present the effects of atmospheric loading during atmospheric re-entry.

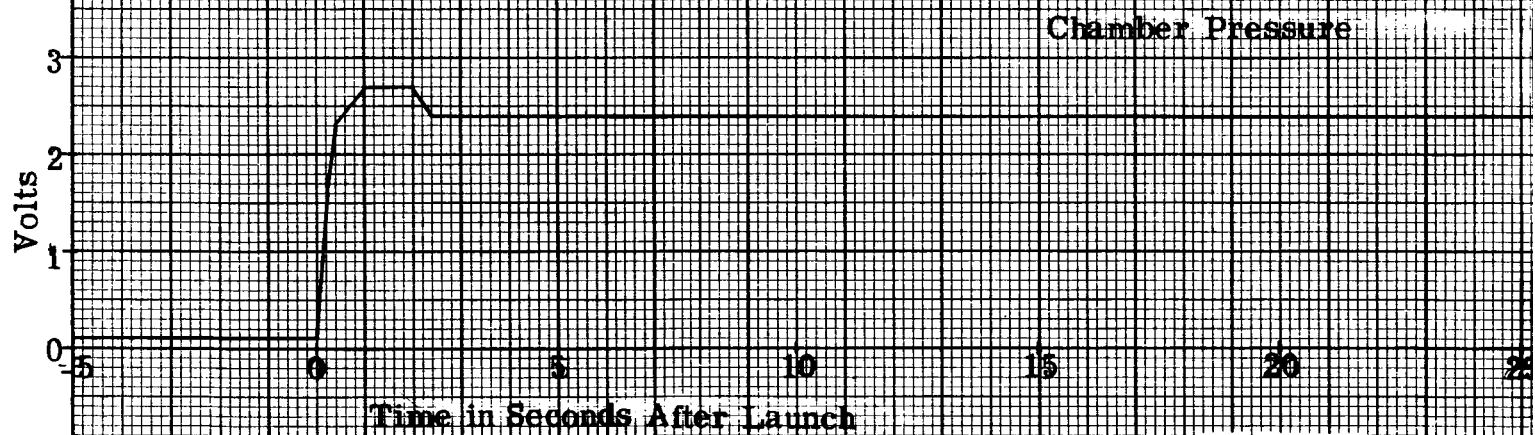
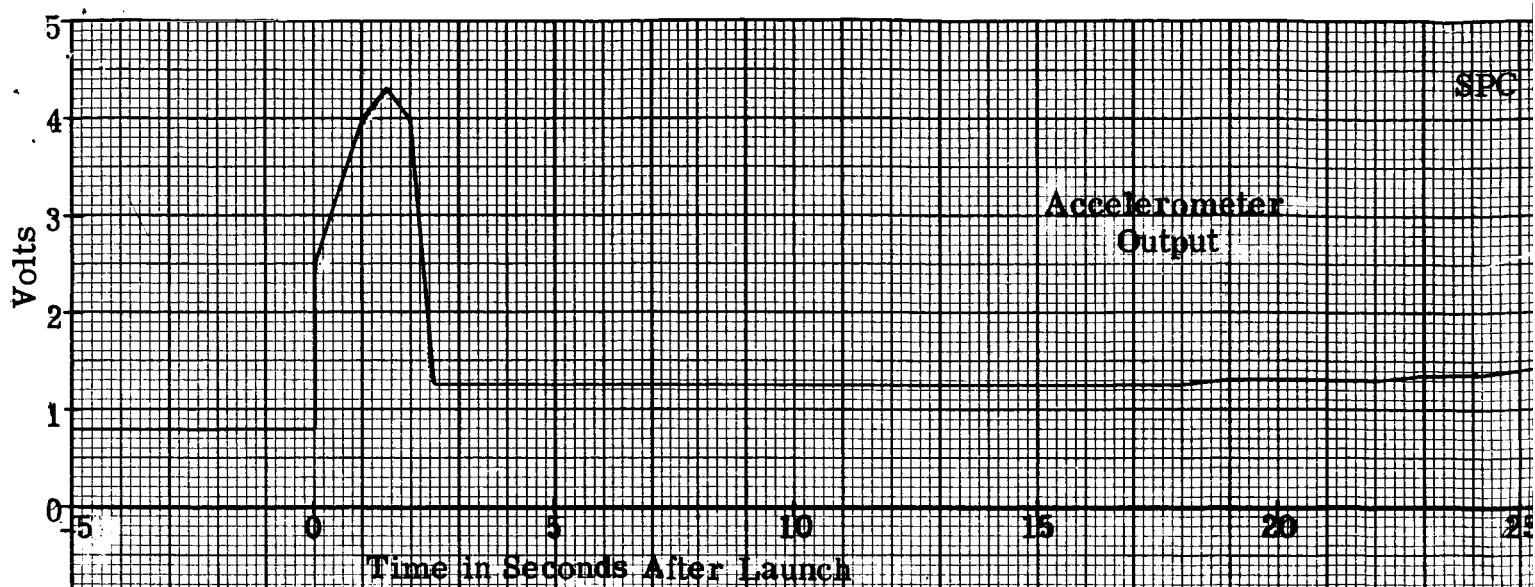
4.3 CONCLUSIONS

Flight performance of the pointing control telemetry system was excellent. An appreciable increase in pointing accuracy was accomplished by the pointing control modifications which permitted the ejection of the nose skin assembly prior to the pointing phase of the flight. Ejection of the nose cone changed the mass and structural resonance of the payload sufficiently to reduce the effects of forcing functions on the pointed instrument introduced by the spinning vehicle.

Atmospheric evacuation of the nose cone prior to launch was successfully achieved and flight results indicate that the procedure increased the safe sampling period possible with instruments utilizing open cathode photomultipliers and other high-voltage detectors which must be exposed to low pressure environments. In addition to corona protection this procedure provides a reduction in environmental contamination by allowing primary outgassing of the experiment prior to launch.

Information received from the Harvard College Observatory indicates that data acquisition was very good and that the performance of the pointing control and telemetry system was well within the requirements of the experiment.



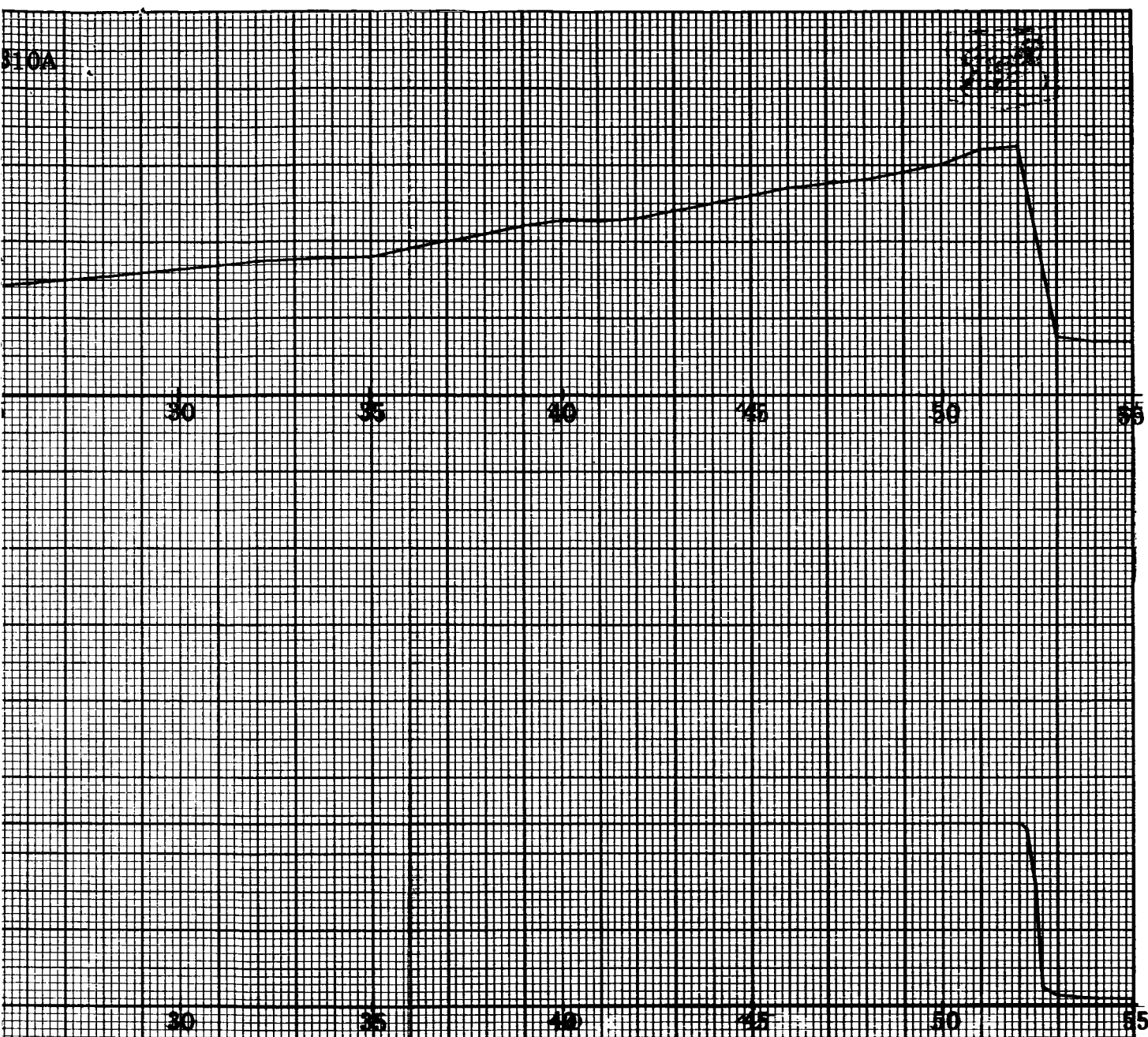


SPC 810A
Accelerometer and Chamber Pressure Transducer

NASA Aerobee Rocket 4.22 US

Launched from WSMR on Sept

T-O Time: 77401.6 G-2



Voltages Vs. Time

ember 6, 1968

Fig. 4-2 Accelerometer and Chamber Pressure Transducer Voltages vs. Time

SXC 31

Elevation and Azimuth

Elevat

Azimu

Error (Minutes of Arc From Center of Sun)
Above
Below

Error (Minutes of Arc From Center of Sun)
Left
Right

Time (Seconds After)



0A

Error Vs. Time

Ion

128 132 136 140 144 148 152 156

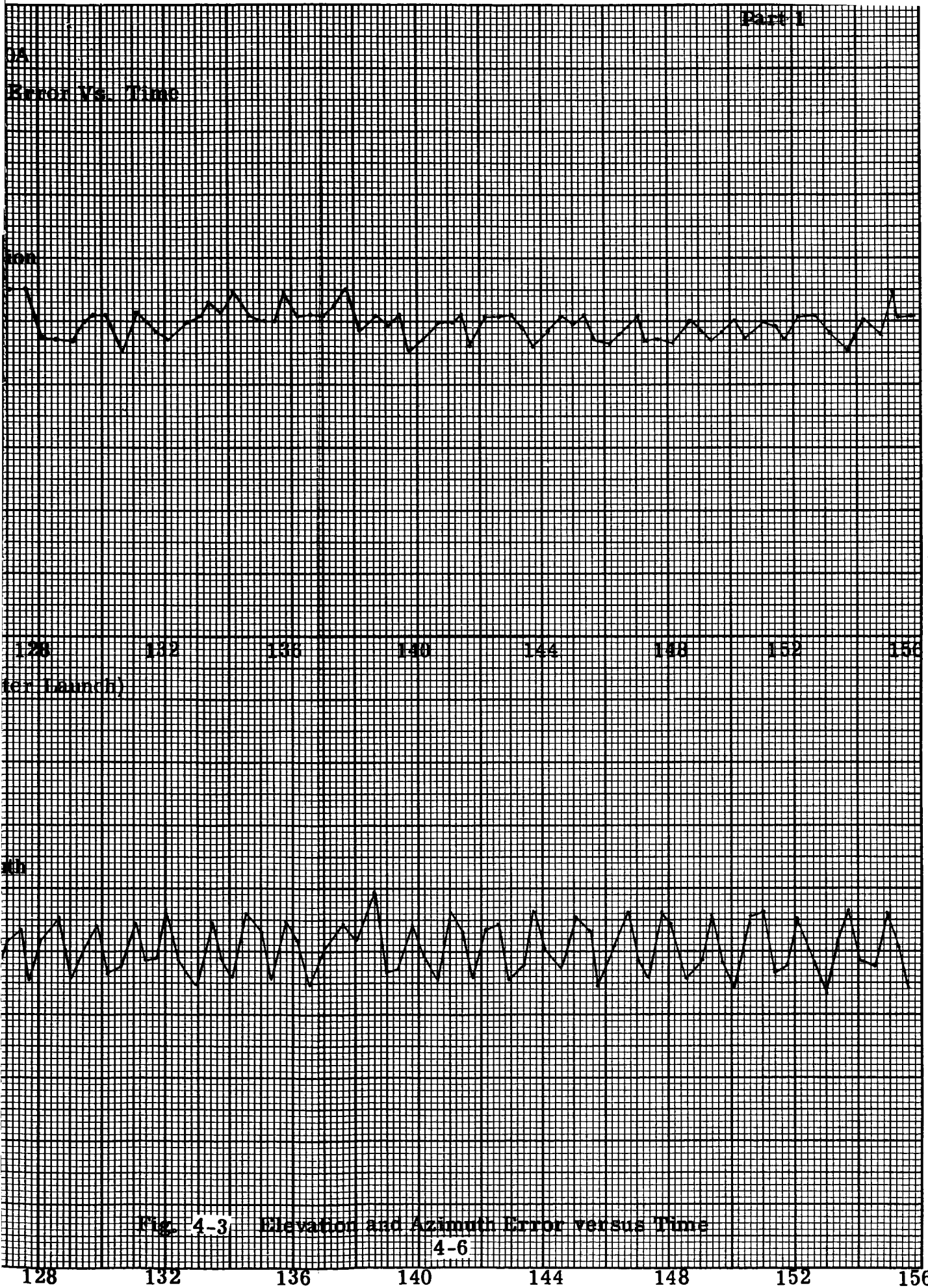
(for launch)

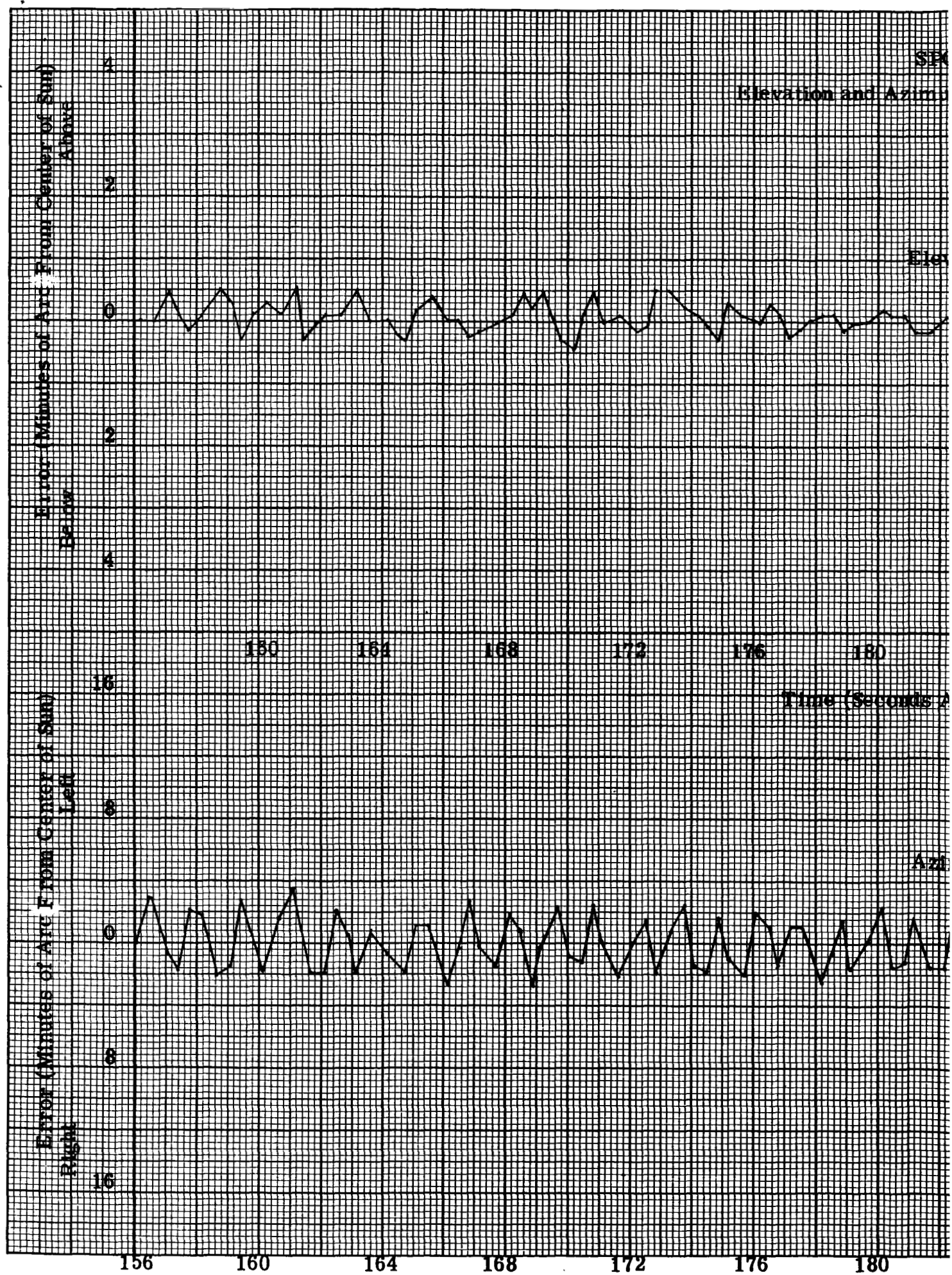
4b

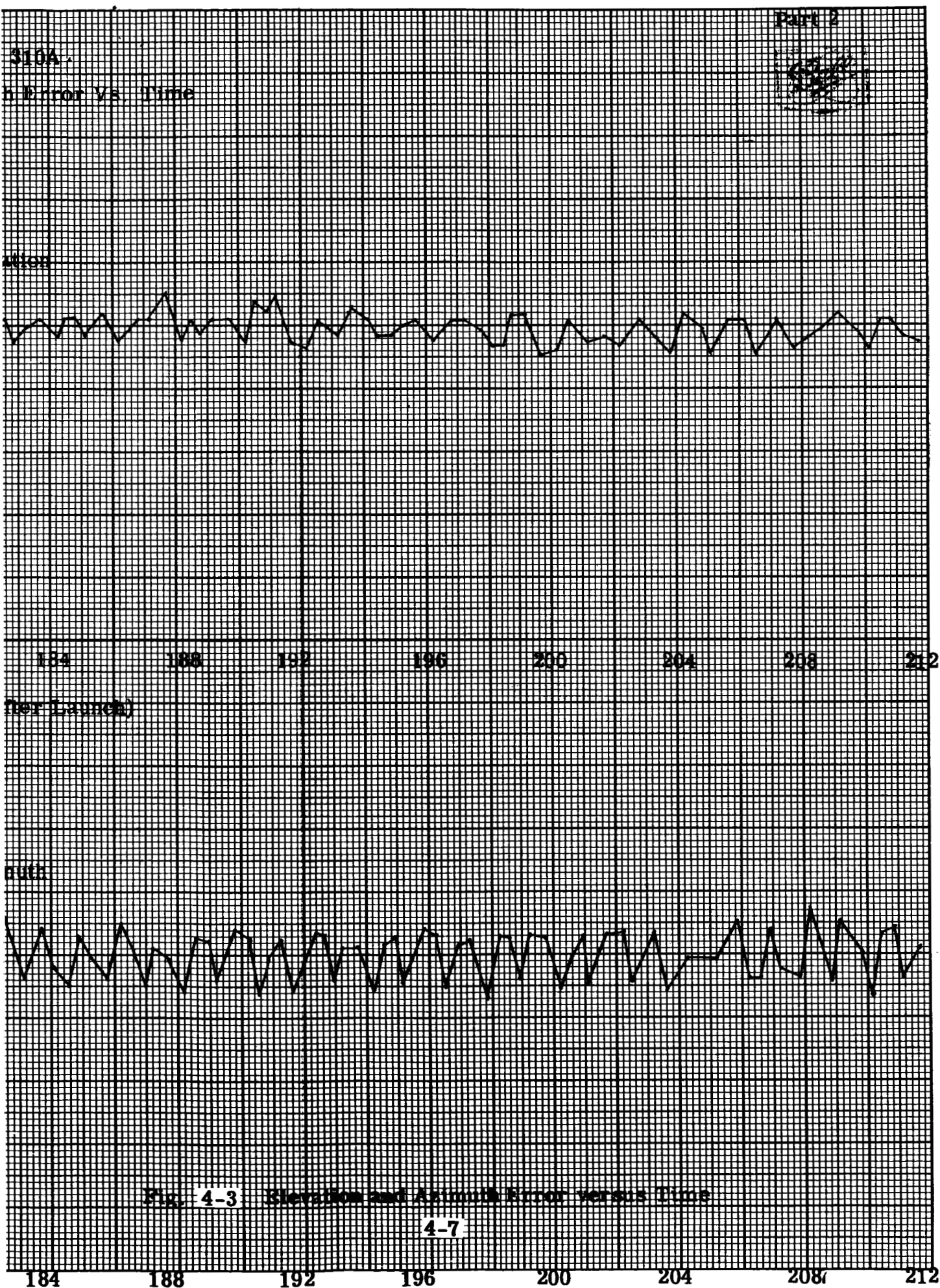
Fig. 4-3 Elevation and Azimuth Error versus Time

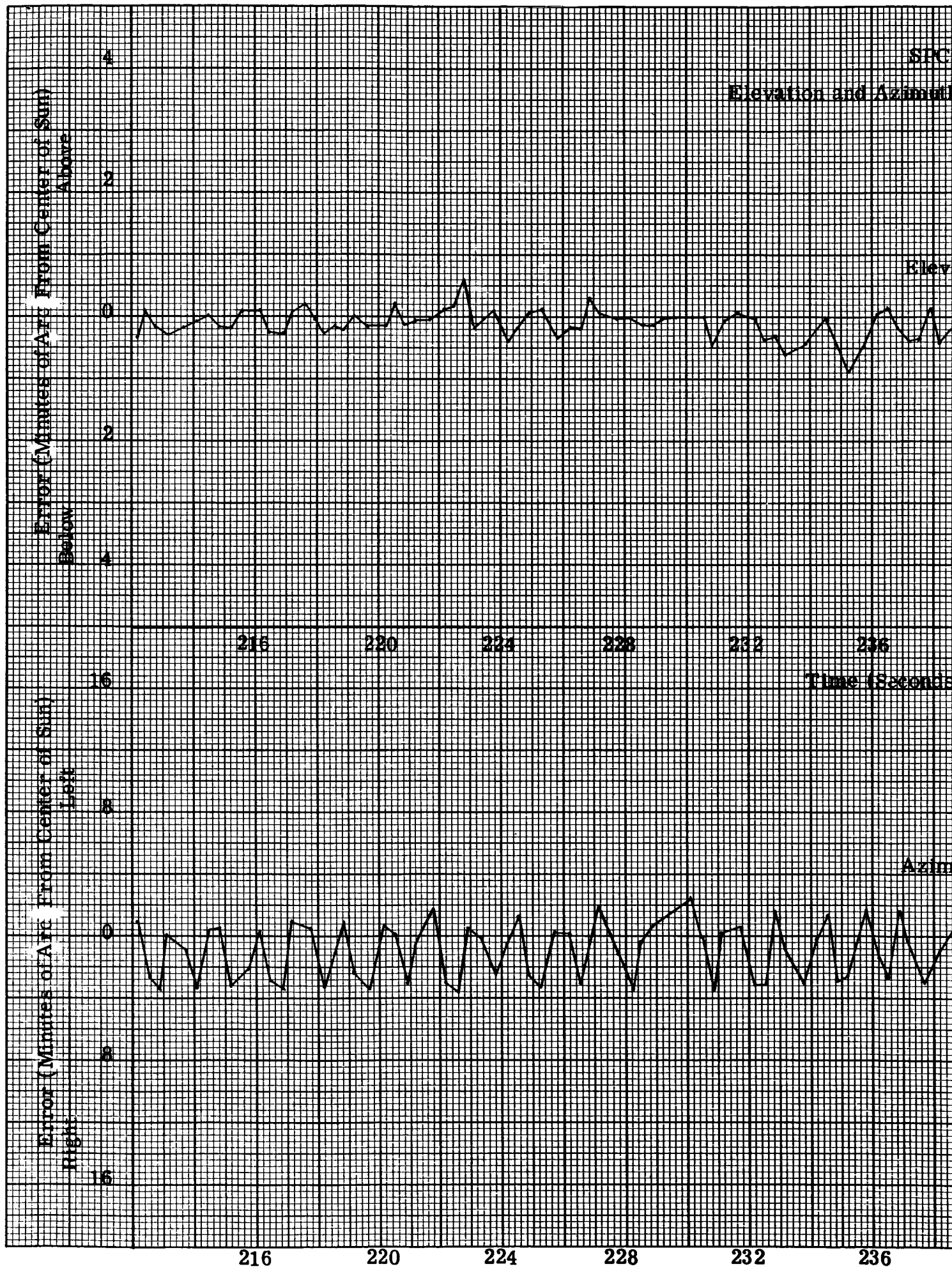
4-6

128 132 136 140 144 148 152 156









310A

Error Vs. Time

Elevation

240 244 248 252 256 260 264 268

After Launch)

Azimuth

Fig. 4-3 Elevation and Azimuth Error versus Time

4-8

240

244

248

252

256

260

264

268

SPC

Elevation and Azimuth

Elev

Azim

Error (Minutes of Arc From Center of Sun)

Above

Below

Error (Minutes of Arc From Center of Sun)

Left

Right

Time (Seconds AT

268

272

276

280

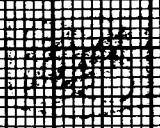
284

288

292

S10A

Error Vs. Time



ation



296 300 304 308 312 316 320 324

or Launch)

1015

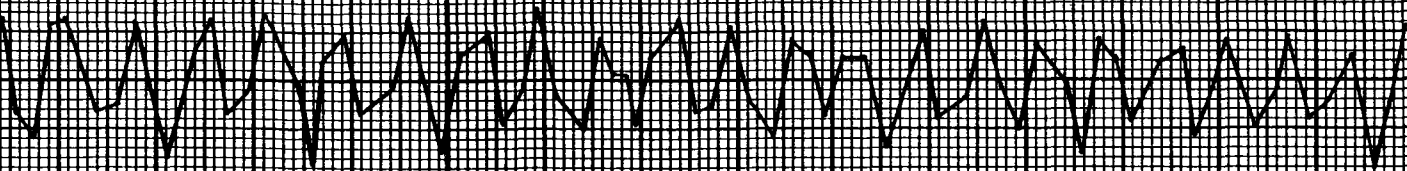
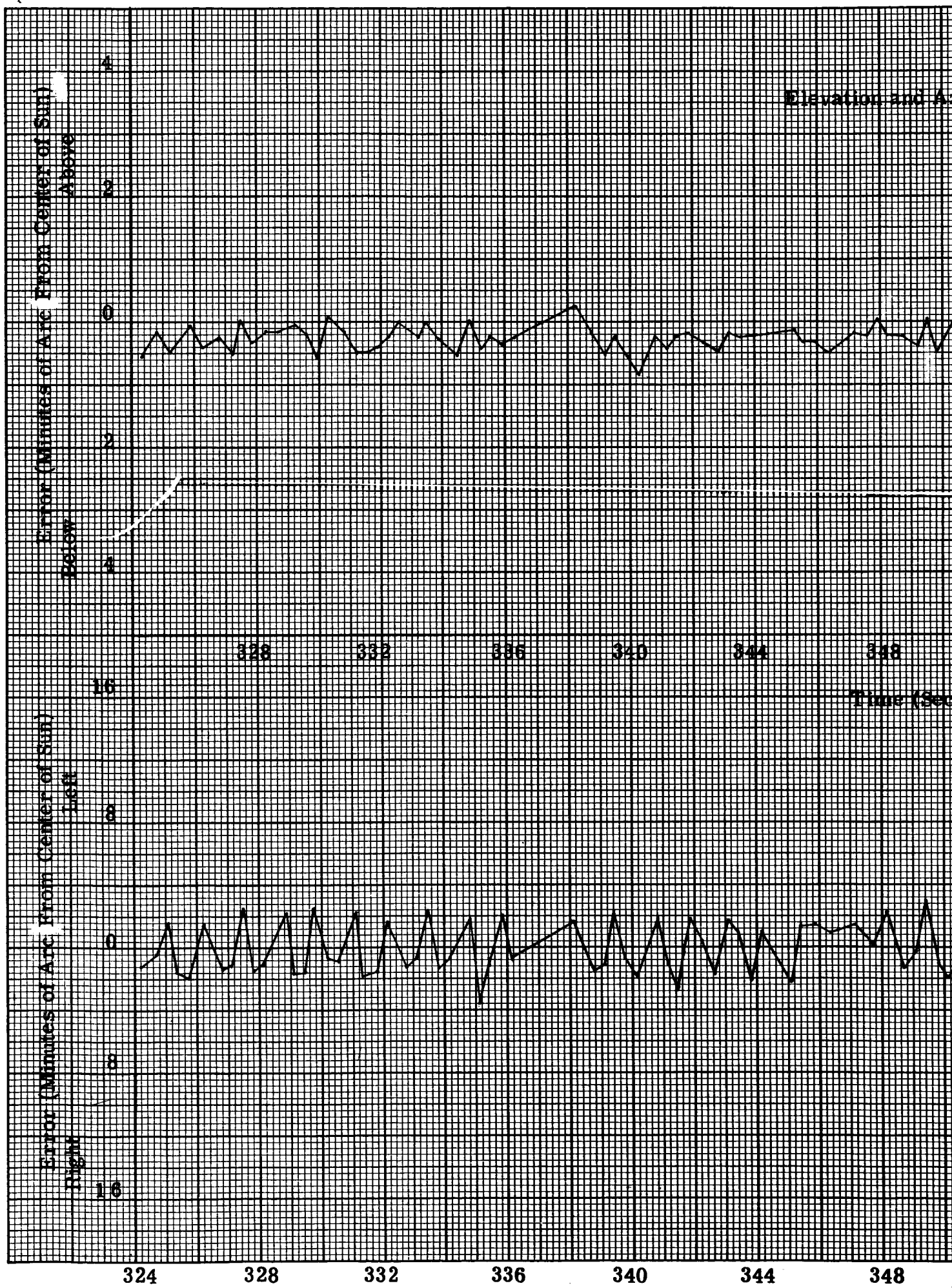


Fig. 4-3 Elevation and Azimuth Error versus Time

4-9

296 300 304 308 312 316 320 324



SPC 3104

Part 5

Azimuth Error Vs. Time

Elevation

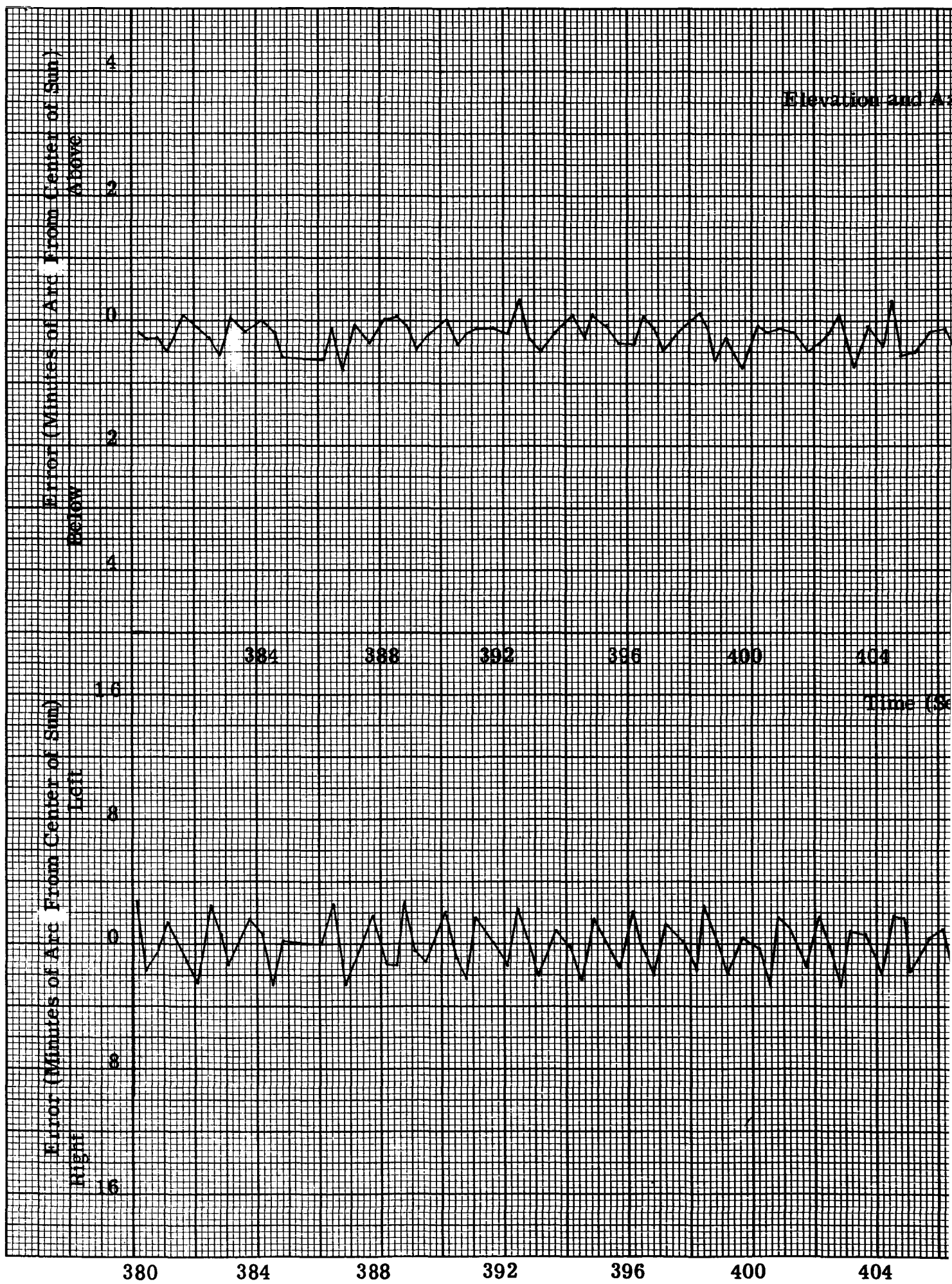
352 356 360 364 368 372 376 380
Seconds After Launch

Azimuth

Fig. 4-3 Elevation and Azimuth Error versus Time

4-10

352 356 360 364 368 372 376 380



SPC 310A

Launch Error Vs. Time

Elevation

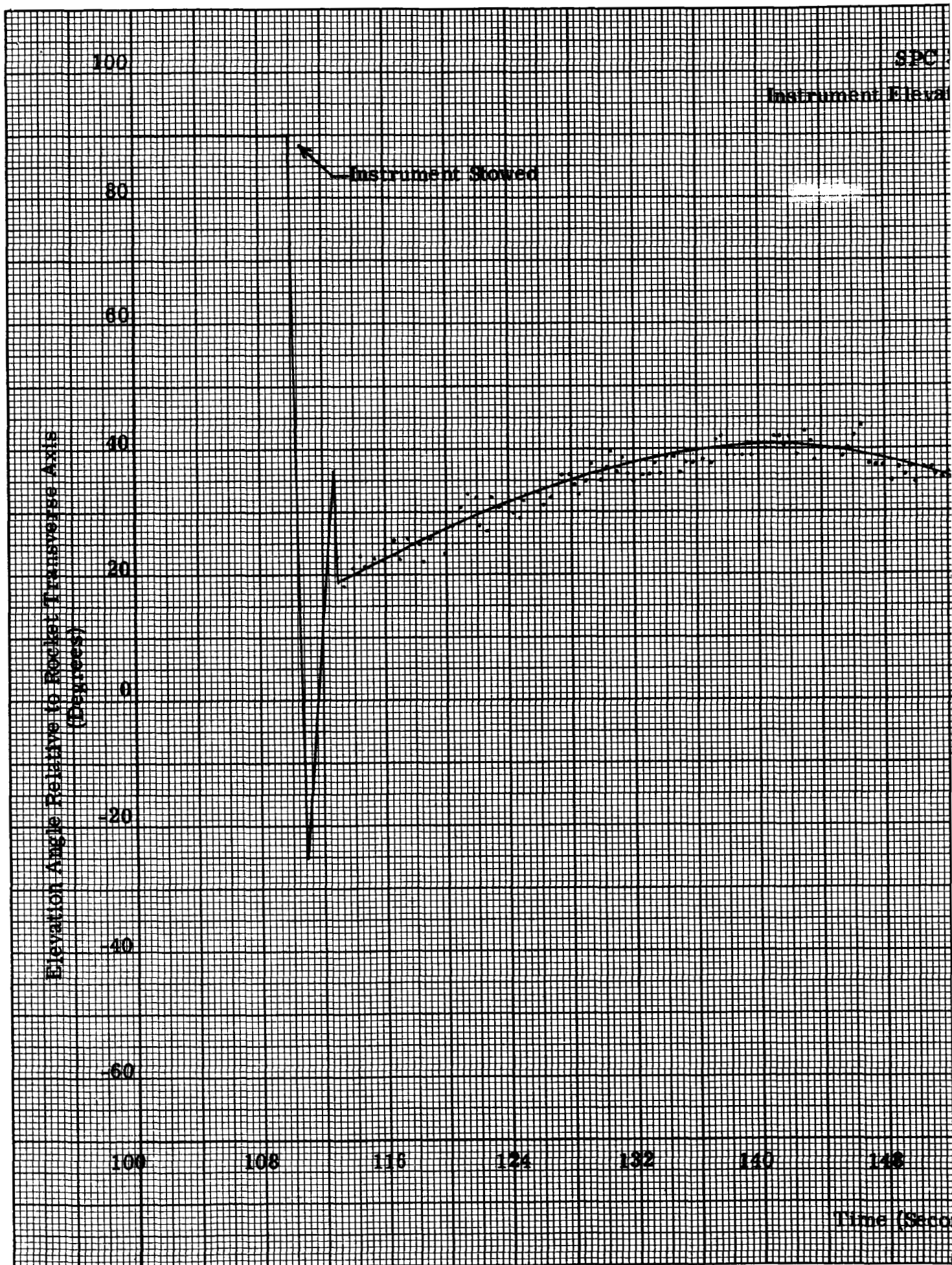
408 412 416 420 424 428 432 436

conds After Launch)

Azimuth

Fig. 4-3: Elevation and Azimuth Error versus Time
4-11

408 412 416 420 424 428 432 436



gle Vs. Time

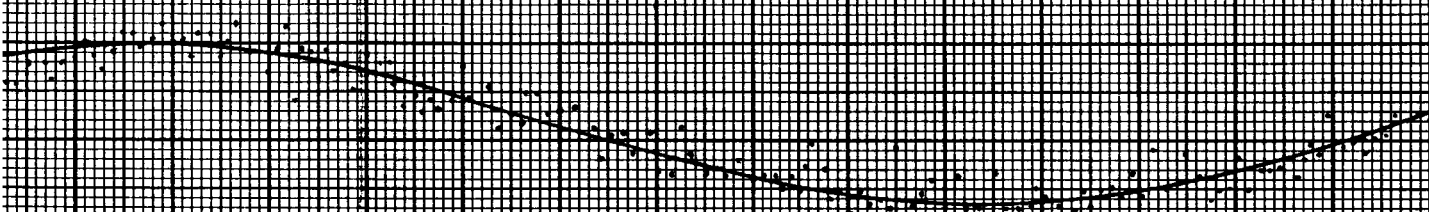


Fig. 4-4 Instrument Elevation Angle versus Time

4-13

276

284

292

300

308

316

324

332

(Launch)

Elevation Angle Relative to Rocket Transverse Axis
(Degrees)

100

80

60

40

20

0

-20

-40

-60

212

220

228

236

244

252

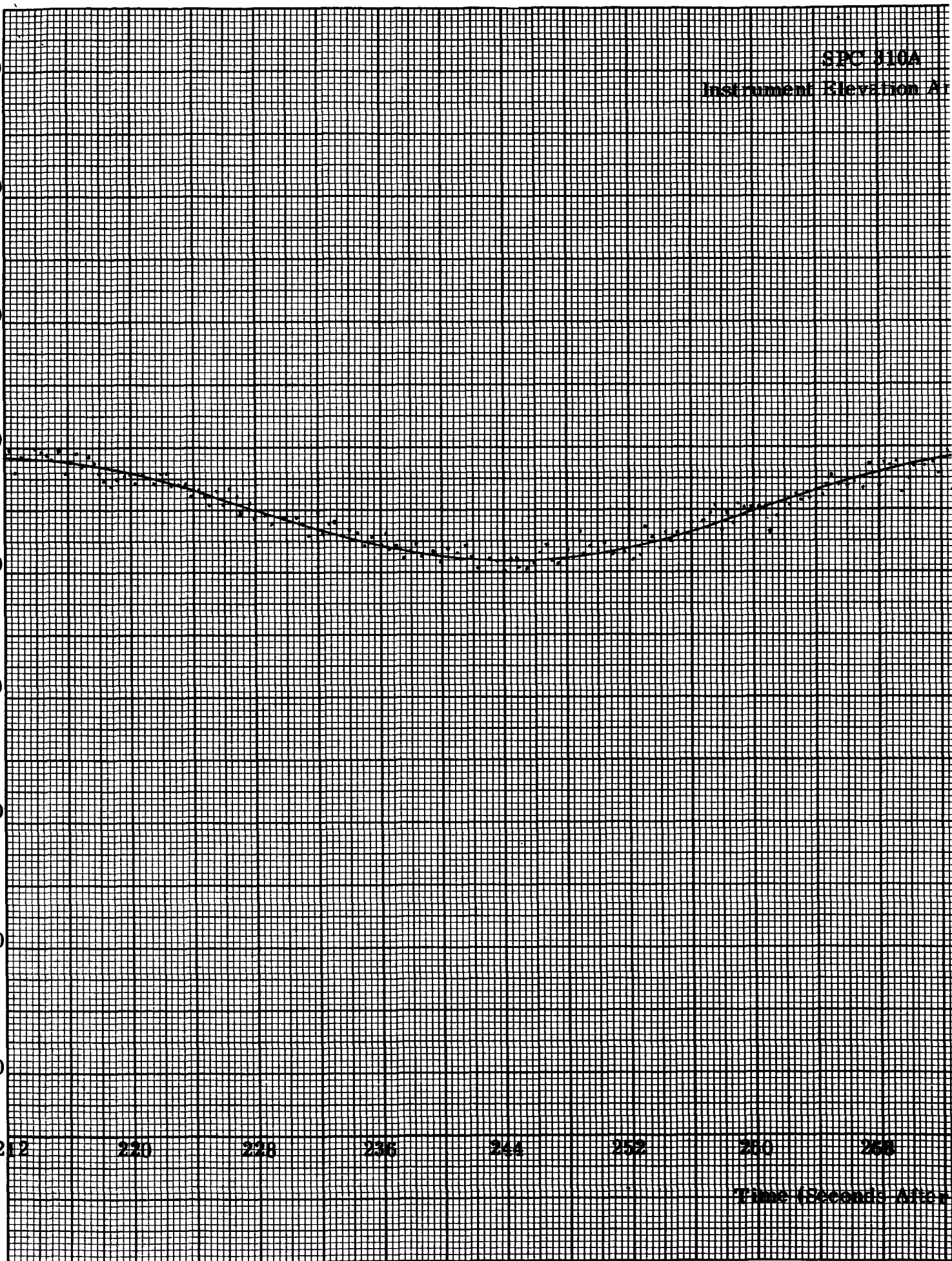
260

268

Time (Seconds After)

SFC 310A

Instrument Elevation At



110A

ion Angle Vs. Time

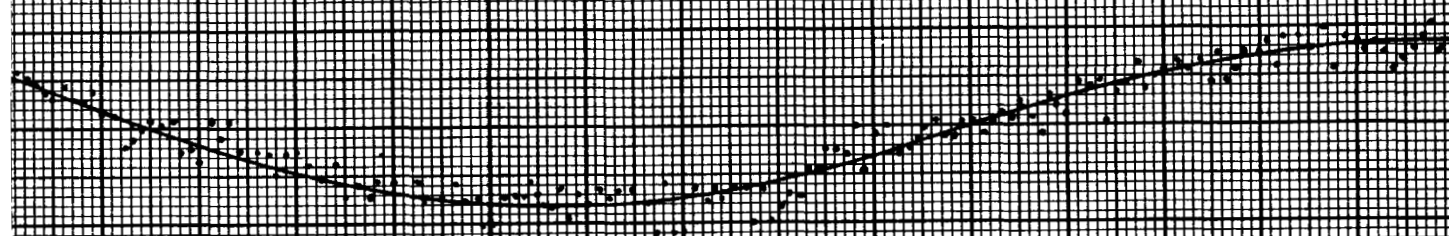


Fig. 4-4 Instrument Elevation Angle versus Time

4-12

156 164 172 180 188 196 204 212

ids After Launch)

Elevation Angle Relative to Rocket Transverse Axis
(Degrees)

80
60
40
20
0
-20
-40
-60

340

348

356

364

372

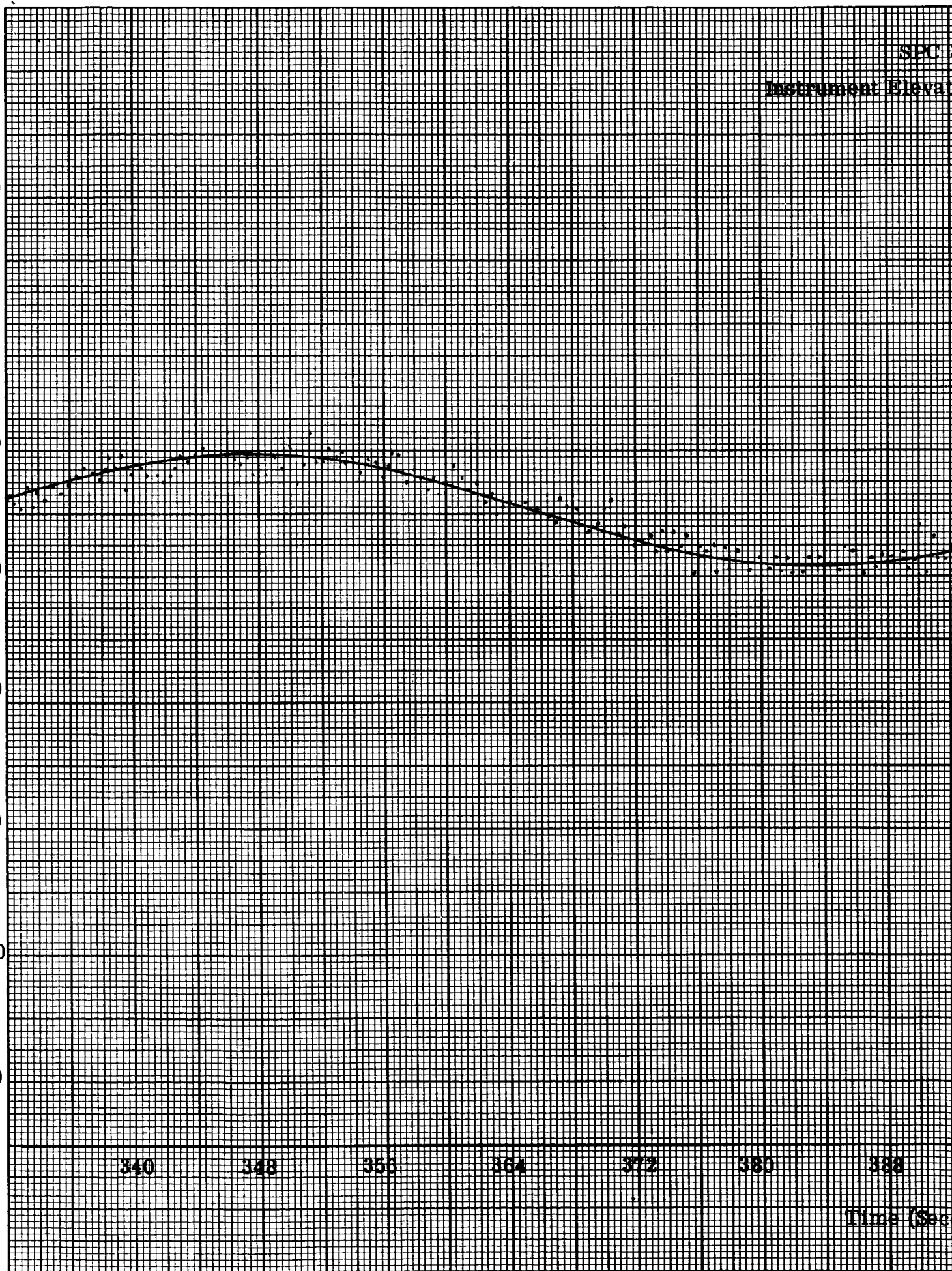
380

388

Time (Sec)

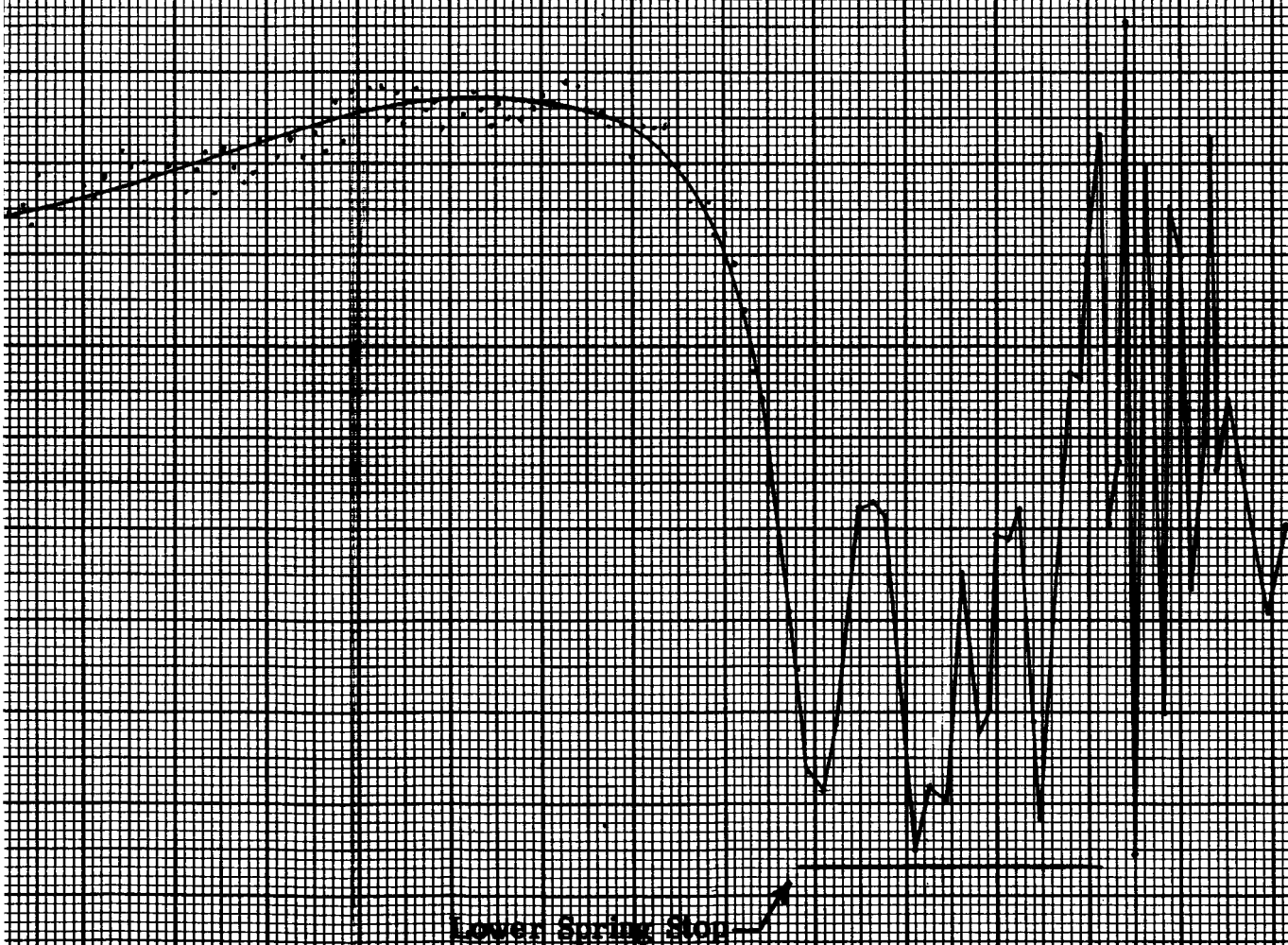
SPC 1

Instrument Elevat



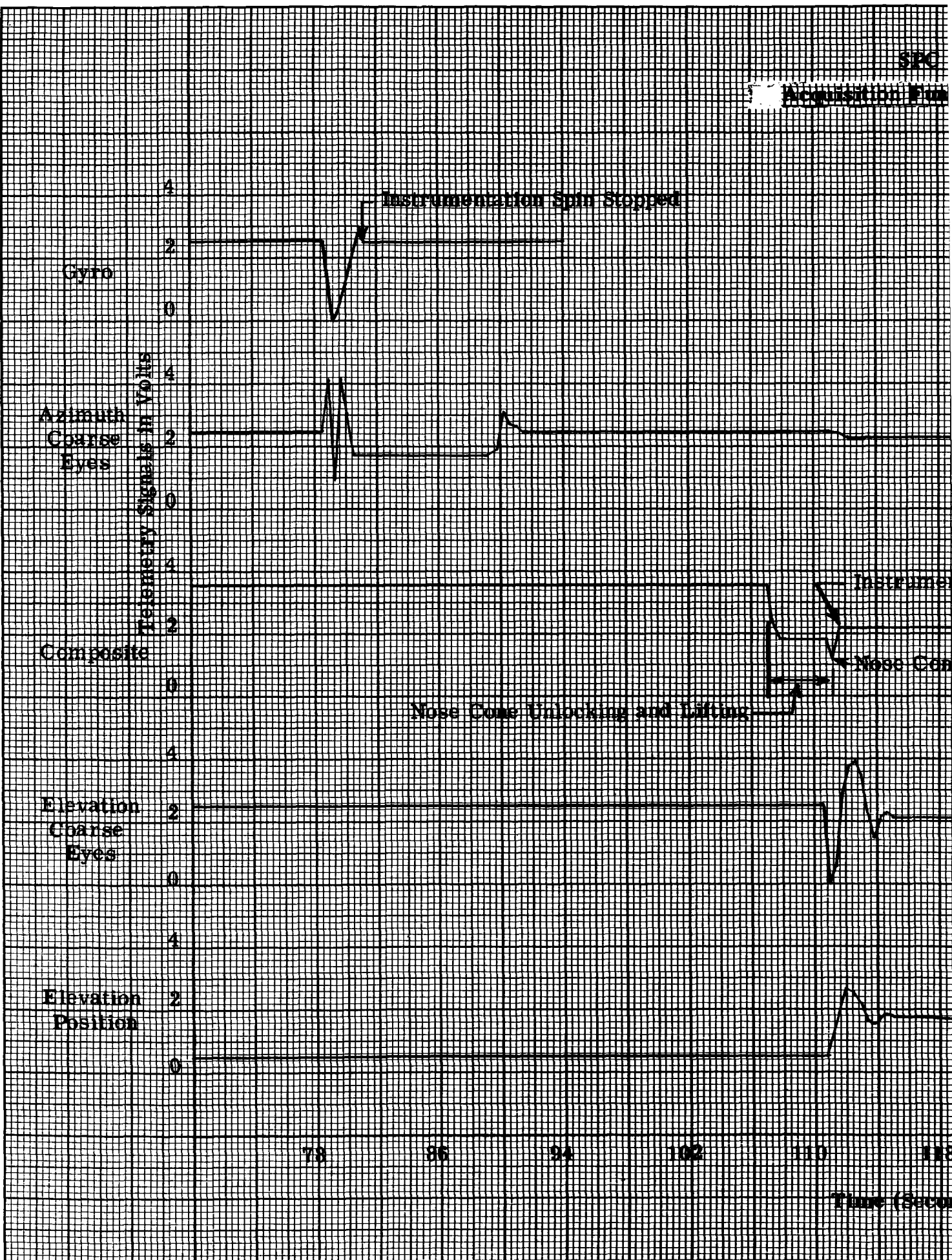
10A

on Angle Vs. Time



nds After Launch)

Fig. 4-4 Instrument Elevation Angle versus Time



310A

Functions Vs. Time

if Unlocked

e Ejected

ms After Launch

Fig. 4-5 Acquisition Functions versus Time



Section 5
FLIGHT OF SPC 309B AND TEL 311

5.1 GENERAL

SPC 309B and TEL 311 were launched on NASA Aerobee 4.116GS at 12:30 p. m. MST, October 30, 1964.

Telemetry records monitored during flight indicated that SPC 309B and TEL 311 operated normally, but recovery could not be immediately effected.

The prime scientific experiment on this flight was the prototype model of the NASA-GSFC pointed instrument to be flown on OSO-C. This instrument, developed at the NASA Goddard Space Flight Center under the direction of Dr. John Lindsay, consisted of three Bragg spectrometers operating in the 1 to 2.5, 2.5 to 6.4, and 6.4 to 25 Angstrom spectral regions, a concave grating spectrometer operating in the 25 to 400 Angstrom region, and two beryllium window, Xenon filled ion chambers for solar flux measurements in the 2 to 8 Angstrom region. A secondary experiment, developed by the Planetary Atmospheres Branch at NASA-GSFC, was included in the telemetry extension to measure ionospheric electron density by Faraday rotation.

A continued recovery effort was maintained by the WSMR recovery team and by American Machine and Foundry personnel until recovery was effected on November 18, 1964. Investigation of the recovered equipment indicated that the recovery package did not operate properly and therefore the parachute melted and burned due to heating during re-entry. No usable equipment was recovered.



5.2 REDUCED FLIGHT DATA

The evaluation of the flight record shows that the pointing accuracy was good and that SPC 309B and TEL 311 functioned normally. The following tabulated data compares the predicted flight performance with the actual flight performance.

<u>Occurrence</u>	<u>Predicted</u>	<u>Actual</u>
Zenith altitude	113.4 miles	118.6 miles
Spin rate (before acquisition)	1.6 rps	1.5 rps
Spin rate (after acquisition)	1.8 rps	1.85 rps
SPC 309B servo operation initiated	T + 75 seconds	T + 76 seconds
SPC 309B nose cone lift	T + 99 seconds	T + 101 seconds
SPC 309B instrument restow	T + 368 seconds	T + 369 seconds
Payload severance	T + 379 seconds	T + 384 seconds

The performance data listed above and the information that follows was reduced from the telemetry records recorded at Ground Station Jig 44. The following graphs present information regarding pointing control and rocket performance.

Figure 5-1 is a plot of instrument elevation angle versus time. Ninety degrees corresponds to the instrument stowed position parallel to the vehicle longitudinal axis, and zero degrees corresponds to alignment of the instrument optical axis along the vehicle transverse axis. The flight records show that the instrument was released from its stowed position at T + 108 seconds and that the rocket precessed with a cone angle of 37 degrees in a 114-second period; therefore, the average roll rate about the solar



vector was 0.65 degrees per second. The instrument restow operation was initiated at T + 369 seconds, and the instrument was locked in the stowed position at T + 370 seconds.

Figure 5-2 is a plot of the elevation and azimuth pointing errors and illustrates the commutated fine detector error signal outputs versus time. The output of the fine detectors is a direct function of their angular displacement from the solar center. Each fine detector error signal is sampled by the commutator 2.5 times per second with a sample bit duration of 6.65 milliseconds.

The maximum plus and minus error during each second was plotted to generate the envelopes shown. Actual pointing error at any specified time therefore falls within the pointing envelope. The figure shows that the instrument was released from its stowed position at T + 108 seconds and acquired in the coarse pointing mode at T + 118 seconds. Elevation coarse gain was reduced at T + 149 seconds and fine acquisition was complete at T + 150 seconds. Short-term errors were within ± 0.4 arc minutes in elevation and ± 2.5 arc minutes in azimuth. Long-term errors were within ± 0.75 arc minutes in elevation and ± 3.9 arc minutes in azimuth. Long-term errors have a cyclic pattern corresponding to vehicle precessional rate and are the result of variations in reflected earthlight into the coarse detectors.

Figure 5-3 shows the variations in rocket spin rate in cycles per second versus time. It shows that, after sustainer burnout, the spin rate is constant at 1.5 rps until the start of payload despin at T + 76 seconds. At this time, vehicle spin rate was increased to 1.85 rps. Payload despin was



completed at T+79 seconds. After the start of re-entry at T+415 seconds, the figure shows that spin rate changed radically; however, spin rate, as depicted after T+415 seconds, is a combination of vehicle spin and vehicle tumbling, since the aspect eye gives the indication of one revolution each time it is illuminated.

Figure 5-4 presents azimuth rate gyro, azimuth coarse detector, composite nose cone and instrument functions, elevation coarse detector, target detector, and battery voltage outputs as a function of time. These curves are all presented on the same sheet because they illustrate the operational sequence when viewed simultaneously. There is a break in the graph from T+160 seconds to T+350 seconds since there were no changes in these functions during that period. The rate gyro output shows that the azimuth motor was switched on at T+76 seconds, and that payload despin was accomplished by T+79 seconds. The azimuth coarse detector output shows that the rate gyro was switched off at T+91 seconds and that coarse solar azimuth acquisition was complete at T+92 seconds. The nose cone and instrument composite outputs indicate that nose cone lift command was initiated at T+101 seconds and complete at T+108 seconds which allowed release of the instrument from the stow position at T+108 seconds. The instrument restow command was given at T+369 seconds, the instrument was locked in the restow position at T+370 seconds, the nose cone was down, and locked at T+379 seconds. The elevation coarse eye output shows that the instrument was released at T+108 seconds, that the instrument was being pointed in the fine detector region with high gain coarse at T+114 seconds, that the instrument started the restow operation at T+369 seconds, and was in the restow position at T+370 seconds. The target eye curve shows that the instrument was on target with high coarse



gain at T + 114 seconds and on target with low coarse gain at T + 150 seconds, and that the restow operation was initiated at T + 369 seconds. The battery voltage curve presents the variations in battery voltage resulting from the peak power requirements during the various pointing control operations.

Figure 5-5 presents the changes in the pointing control bias voltage as a function of time. There were no significant changes in the bias voltage for the flight duration. This bias voltage is used by the pointing control as a reference and the slight changes in this voltage are taken into account when determining the pointing error curves.

Figure 5-6 presents the biaxial accelerometer output in G's as a function of time. This figure indicates that the maximum thrust was 10.8 G's at T + 1.8 seconds and that sustainer burnout occurred at T + 53 seconds. This figure indicates that severance occurred at T + 384 seconds and that a shock of larger than 30 G's was experienced. This figure indicates that re-entry loading started occurring at T + 412 seconds and reached a peak of approximately 11 G's at T + 427 seconds. The figure also shows another peak of approximately 7 G's at T + 472 seconds. Tumbling about the payload CG could be additive to re-entry loading; therefore, it must be kept in mind when analyzing this data that there are forces in more than one direction and that a biaxial accelerometer only gives part of the total force picture.

Figure 5-7 presents the NASA chamber pressure transducer output voltage as a function of time. The chamber pressure transducer was mounted in the rocket tail section and its output routed through the BBRC telemetry section. This curve indicates that sustainer burnout occurred at T + 53 seconds. Chamber pressure data was not plotted since the transducer calibration curves are not available at BBRC.



Figure 5-8 presents the temperature in degrees Centigrade on the inside of the casting at Station 87 as a function of time. The curve indicates that the temperature rose to 77°C at T + 54 seconds, then dropped to 67.5°C and remained constant until the start of re-entry. At T + 440 seconds, the temperature rose to 100°C due to re-entry heating, then dropped to 37.5°C in the denser atmosphere.

5.3 CONCLUSIONS

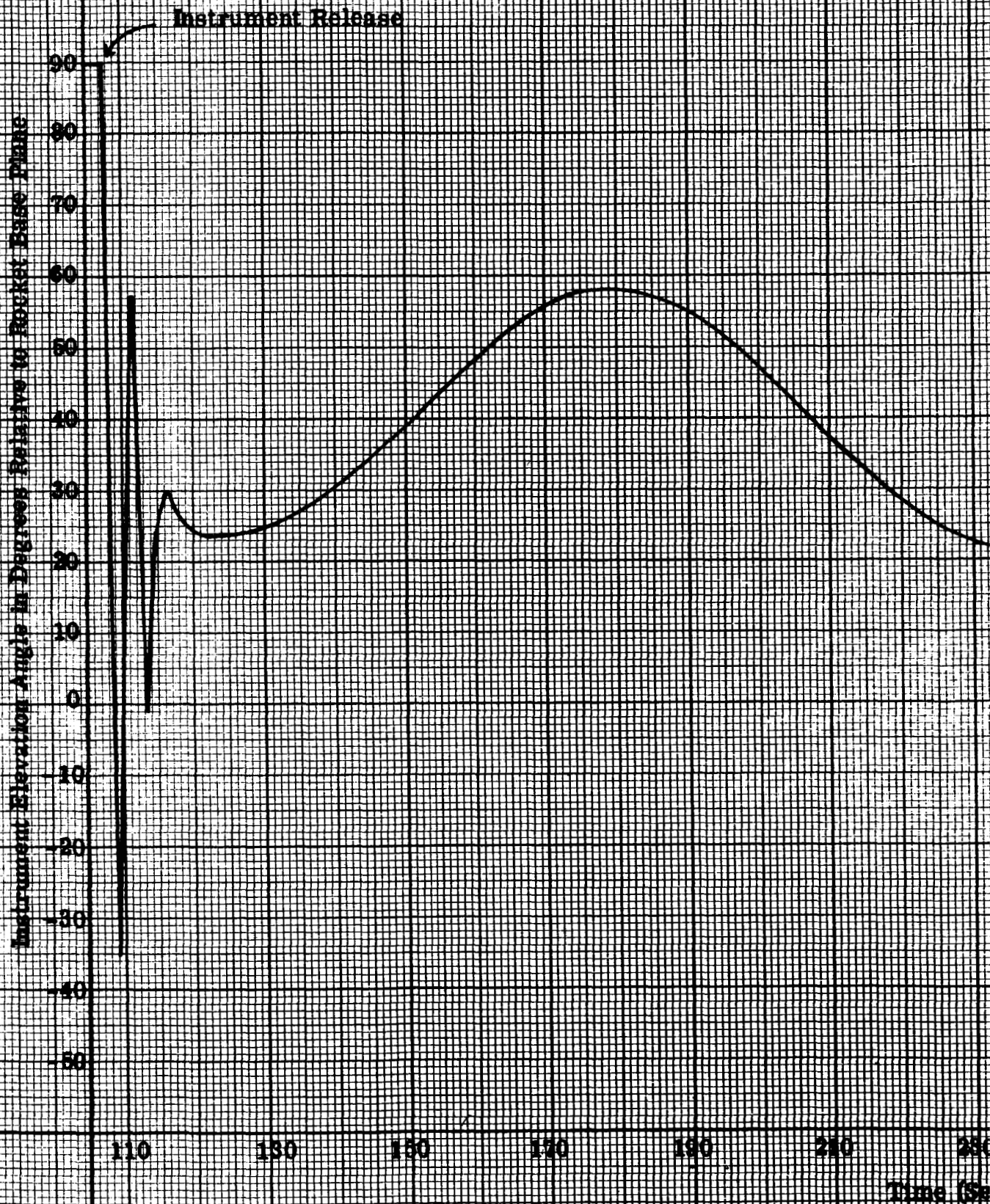
Flight performance of the solar pointing control and the telemetry system was excellent. The pointing accuracy was typical of a model SPC 300 pointing control and was exceptionally good for this particular unit considering the extra long and heavy nose cone that was required for this flight.

The major forcing functions affecting pointing accuracy are introduced by mass unbalance of the rocket vehicle about its spin axis. The extra length and weight of the nose cone add to the pointing control's reaction to these forcing functions. Reduction of the spin rate reduces the amplitude of these forcing functions and correspondingly increases short-term pointing accuracy. Unfortunately, reduction of the spin rate also reduces vehicle stability as reflected by the 37-degree precessional cone, illustrated in Figure 5-1 of this report. This precessional motion is corrected by the pointing control in the two control axes. The third axis motion, however, introduces roll of the instrument about the solar vector. In addition, the excessive precessional motion contributed to long-term pointing inaccuracies by increasing the effects of reflected earthlight on the coarse detectors.

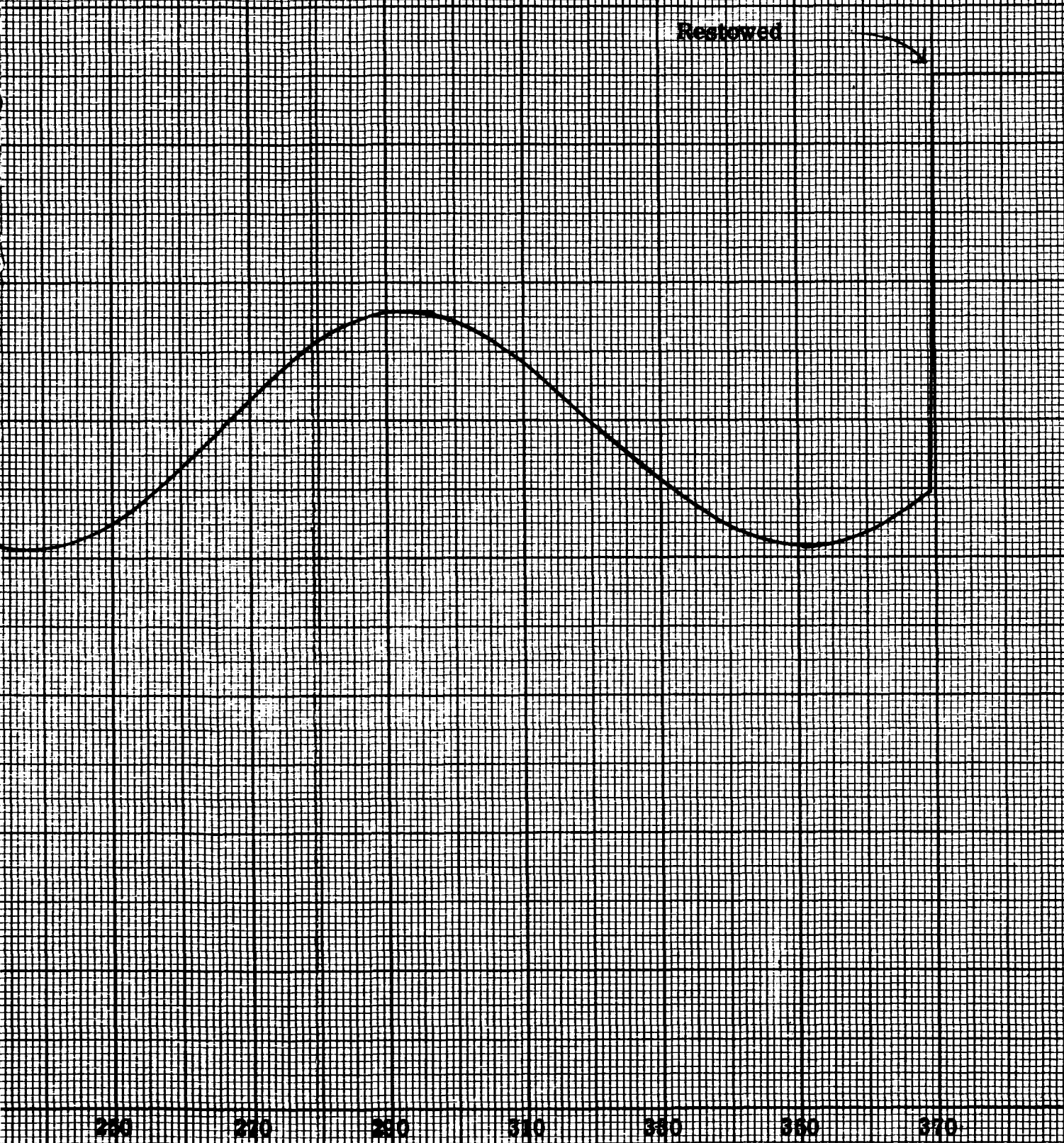


The effects of this reflected light are illustrated by Fig. 5-2.

The pointing errors introduced by reflected light on the coarse detectors are eliminated in more advanced pointing controls, the BBRC type SPC 400, and the BBRC type SPC 300D. This is accomplished by disabling the coarse detectors when the sun is in the fine field of view.

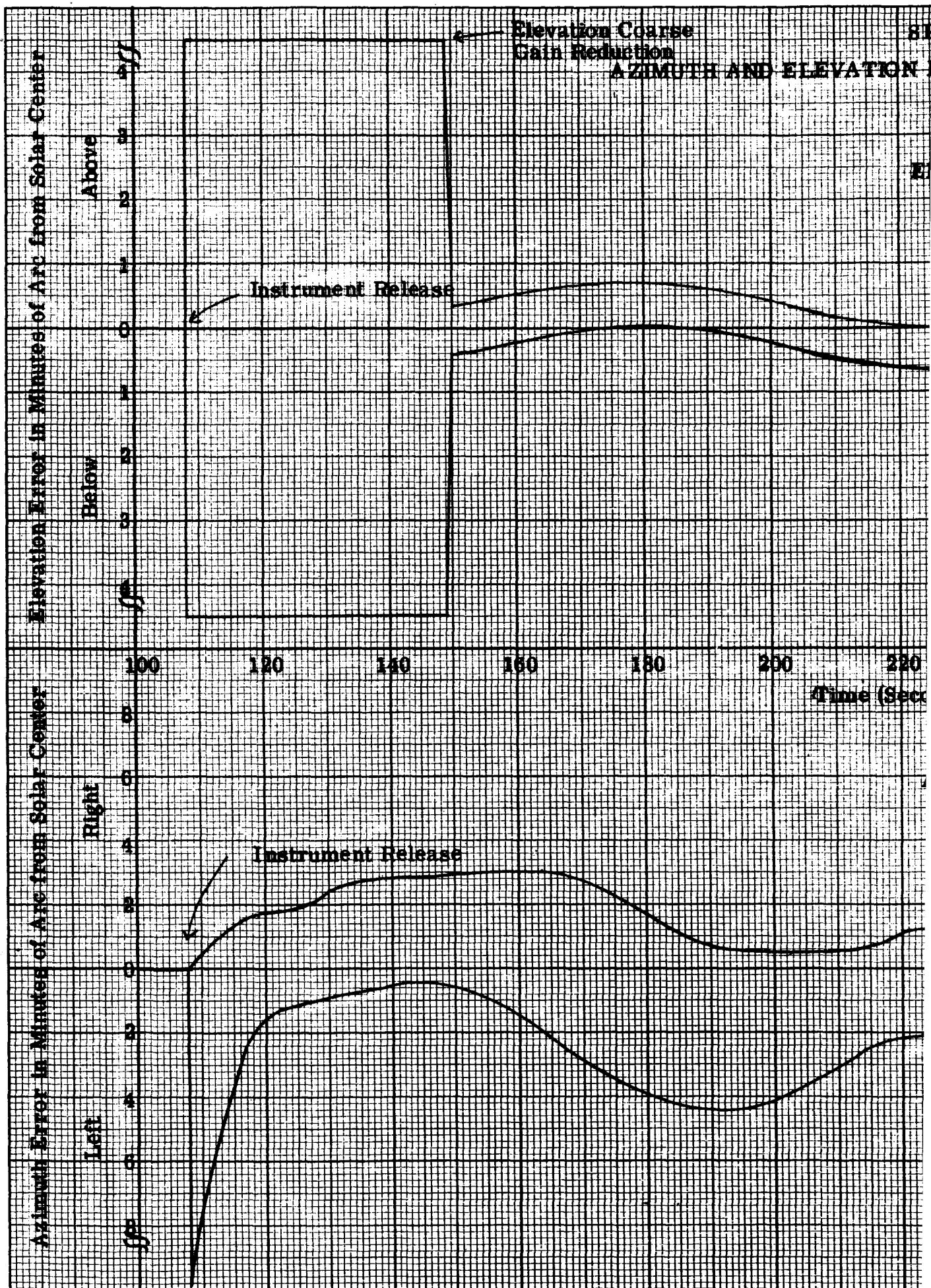


ELEVATION ANGLE VERSUS TIME



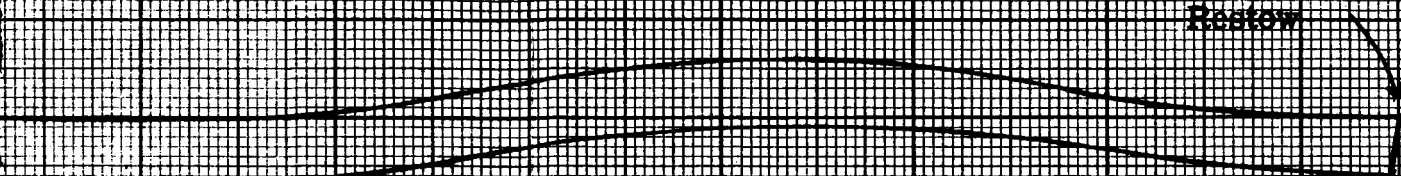
seconds After Launch)

Fig. 5-1 Instrument Elevation Angle versus Time



POINTING ERRORS VERSUS TIME

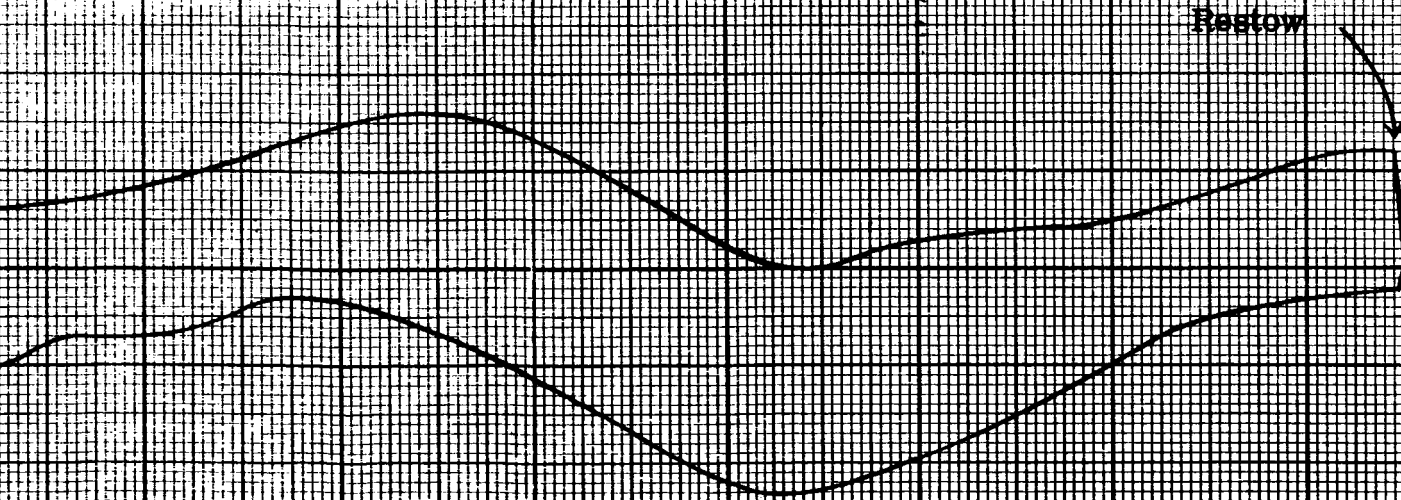
Elevation



240 260 280 300 320 340 360

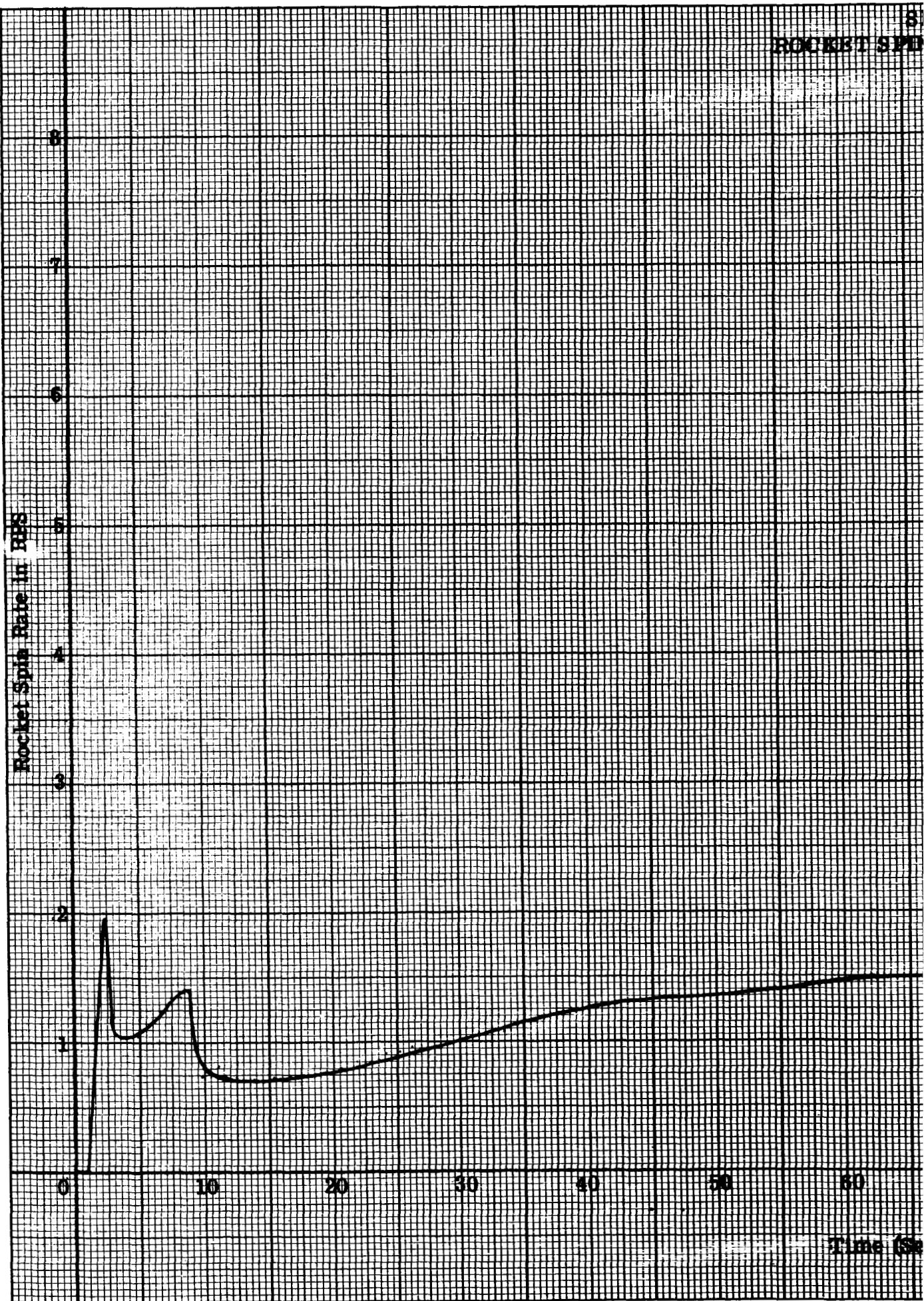
Seconds After Launch)

Azimuth



Note: This graph shows the envelope of the maximum error points recorded each second.

Fig. 5-2 Azimuth and Elevation Pointing Errors versus Time



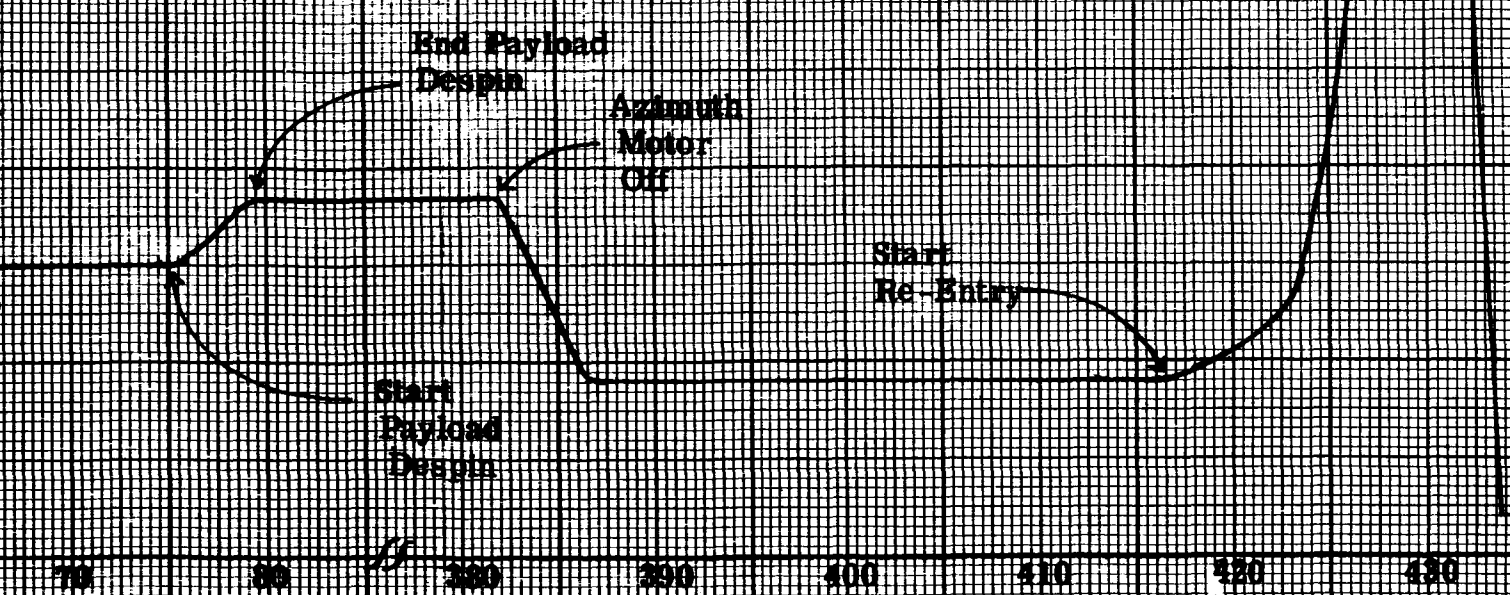
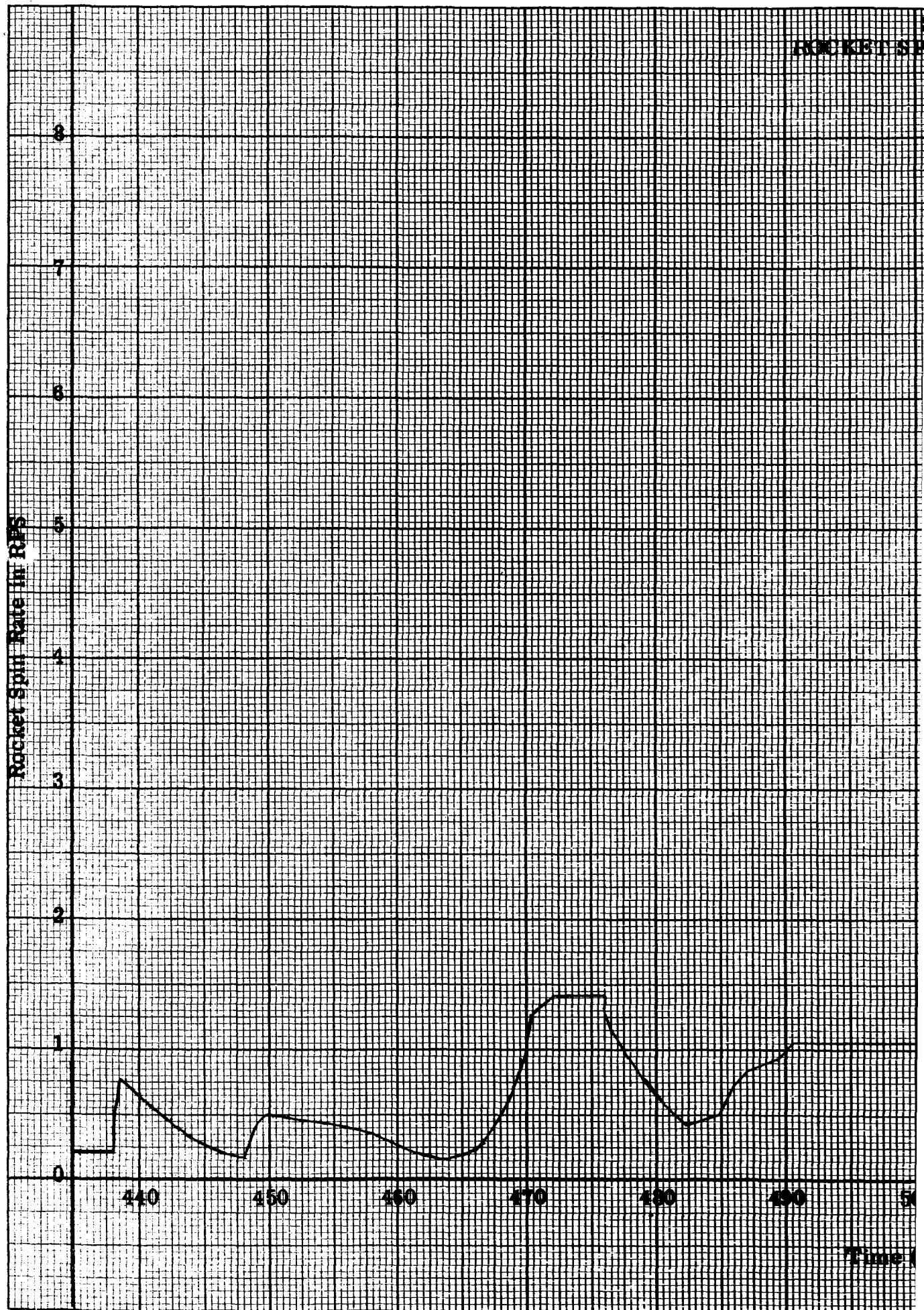
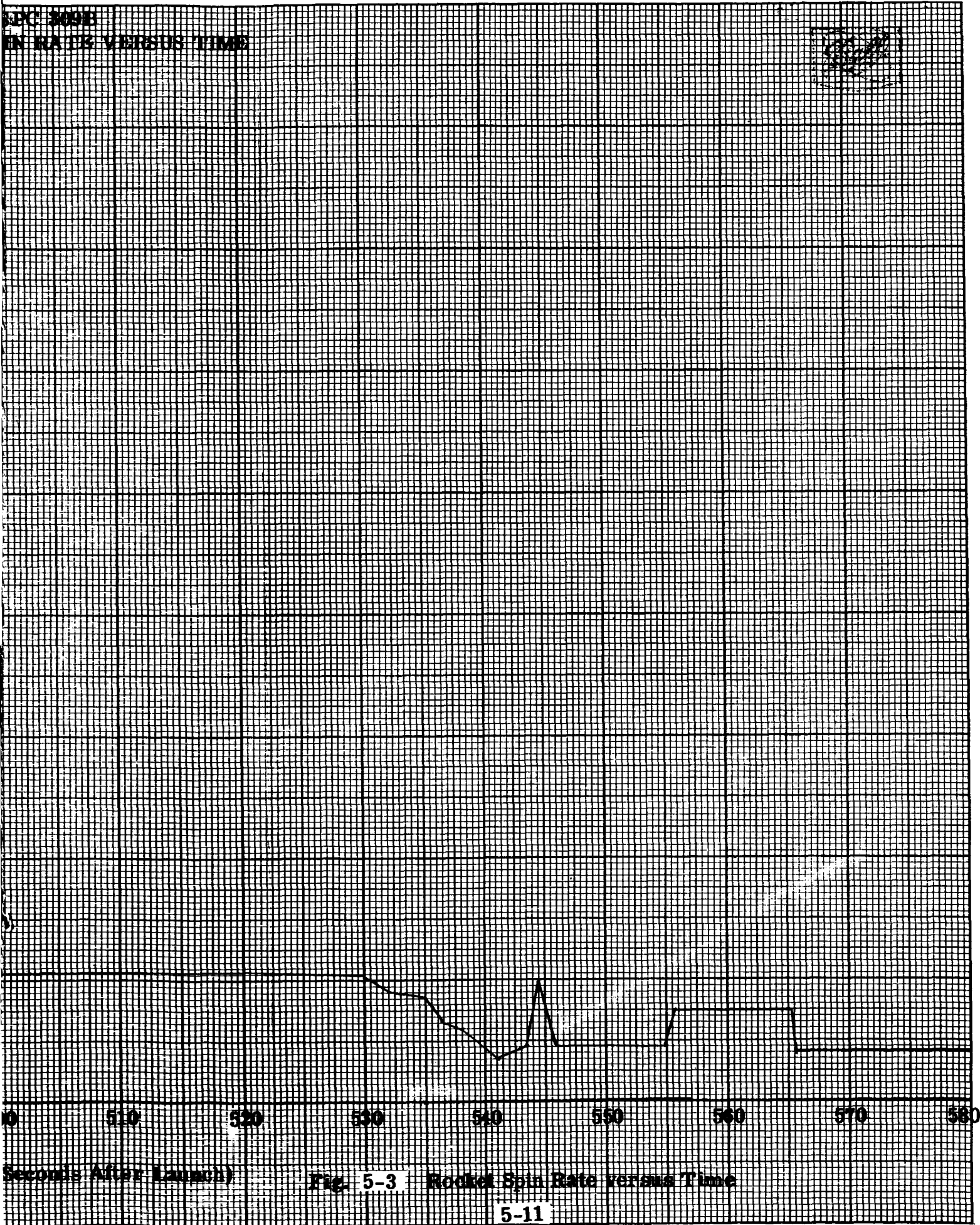


Fig. 5-3 Rocket Spin Rate versus Time

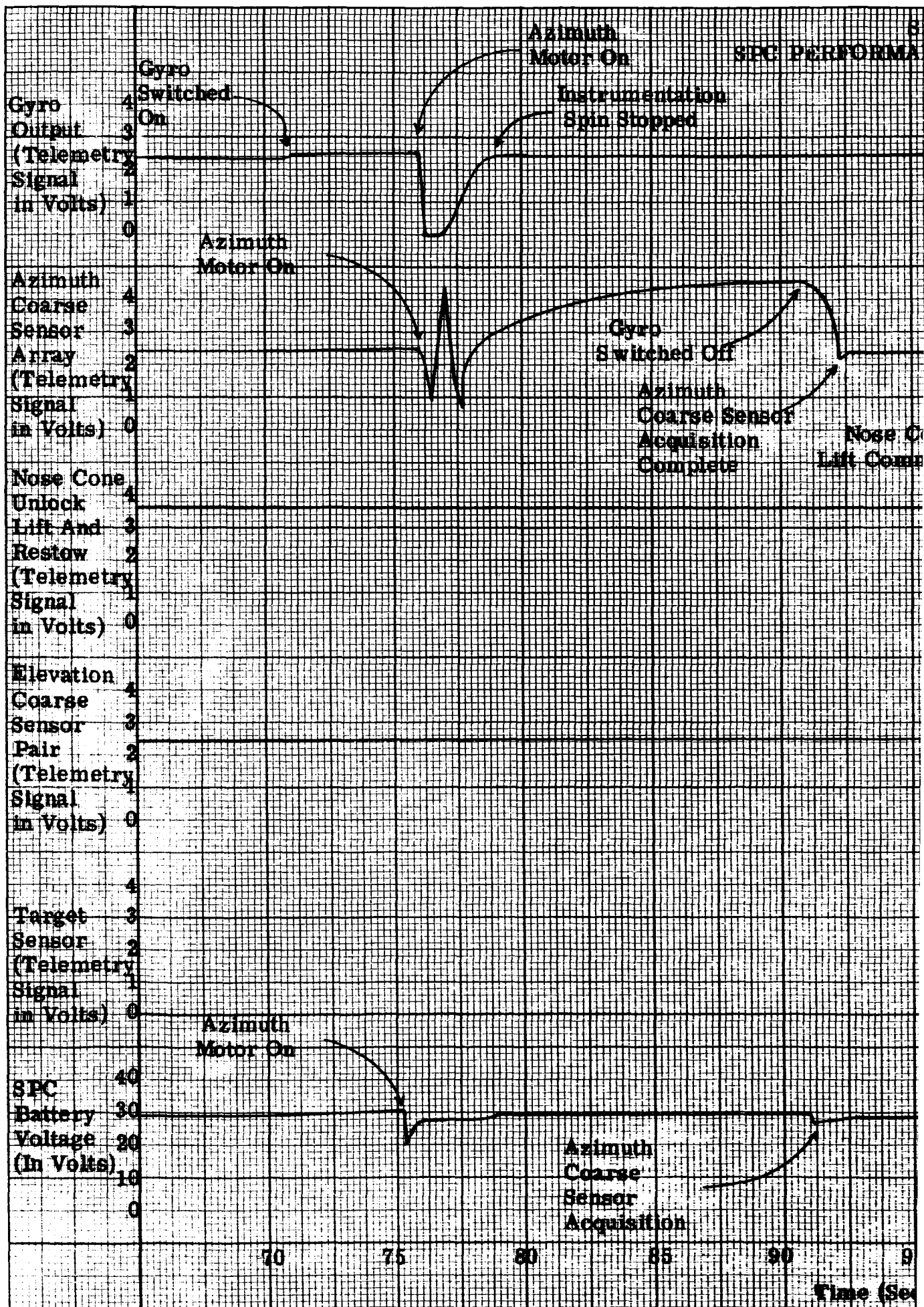


SPC 309B
IN RATE VERSUS TIME



Seconds After Launch)

Fig. 5-3 Rocket Spin Rate versus Time



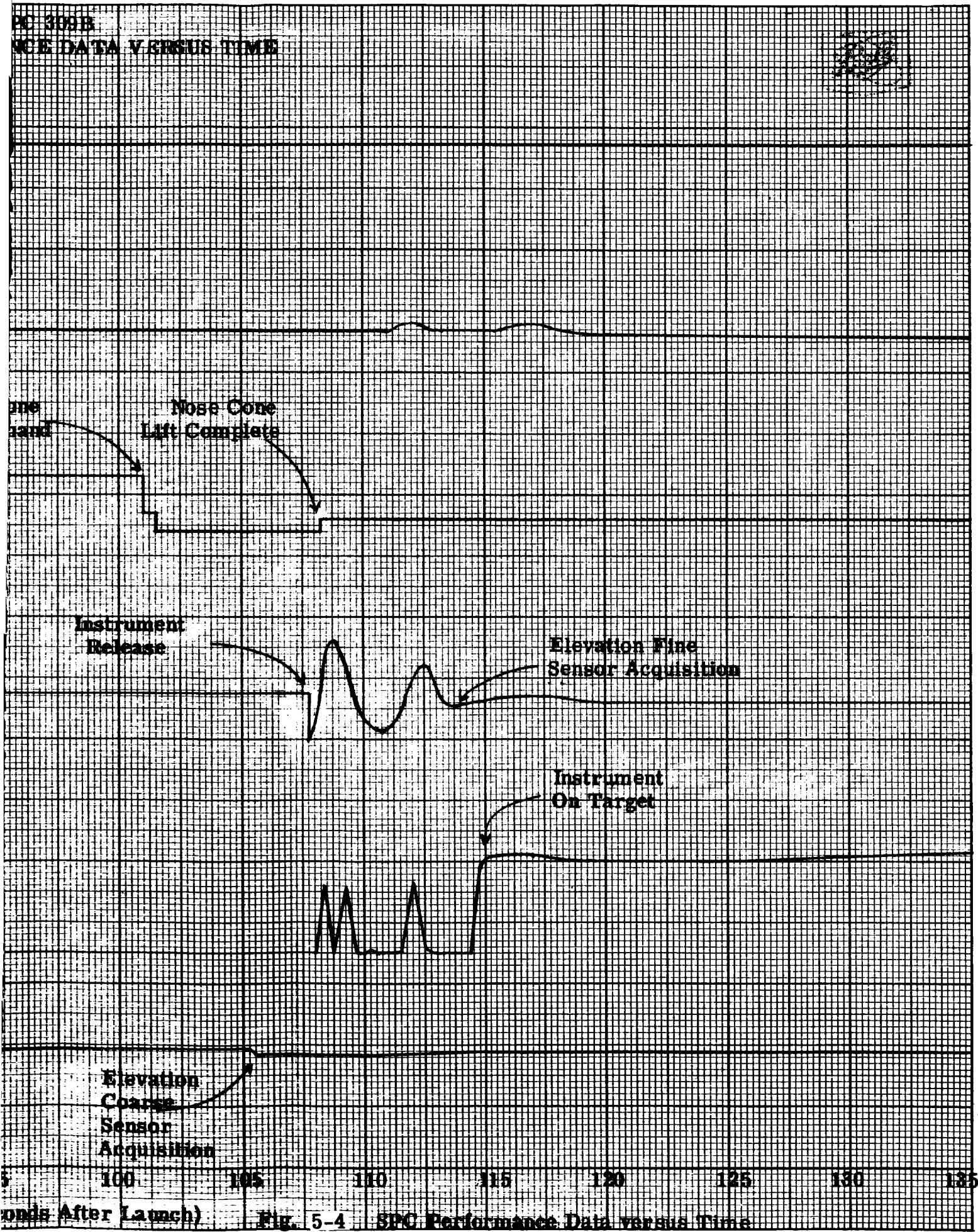


Fig. 5-4 SPC Performance Data versus Time

SPC PERFORMANCE

Gyro 4
Output 3
(Telemetry
Signal 1
in Volts) 1
0

Azimuth 4
Coarse 4
Sensor 2
Array 2
(Telemetry
Signal 1
in Volts) 0

Nose Cone 4
Unlock 4
Lift and 3
Restow 2
(Telemetry
Signal 1
in Volts) 0

Elevation 4
Coarse 4
Sensor 3
Pair 2
(Telemetry
Signal 1
in Volts) 0

Target 4
Sensor 3
(Telemetry
Signal 1
in Volts) 0

SPC 40
Battery 30
Voltage 20
(in Volts) 10
0

Elevation
Coarse Gain
Reduced

135

140

145

150

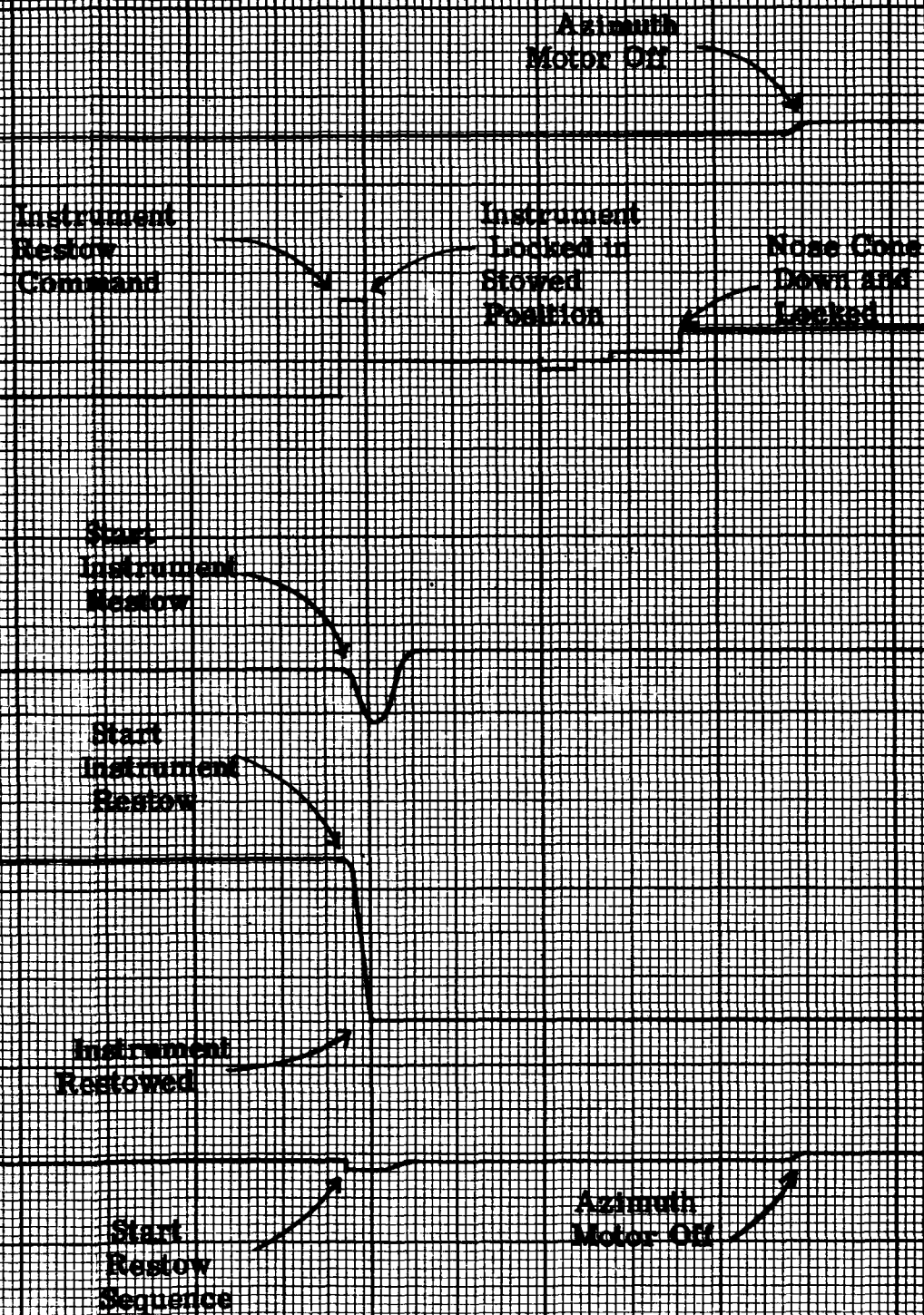
155

160

165

Time (Second)

3000
DATA VERSUS TIME



355

360

365

370

375

380

385

(After Launch)

Fig. 5-4 SPC Performance Data versus Time

S
SPC BIAS VO

SPC Bias Voltage in Volts

5

4

3

2

1

0

40

80

120

160

200

240

Time (S)

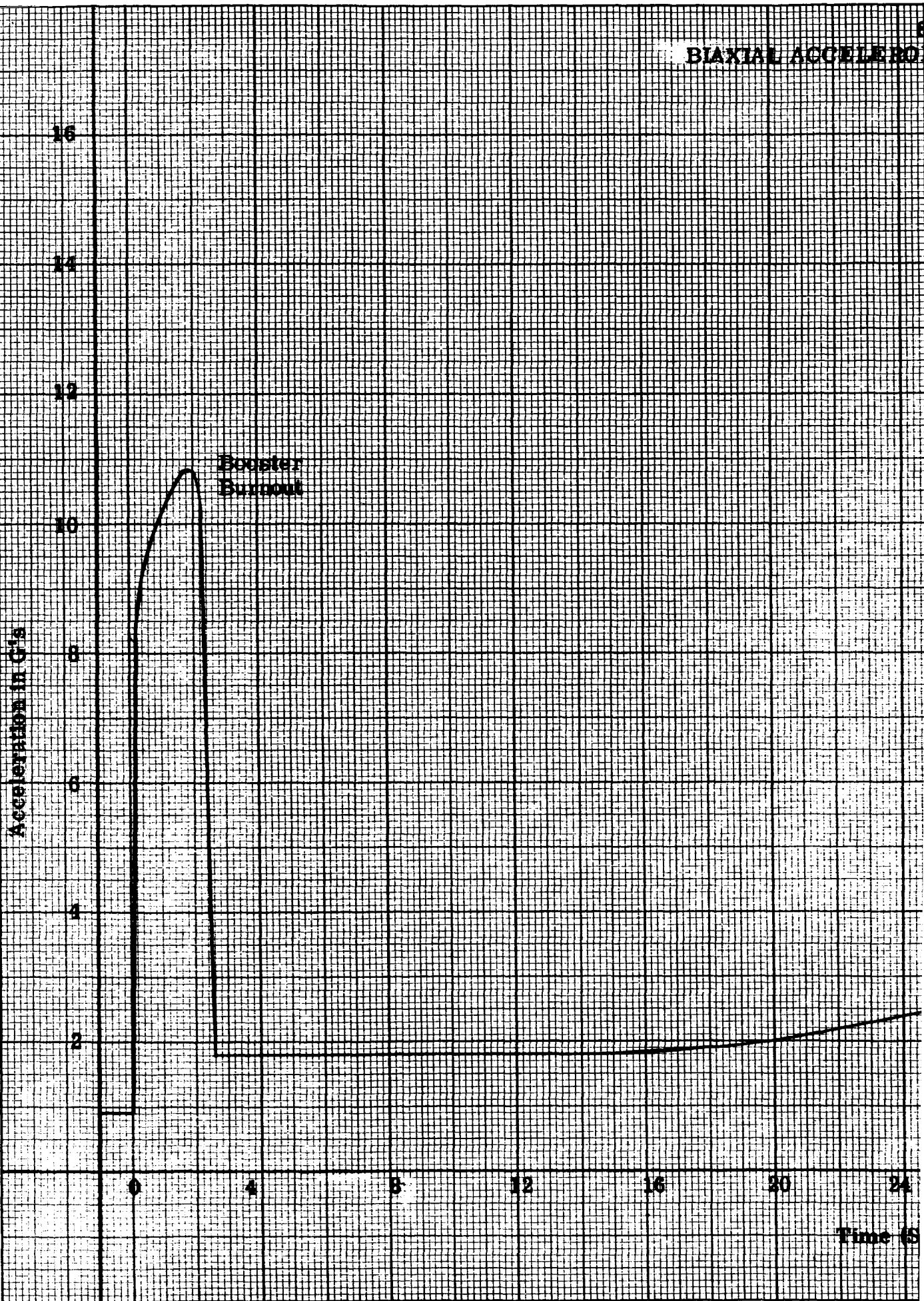
PC 309B
STAGE VERSUS TIME



0 280 320 360 400

Seconds After Launch)

Fig. 5-5 SPC Bias Voltage versus Time



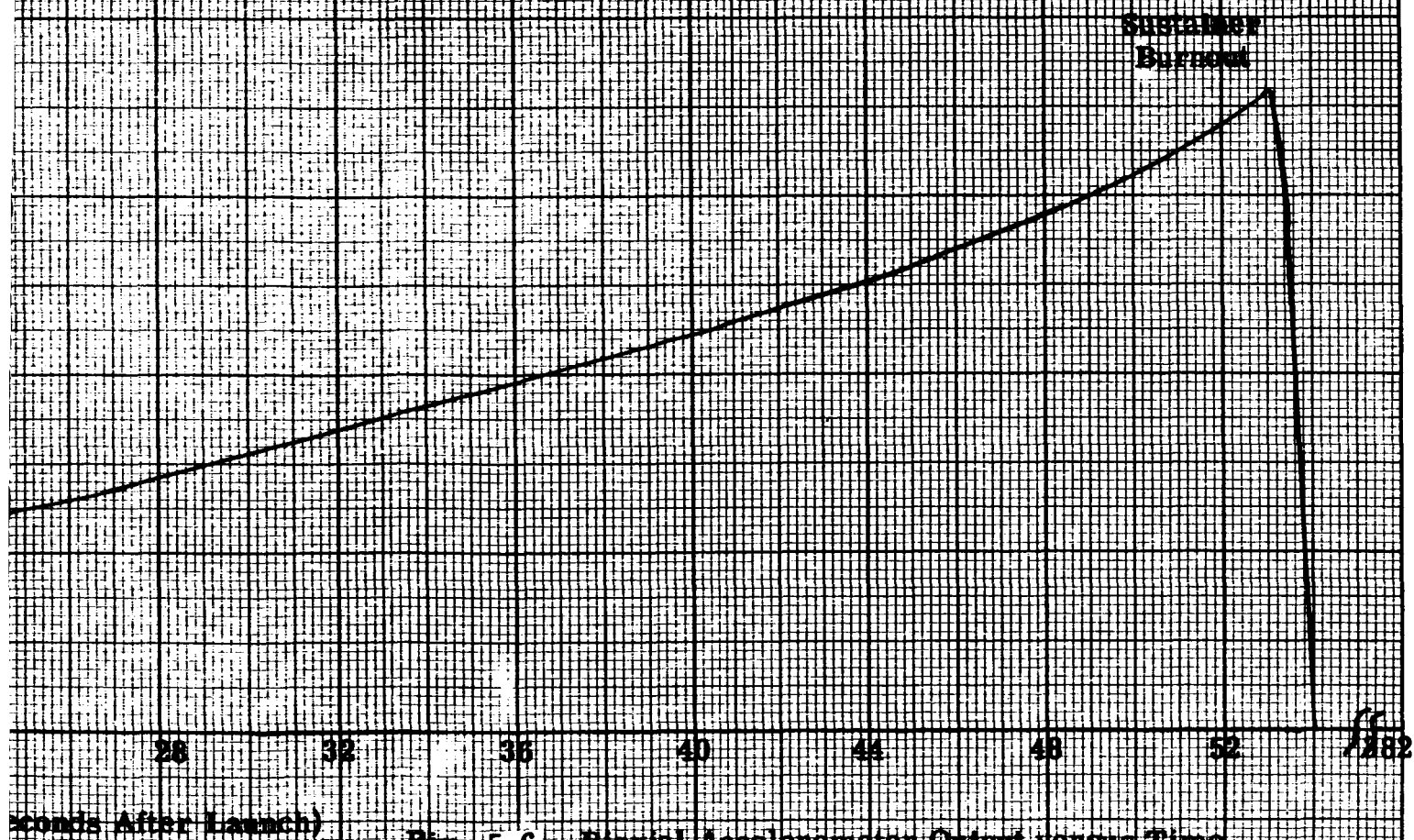
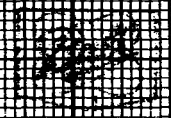
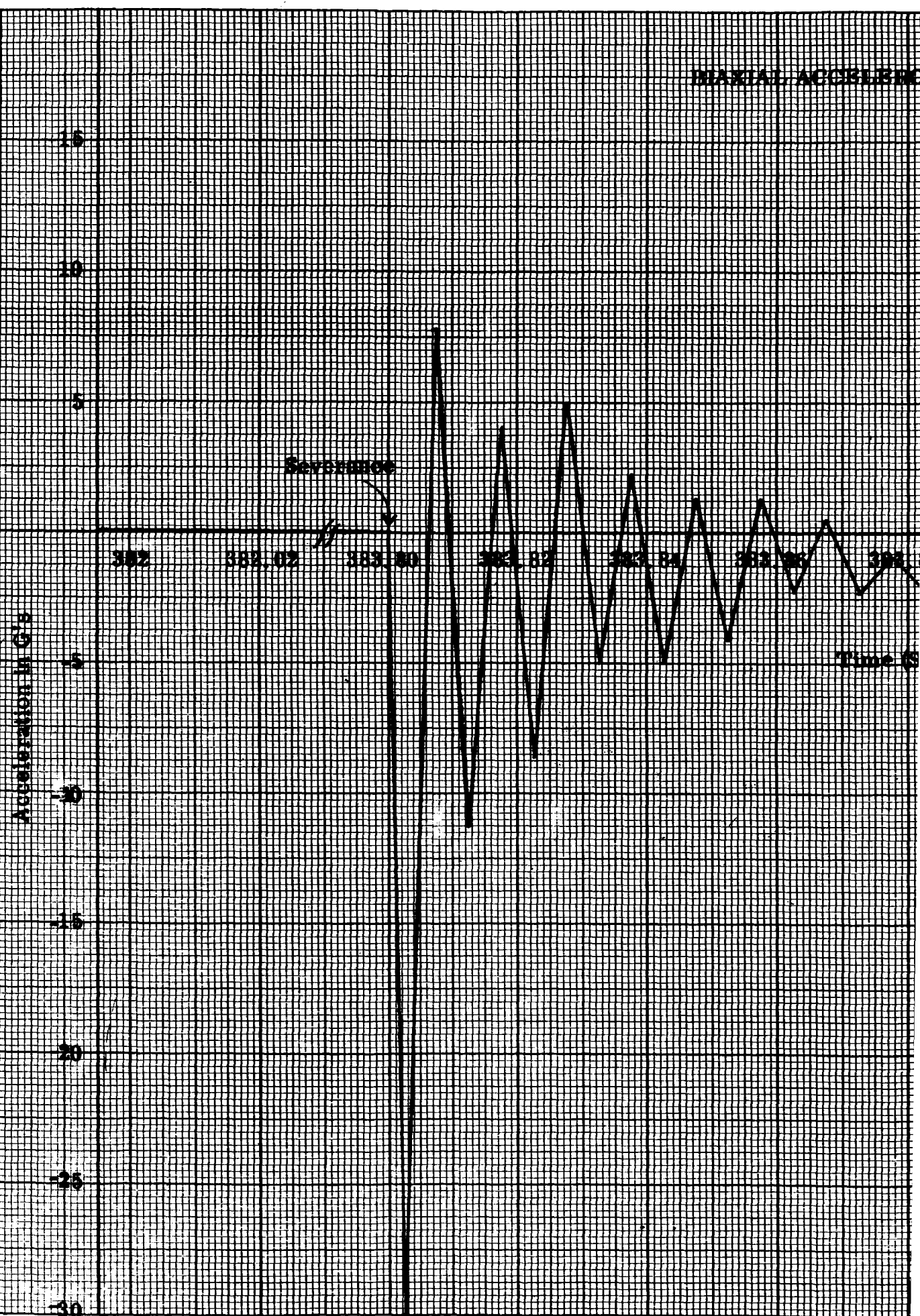


Fig. 5-6 Biaxial Accelerometer Output versus Time

MAXIAL ACCS13NO



PC 302B

METER OUTPUT VERSUS TIME

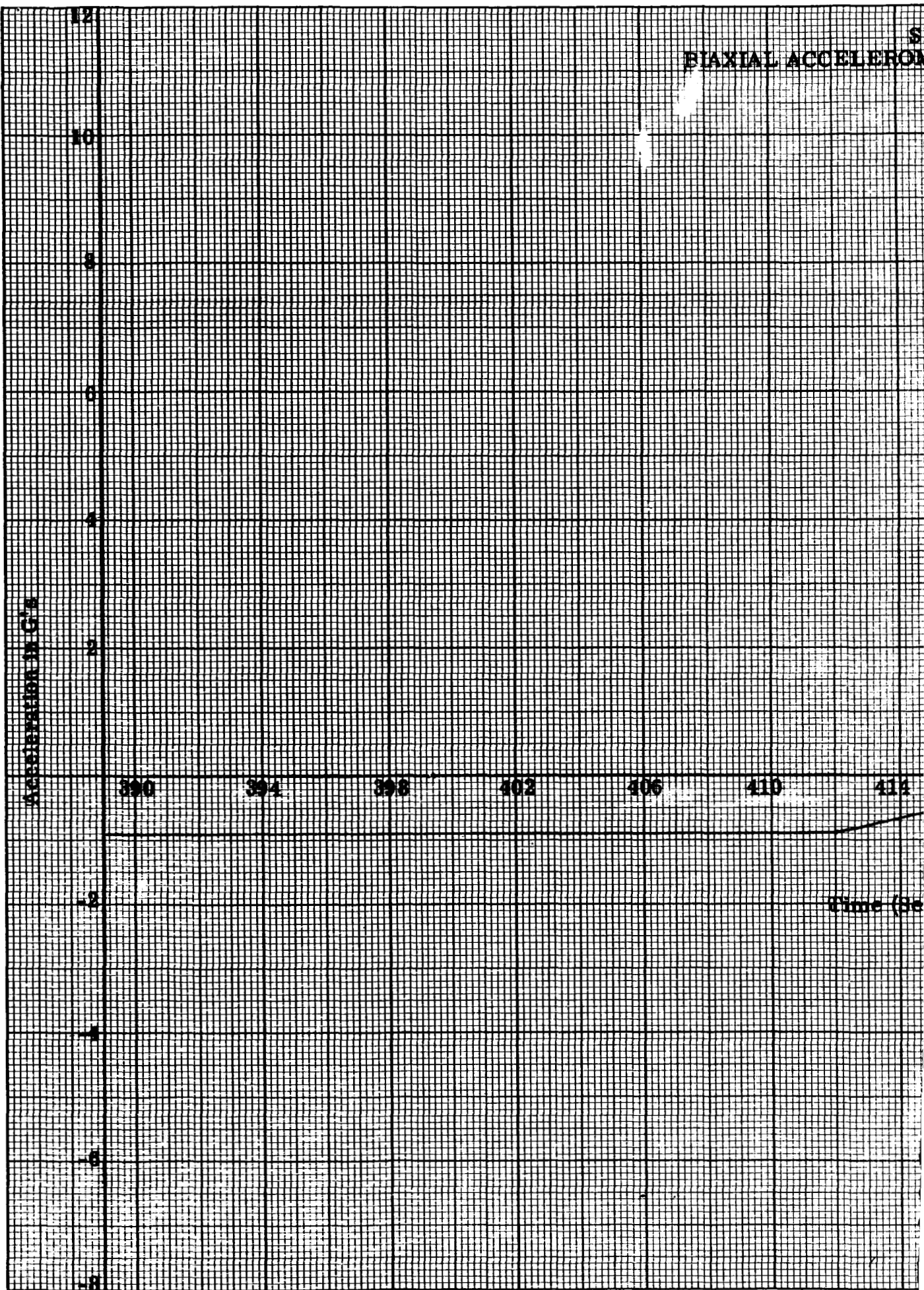


383.90 383.92 383.94 383.96 383.98 384 384.02 384

seconds After Launch)

Fig. 5-6 Biaxial Accelerometer Output versus Time

BIAXIAL ACCELEROMETER



PC 300B
METER OUTPUT VERSUS TIME

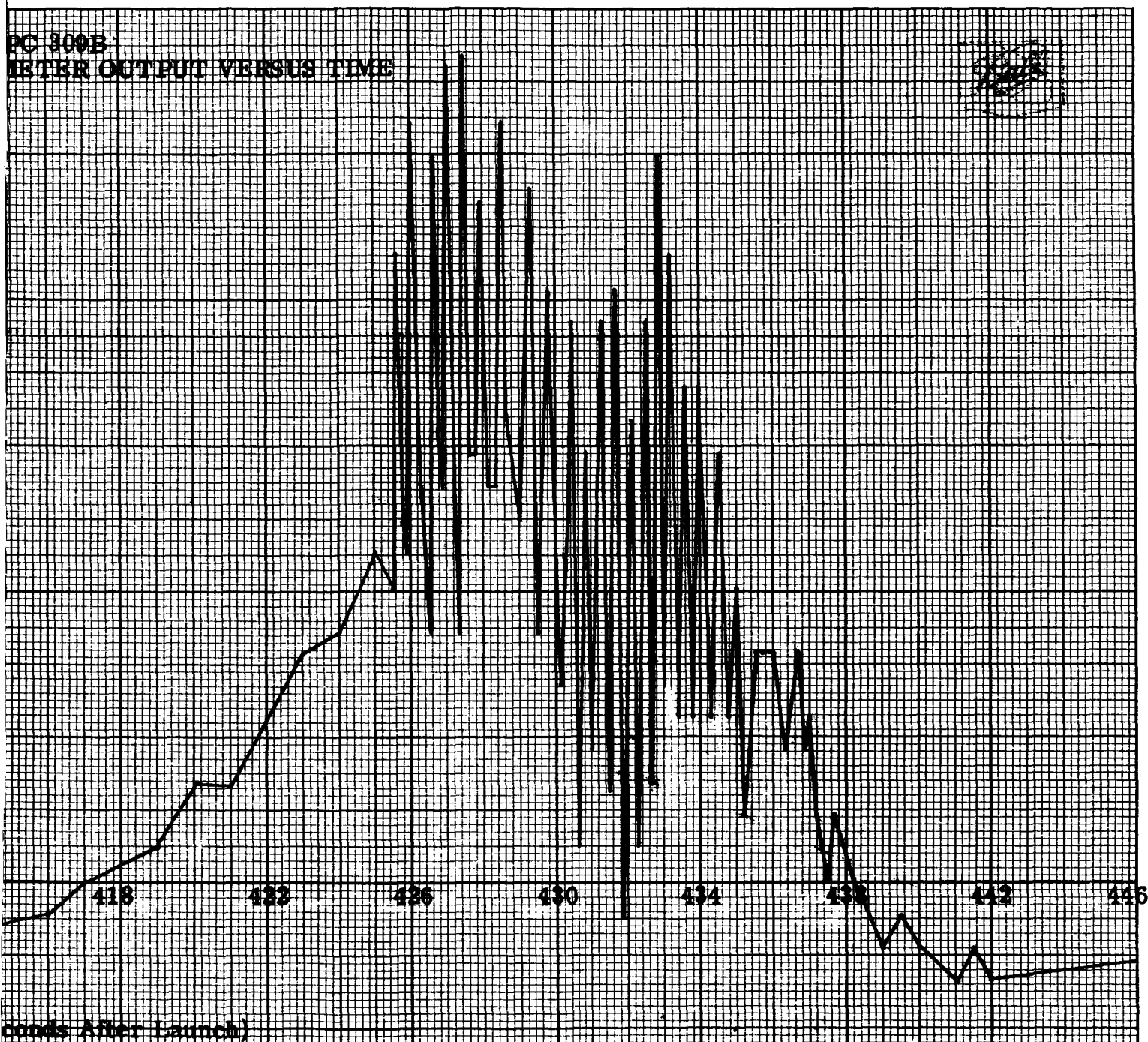
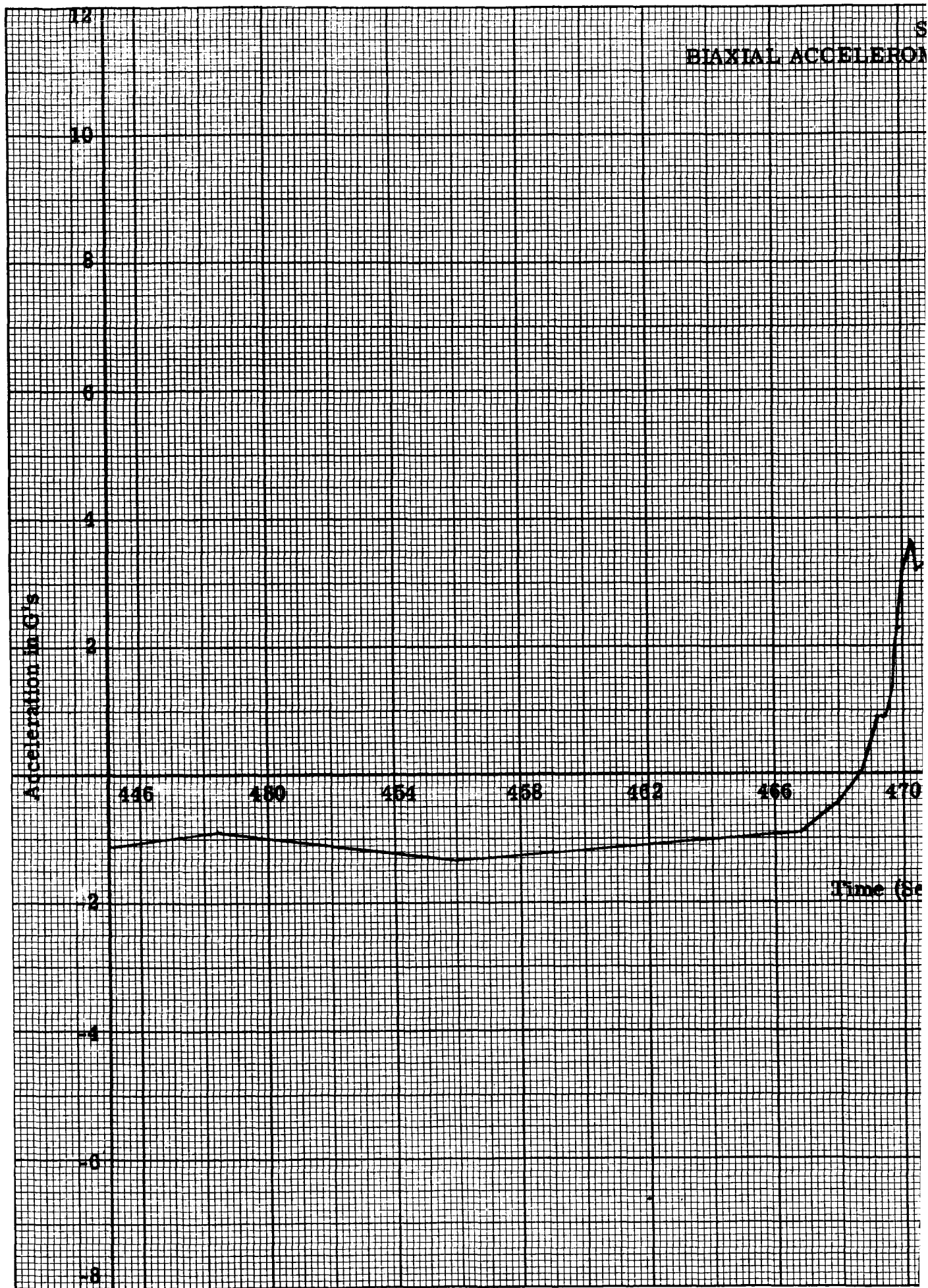
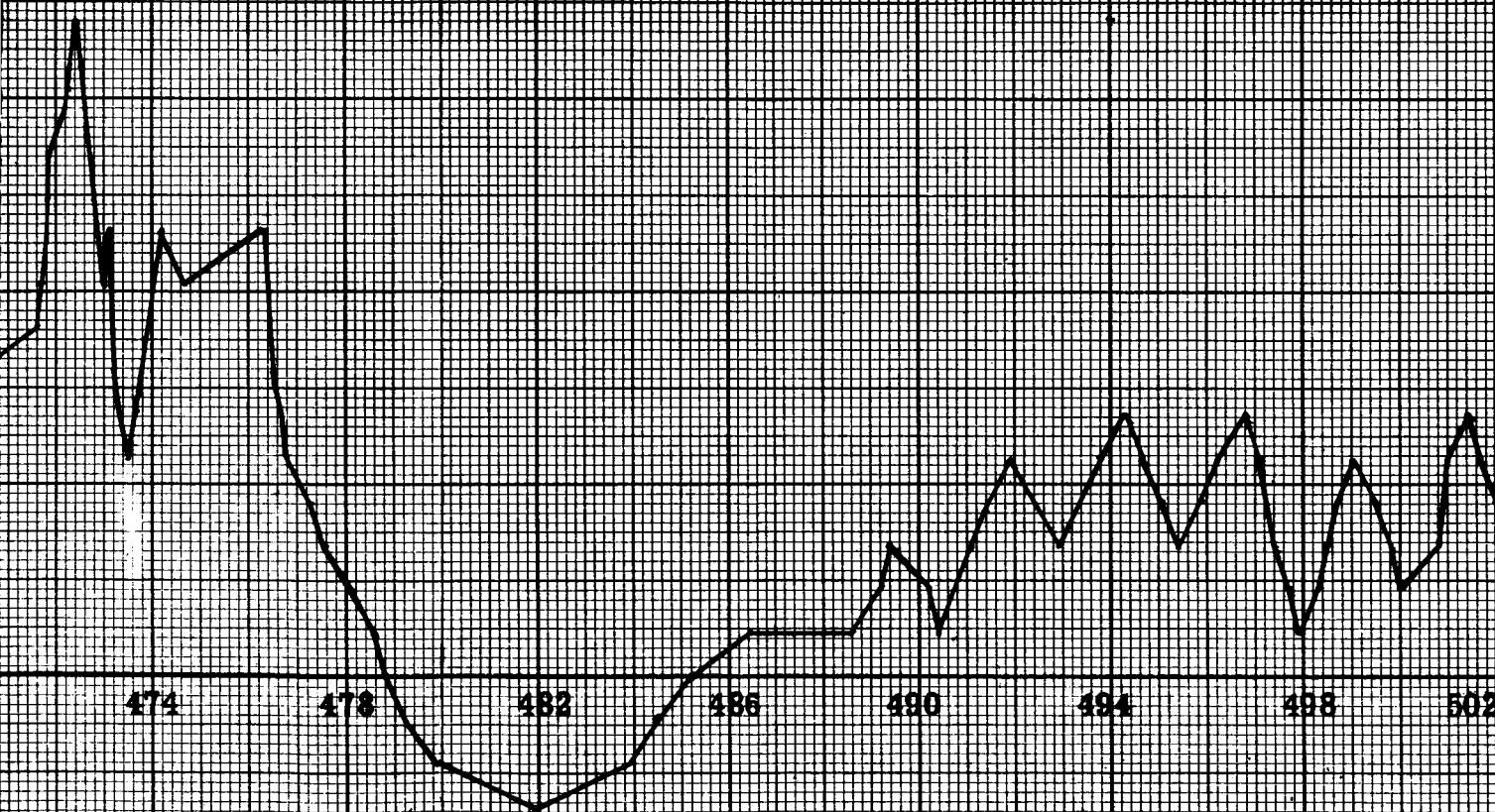


Fig. 5-6 Biaxial Accelerometer Output versus Time



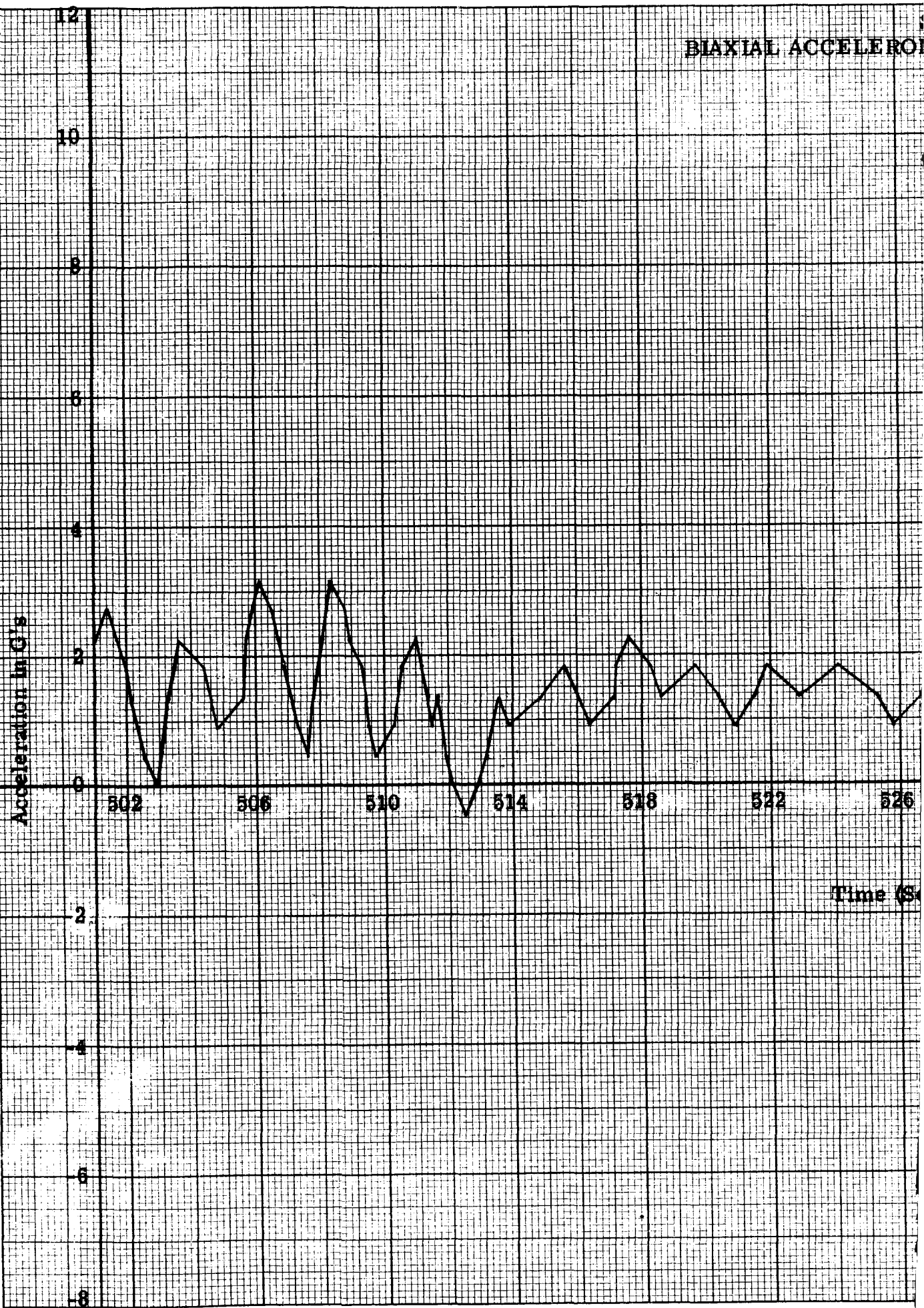
PC 309B
METER OUTPUT VERSUS TIME



conds After Launch)

Fig. 5-6 Biaxial Accelerometer Output versus Time

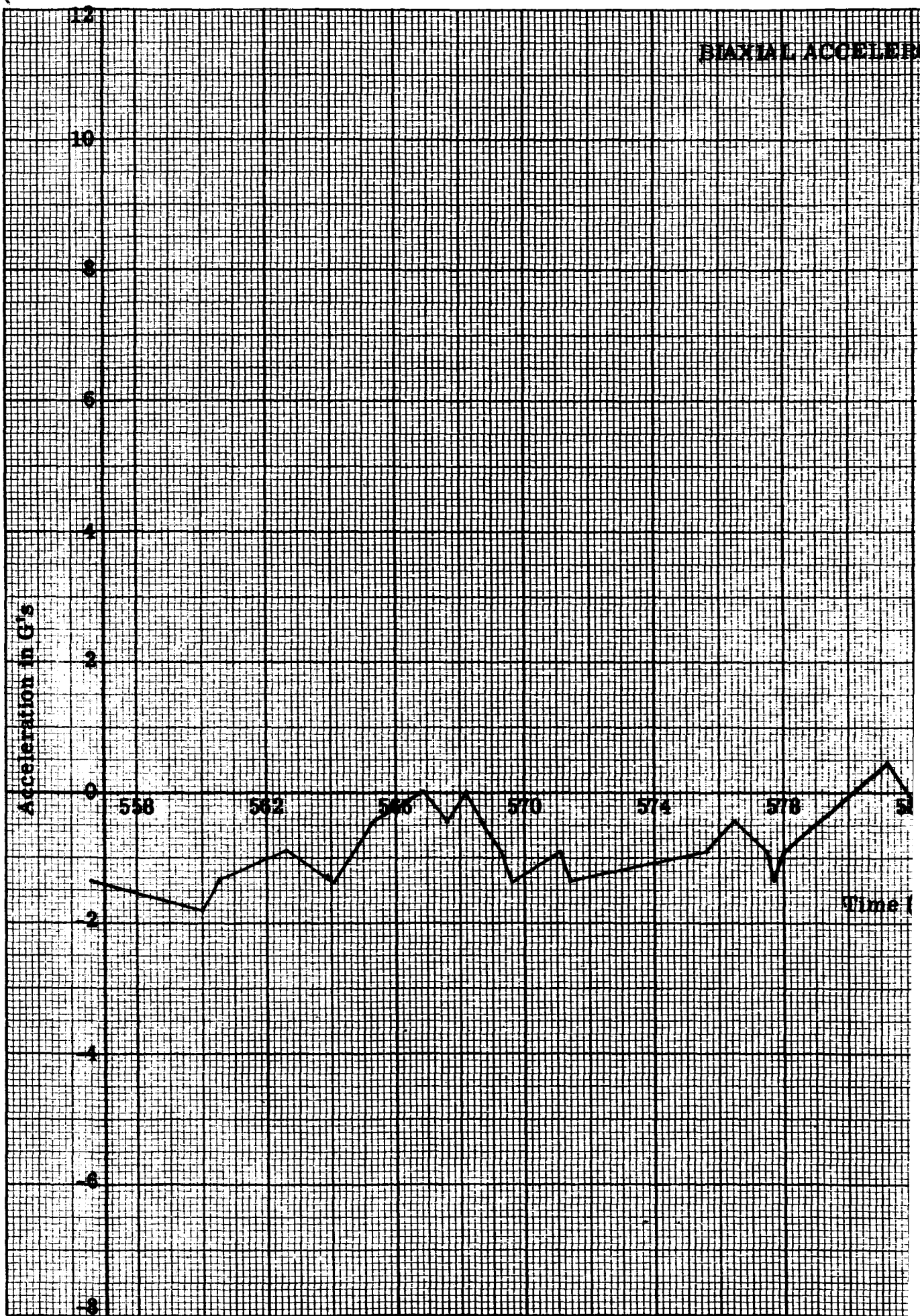
BIAXIAL ACCELEROMETER



SPC 309B
METER OUTPUT VERSUS TIME



Fig. 5-6 Biaxial Accelerometer Output versus Time



SPC 309B
ACCELEROMETER OUTPUT VERSUS TIME

588 590

(Seconds After Launch)

Fig. 5-6 Bixial Accelerometer Output versus Time

Chamber Pressure Transducer Output in Volts

5
4
3
2
1
0

0

4

8

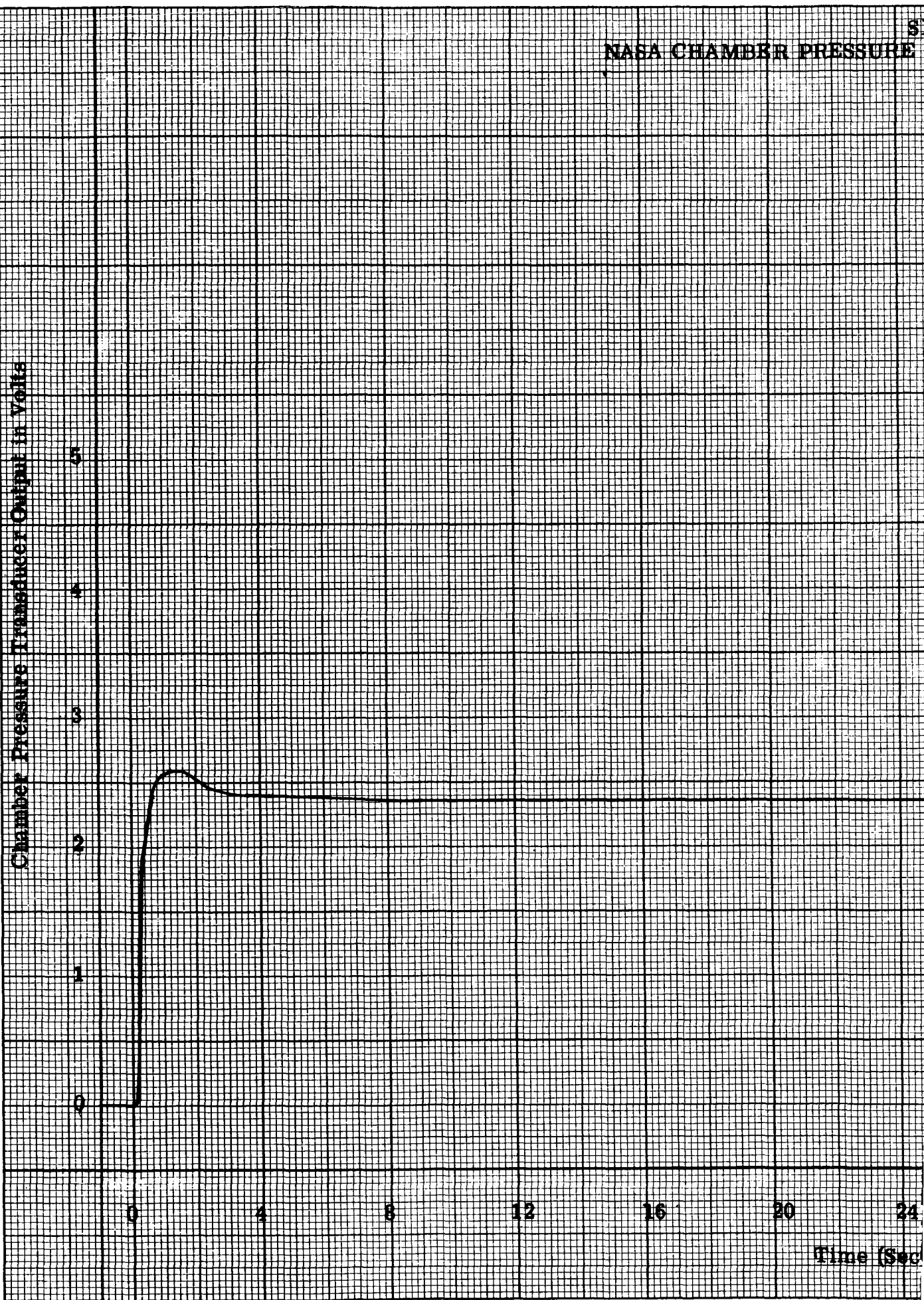
12

16

20

24

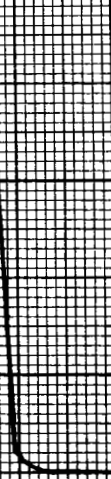
Time (Sec)



IC 309B
TRANSDUCER OUTPUT VERSUS TIME



Sustainer
Burnout



28

32

36

40

44

48

52

54

nds After Launch)

Fig. 5-7 NASA Chamber Pressure Transducer Output versus Time

SE
TEMPERATURE ON INSIDE OF

Temperature in Degrees Centigrade

110

100

90

80

70

60

50

40

30

°C

0

20

40

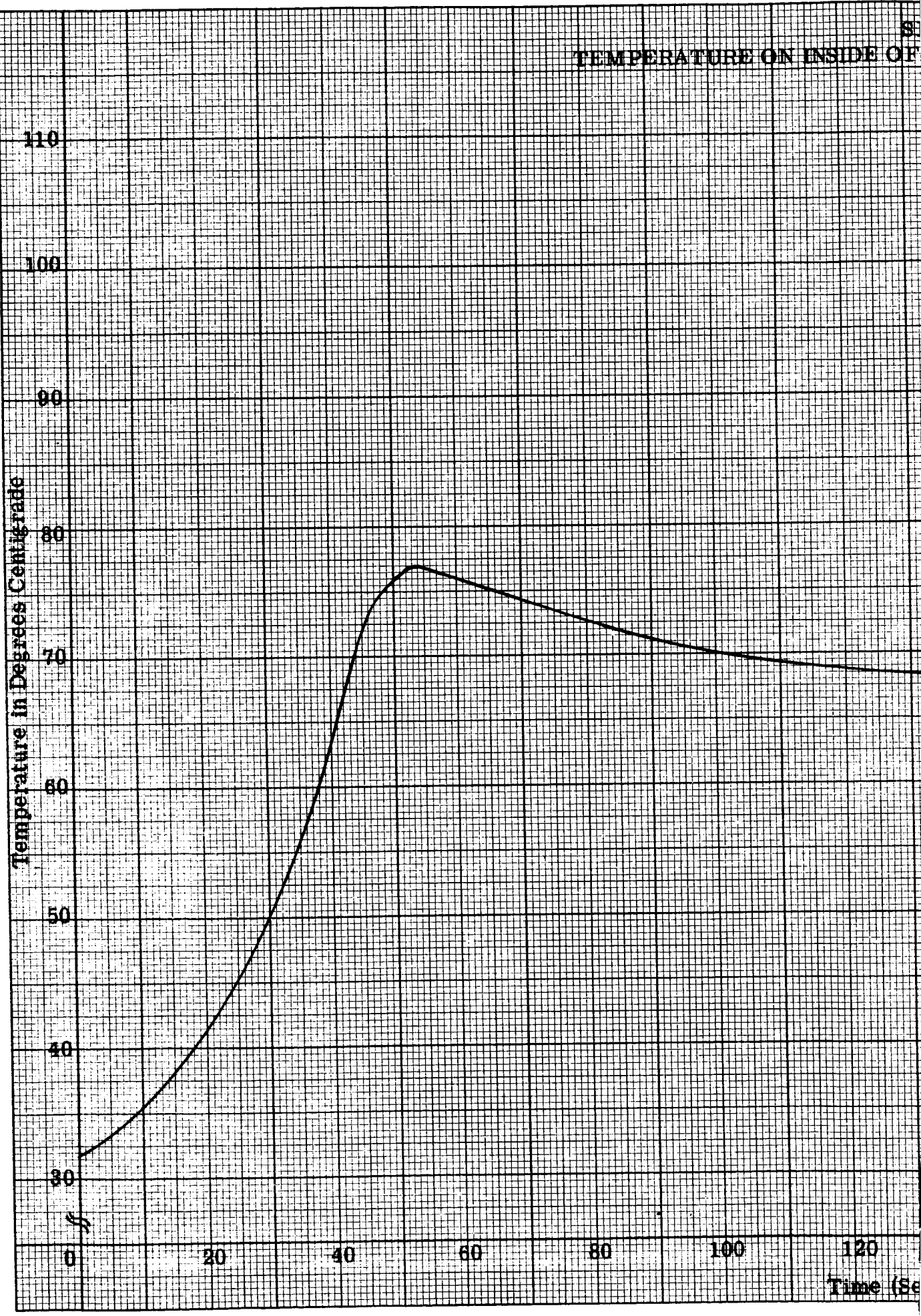
60

80

100

120

Time (Sec)

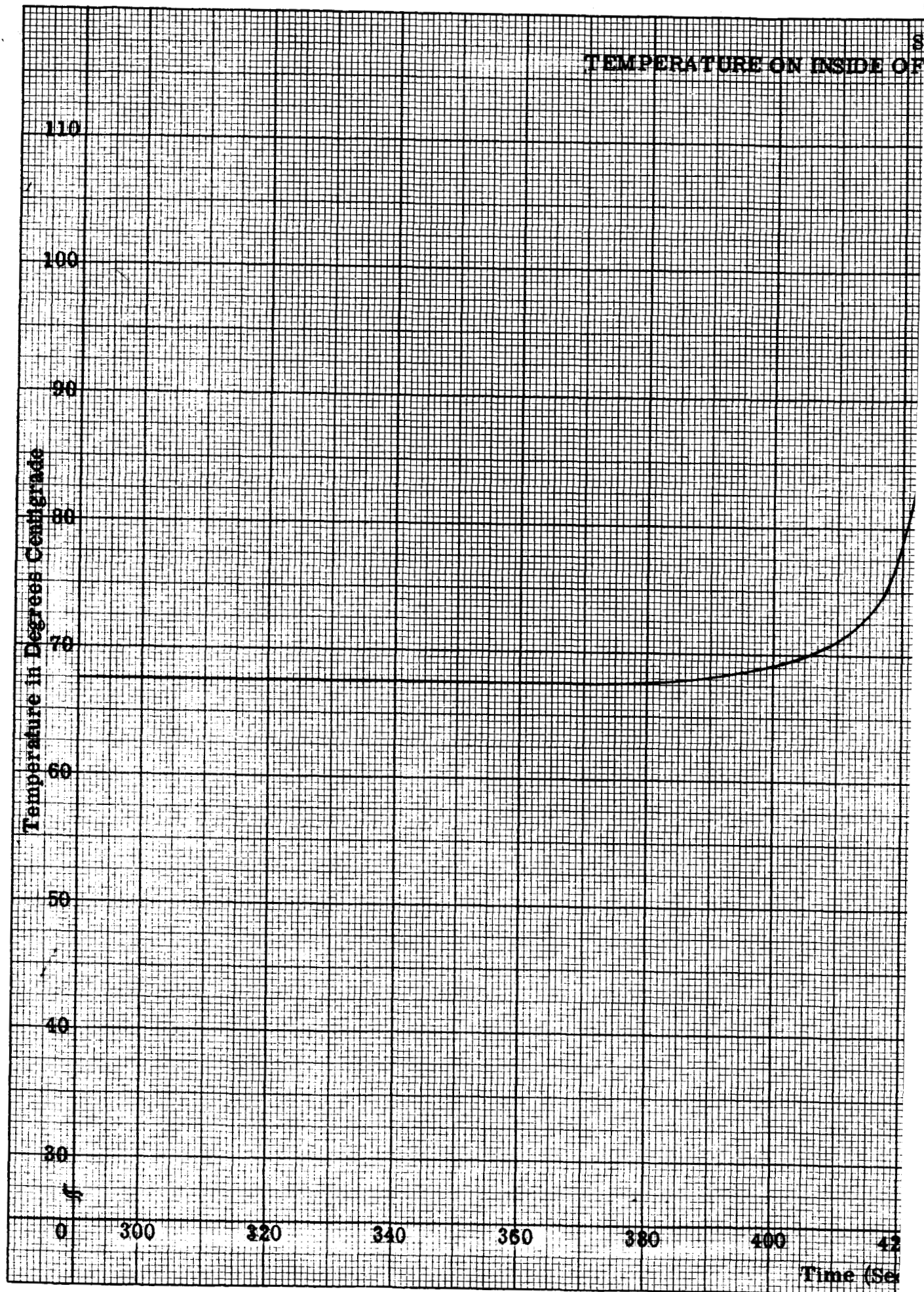


PC 309B
CASTING AT STATION 87 VERSUS TIME



140 160 180 200 220 240 260 280
conds After Launch) Fig. 5-8 Temperature on Inside of Casting at Station 87r versus Time

TEMPERATURE ON INSIDE OF



PC 309B
CASTING AT STATION 87 VERSUS TIME

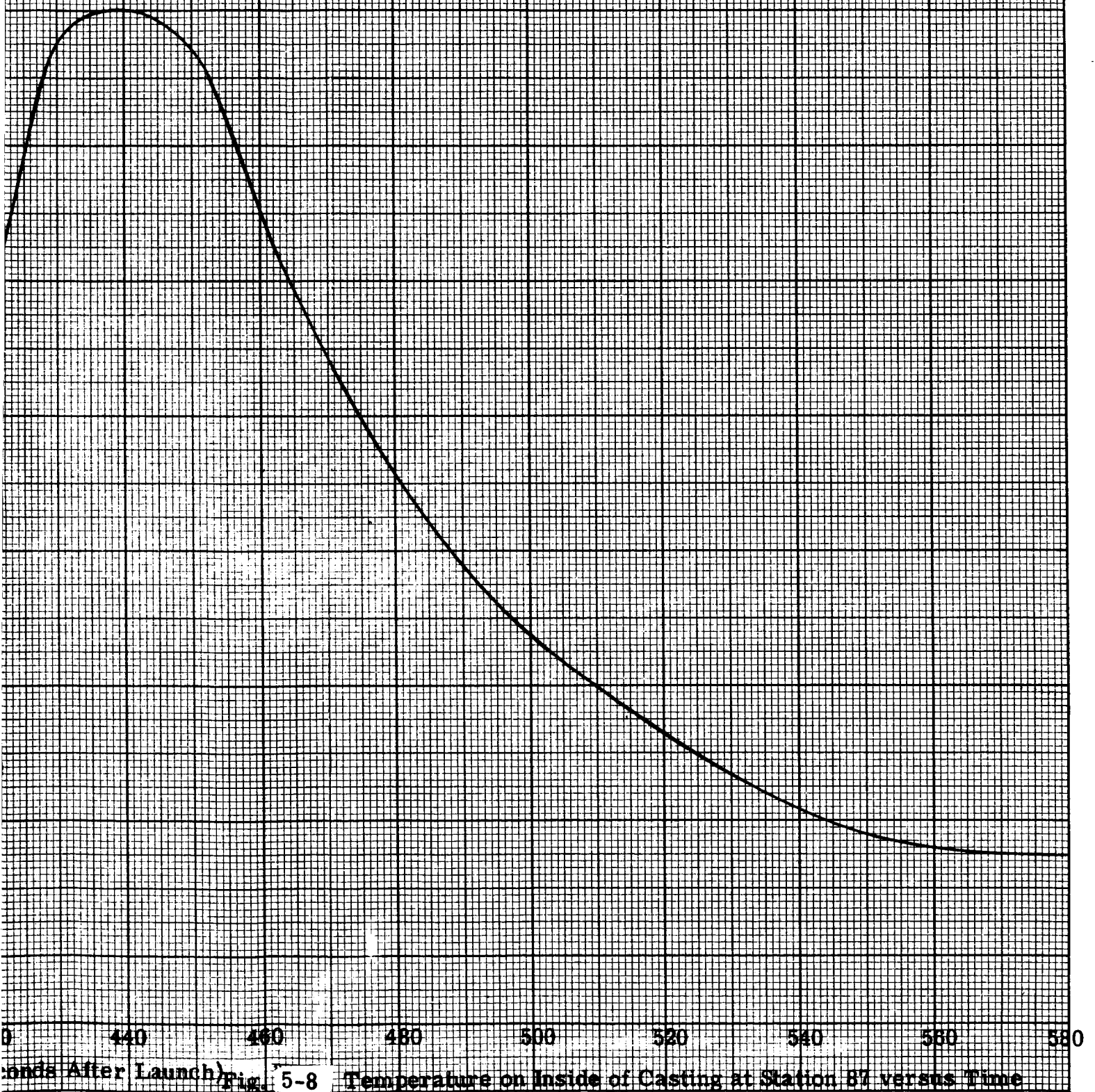


Fig. 5-8 Temperature on Inside of Casting at Station 87 versus Time